



Fakultät für Medizin der Technischen Universität München (TUM)

**Investigating the *MAPT* Haplotype as a Risk Factor
for Neurodegenerative Diseases with
Induced Pluripotent Stem Cells**

Tabea Strauß

Vollständiger Abdruck der von der Fakultät für Medizin der Technischen Universität München zur Erlangung einer

Doktorin der Naturwissenschaften (Dr.rer.nat.)

genehmigten Dissertation.

Vorsitzender:

Prof. Dr. Mikael Simons

Prüfende/-r der Dissertation:

1. Prof. Dr. Günter Höglinger
2. Prof. Dr. Wolfgang Wurst
3. Prof. Dr. Dr. Andreas Hermann

Die Dissertation wurde am 14.03.2022 bei der Technischen Universität München eingereicht und durch die Fakultät für Medizin am 11.10.2022 angenommen.

Acknowledgment

First of all, my sincere thanks goes to Prof. Dr. Günter Höglinger for giving me the opportunity to work in his group on such an interesting topic and making this thesis possible. Thank you for your time, guidance and support, especially during the last phase of my work. I would also like to thank my co-advisor Prof. Dr. Wolfgang Wurst for his help and input. I specially thank my mentor Dr. Sigrid Schwarz for her time and support throughout my thesis. Furthermore, I would like to thank Prof. Dr. Paul Lingor for kindly agreeing to be the first examiner for this thesis.

I sincerely want to thank Prof. Dr. Peter Heutink for welcoming me in his group in Tübingen multiple times and his support during our collaboration. I especially would like to thank Ashutosh Dhingra and Dr. Eldem Sadikoglou for their time, patience and help in the lab, as well as their expertise and advice.

I further thank Prof. Dr. med. Alexander Storch for the valuable experience in his lab in Rostock and Dr. Anna-Maria Pielka for her guidance.

I want to express my gratitude to the whole Höglinger team, in particular to Lena, Tasnim, Elisabeth, Valentin and Niko for their support and friendship during the last five years. Thank you for sharing so many funny moments with me and being there during the difficult ones. Additionally, thanks to Zoë for her friendship and generosity during my time in Tübingen.

I am immensely thankful for my great family who always supported me. I know I can always count on you. To my mum and my sister: Thank you for your love, guidance and being my role models.

My deepest gratitude goes to my fiancé for always being there and for always having my back. Thank you for your patience, encouragement and love. You are my rock and my sunshine.

Summary

A hallmark of neurodegenerative diseases are pathological deposits of different proteins in the human brain. The subgroup of tauopathies, for example, is characterized by intracellular deposits of the microtubule-associated protein TAU (MAPT) in neurons. The corresponding *MAPT* gene encoding TAU exists as the two haplotypes H1 and H2, which span a region of approximately 2 Mb on human chromosome 17q21. The H1 haplotype of the *MAPT* gene has previously been identified as a common genetic risk factor for some tauopathies and synucleinopathies, including progressive supranuclear palsy, corticobasal degeneration and Parkinson's disease. The mechanism behind the increased risk of the named diseases, however, remains largely unclear.

The present work aims to contribute to the elucidation of the cell-based background of the H1-related risk for neurodegenerative diseases and introduces a cell model that could also be applied for further studies in the future. This cell model is used to identify *MAPT*-dependent phenotypes in neurons which are generated from induced pluripotent stem cells (iPSCs). In the investigations, eight homozygous *MAPT* cell lines are compared systematically, four of the H1/H1 and four of the H2/H2 genotype. Within the scope of the analysis, the cell lines are first pre-differentiated from iPSCs to small molecule neural precursor cells (smNPCs), which subsequently can be differentiated into the desired neurons in a fast and reproducible manner. The comparison of all cell lines regarding their differentiation efficiency and cell composition showed a high and comparable number of neurons as early as five days after the start of differentiation. With increasing differentiation time, the neurons continued to mature so that the adult 4R isoform of the TAU protein could already be detected after 15 days. Furthermore, a systematic comparison of the TAU expression profile at mRNA and protein level of the cell lines was carried out within a differentiation period of 30 days. In contrast to the primary hypothesis, no significant differences in total TAU and TAU isoform expression could be observed between the examined cell lines. After 30 days, however, the insoluble protein fraction of the H2/H2 cells showed, compared to H1/H1 cells, higher levels of a conformationally altered TAU protein, which can lead to increased TAU deposits in the human brain. In additional analysis with the protein α -SYNUCLEIN – known to be involved in Parkinson's disease – a higher expression level in H1/H1 cells than in H2/H2 cells could be detected both at the mRNA and protein level. These differences form an interesting basis for further studies on the role of the *MAPT* haplotypes in neurodegenerative diseases.

In conclusion, the presented work describes a method for efficient and comparable differentiation of iPSC lines into neurons. Thereby, differences in the expression profiles of the disease-relevant proteins TAU and α -SYNUCLEIN between H1/H1 and H2/H2 haplotype groups can be identified. The described cell model offers a helpful resource for future modeling of sporadic tauopathies using iPSC lines.

Zusammenfassung

Ein Hauptmerkmal neurodegenerativer Erkrankungen sind krankhafte Ablagerungen verschiedener Proteine im menschlichen Gehirn. So wird die Untergruppe der Tauopathien beispielsweise durch intrazelluläre Ablagerungen des Mikrotubuli-assoziierten Proteins TAU (MAPT) in Nervenzellen charakterisiert. Das entsprechende für TAU codierende *MAPT*-Gen existiert in Form der zwei Haplotypen H1 und H2, die eine Region von etwa 2 Mb auf dem menschlichen Chromosom 17q21 umspannen. Der H1-Haplotyp des *MAPT*-Gens wurde in der Vergangenheit als gemeinsamer genetischer Risikofaktor für einige Tauopathien und Synucleinopathien identifiziert. Beispiele sind die progressive supranukleäre Blickparese, die kortikobasale Degeneration sowie die Parkinson-Krankheit. Bis heute ist der Mechanismus hinter diesem erhöhten Risiko für die genannten Krankheiten jedoch weitgehend ungeklärt.

Die vorliegende Arbeit leistet einen Beitrag zur Aufklärung der zellbasierten Hintergründe des H1-bedingten Risikos für neurodegenerative Erkrankungen und führt ein Zellmodell ein, das auch für weitergehende Studien genutzt werden könnte. Dieses Zellmodell dient der Identifizierung von *MAPT*-abhängigen Phänotypen in Neuronen, die aus induzierten pluripotenten Stammzellen (iPSCs) generiert werden. In den Untersuchungen werden acht homozygote *MAPT*-Zelllinien systematisch verglichen, je vier des H1/H1- und des H2/H2-Genotyps. Im Rahmen der Analysen werden die Zelllinien zunächst von iPSCs zu neuronalen Vorläuferzellen (smNPCs) vordifferenziert, da diese anschließend schnell und reproduzierbar zu den gewünschten Nervenzellen differenziert werden können.

Der Vergleich aller Zelllinien bezüglich ihrer Differenzierungseffizienz und Zellzusammensetzung zeigte bereits fünf Tage nach Differenzierungsstart eine hohe und vergleichbare Anzahl an Neuronen. Mit fortlaufender Differenzierungsdauer reifen die Neuronen weiter heran, sodass bereits nach 15 Tagen die adulte 4R-Isoform des TAU-Proteins nachgewiesen werden konnte. Des Weiteren wurde ein systematischer Vergleich des TAU-Expressionsprofils der Zelllinien innerhalb eines Differenzierungszeitraum von 30 Tagen auf mRNA- sowie auf Proteinebene durchgeführt. Entgegen der ursprünglichen Hypothese konnten keine signifikanten Unterschiede in der absoluten TAU-Expression sowie in der Expression der TAU-Isoformen zwischen den untersuchten Zelllinien beobachtet werden. Verglichen mit H1/H1-Zellen zeigten sich jedoch nach 30 Tagen in der unlöslichen Proteinfraction der H2/H2-Zellen höhere Konzentrationslevel eines in seiner Konformation veränderten TAU-Proteins, das zu verstärkten TAU-Ablagerungen im menschlichen Gehirn führen kann. In ergänzenden Analysen des Proteins α -SYNUCLEIN, dessen Aggregate ein typisches Merkmal für Parkinson sind, konnten in H1/H1-Zellen sowohl auf mRNA- als auch auf Proteinebene ein höheres Expressionsniveau gegenüber H2/H2-Zellen nachgewiesen werden. Diese Unterschiede bilden eine interessante Grundlage für

weiterführende Studien zur Rolle der verschiedenen Haplotypen bei der Entwicklung neurodegenerativer Erkrankungen.

Die vorliegende Arbeit beschreibt damit eine Methode zur effektiven, schnellen und vergleichbaren Differenzierung unterschiedlicher iPSC-Linien zu Neuronen. Dadurch können Unterschiede in den Expressionsprofilen der krankheitsrelevanten Proteine TAU und α -SYNUCLEIN zwischen den H1/H1- und den H2/H2-Haplotypgruppen identifiziert werden. Das beschriebene Zellmodell bietet daher ein hilfreiches Werkzeug zur zukünftigen Modellierung sporadischer Tauopathien mit Hilfe von iPSC-Linien.

Table of Contents

Acknowledgment	I
Summary	II
Zusammenfassung	III
Table of Contents	V
List of Figures	VII
List of Tables	VIII
List of Abbreviations	IX
1. Introduction and theoretical background	1
1.1. Tauopathies	2
1.1.1. Classification of tauopathies	2
1.1.2. TAU protein – structure, function and role in neurodegenerative diseases.....	4
1.1.3. The <i>MAPT</i> gene and its haplotypes	9
1.2. Synucleinopathies.....	12
1.2.1. Classification of synucleinopathies.....	12
1.2.2. α -SYNUCLEIN protein – structure, function and role in neurodegenerative diseases..	13
1.3. The interplay of TAU and α -SYNUCLEIN in neurodegenerative diseases.....	14
1.4. Cell culture models for neurodegenerative diseases	14
1.4.1. iPSC-derived neuronal cell models	14
1.4.2. iPSC models for tauopathies	16
1.5. Aims of this thesis.....	17
2. Material and methods	18
2.1. Cell line identification and cell differentiation	18
2.1.1. Identification and selection of iPSC lines	18
2.1.2. Genotyping	19
2.1.3. Cell culture.....	19
2.2. Analytical methods.....	22
2.2.1. Immunocytochemistry	22
2.2.2. Semi-quantitative real-time PCR	23
2.2.3. Western blot.....	25
2.2.4. Cell survival without antioxidants	26
2.2.5. Toxin treatment.....	27
2.3. Statistical analysis.....	27

3. Results.....	28
3.1. Generation of <i>NGN2</i> _smNPCs from iPSC lines.....	28
3.2. Differentiation and characterization of <i>NGN2</i> _smNPC lines	30
3.2.1. Evaluation of cell survival at day 30 and 60 of differentiation.....	30
3.2.2. Evaluation of differentiation via <i>SOX2</i> and β -3-TUBULIN expression	31
3.2.3. Identification and quantification of cell types during differentiation via immunocytochemistry	32
3.2.4. Further characterization of differentiated neurons.....	37
3.3. TAU expression in differentiated neurons with homozygous H1 or H2 <i>MAPT</i> haplotypes ..	38
3.3.1. Immunofluorescent and qPCR analysis of TAU	38
3.3.2. Protein analysis of TAU via Western blot.....	40
3.3.3. Genotyping for H1 sub-haplotypes	44
3.4. α -SYNUCLEIN expression in differentiated neurons with homozygous H1 or H2 <i>MAPT</i> haplotypes.....	44
3.4.1. Analysis of α -SYNUCLEIN expression on mRNA and protein level	44
3.4.2. α -SYNUCLEIN expression over time via immunocytochemistry.....	46
3.4.3. Genotyping of <i>SNCA</i> gene for disease conveying SNPs.....	47
3.5. Vulnerability of differentiated neurons with homozygous H1 or H2 <i>MAPT</i> haplotypes to external stressors	49
4. Discussion.....	52
4.1. Cell differentiation and characterization	52
4.2. TAU expression in differentiated <i>NGN2</i> _smNPCs.....	53
4.2.1. TAU expression over the 30-day differentiation period.....	53
4.2.2. TAU expression in homozygous H1 and H2 neurons.....	54
4.3. α -SYNUCLEIN expression in homozygous H1 and H2 neurons.....	55
4.4. Vulnerability of homozygous H1 and H2 neurons to external stressors.....	56
5. Conclusion.....	58
List of publications	59
Declaration of contribution.....	60
References.....	61

List of Figures

Figure 1.1: Histopathological features of tauopathy subtypes.	3
Figure 1.2: Mutations in the <i>MAPT</i> gene.	4
Figure 1.3: The human <i>MAPT</i> gene and the isoforms of the TAU protein.	5
Figure 1.4: Structure and function of TAU.	6
Figure 1.5: Structure of the <i>MAPT</i> haplotypes H1 and H2.	9
Figure 1.6: <i>MAPT</i> gene with haplotype-defining SNPs.	10
Figure 1.7: Characteristic α -SYNUCLEIN inclusions in different synucleinopathies.	12
Figure 2.1: Overview of the differentiation protocol employed in this thesis.	20
Figure 2.2: Scheme of the procedure to convert induced pluripotent stem cells (iPSCs) into small molecule neural precursor cells (smNPC).	21
Figure 2.3: Experimental timeline.	22
Figure 3.1: Conversion of iPSC lines into <i>NGN2</i> _smNPCs.	29
Figure 3.2: Evaluation of cell survival at day 30 and day 60 of differentiation.	30
Figure 3.3: Expression of <i>SOX2</i> and β -3-TUBULIN over a differentiation period of 30 days.	31
Figure 3.4 Quantification of cell types over a differentiation period of 30 days.	32
Figure 3.5: Immunostaining at different time points of differentiation with neural progenitor marker NESTIN and dendritic marker MAP2.	33
Figure 3.6: Immunostaining at different time points of differentiation with glial marker GFAP.	34
Figure 3.7: Immunostaining for the neurotransmitter GABA.	35
Figure 3.8: Immunostaining for the cortical marker BRN2 and neuronal marker TAU at day 30 of differentiation.	36
Figure 3.9: Immunostaining for additional neuronal markers.	37
Figure 3.10: Immunofluorescent and qPCR analysis of TAU and its isoforms.	39
Figure 3.11: Western blot analysis with total TAU, 3R and 4R TAU antibodies over 30 days.	41
Figure 3.12: Western blots for phosphorylated and conformationally changed TAU.	43
Figure 3.13: Analysis of α -SYNUCLEIN expression over time on protein and mRNA levels.	45
Figure 3.14: Immunostaining of α -SYNUCLEIN expression over 30 days.	47
Figure 3.15: Treatment of cells with external stressors.	50

List of Tables

Table 1.1: Studies identifying <i>MAPT</i> haplotype as risk factor for neurodegenerative diseases.....	10
Table 1.2: Sub-haplotypes-defining SNPs in <i>MAPT</i> gene	11
Table 2.1: Purchased cell lines	18
Table 2.2: Antibodies used in immunocytochemistry	23
Table 2.3: Primers used for qPCR	24
Table 2.4: Antibodies used for Western blot	26
Table 3.1: Genotyping of H1 cell lines for H1 sub-haplotypes-defining SNPs.....	44
Table 3.2: Location of SNPs on <i>SNCA</i> gene.....	48
Table 3.3: Genotypes of cell lines for certain SNPs in <i>SNCA</i> gene.....	48
Table 3.4: Sequence of <i>Rep1</i> microsatellite for the different cell lines	49

List of Abbreviations

AA	Ascorbic acid	MSA	Multiple system atrophy
AD	Alzheimer's disease	MTT	3-(4,5-dimethylthiazol-2-yl)- 2,5 diphenyl tetrazolium bromide
AGD	Argyrophilic grain disease	NAC	Non-amyloid component
ALS-PD	Amyotrophic lateral sclerosis and/or parkinsonism with dementia	NFT	Neurofibrillary tangle
ANOVA	Analysis of variance	<i>NGN2</i>	<i>NEUROGENIN2</i>
AO	Antioxidant	nPPS	Novel pluripotency score
ARE	Antioxidant response element	PART	Primary age-related tauopathies
BSA	Bovine serum albumin	PBS	Phosphate-buffered saline
CBD	Corticobasal degeneration	PBS-T	PBS containing 0.2% Tween®
cDNA	Complementary DNA	PD	Parkinson's disease
CHIR	CHIR99021	PHF	Paired helical filament
CTE	Chronic traumatic encephalopathy	PiD	Pick's disease
Ctx	Cortex	PMA	Purmorphamine
DLB	Dementia with Lewy bodies	PPS	Pluripotency score
DMSO	Dimethyl sulfoxide	PSP	Progressive supranuclear palsy
DOR	Dorsomorphin	p-TAU	Phosphorylated TAU
EB	Embryoid body	PVDF	Polyvinylidene fluoride
ECACC	European Collection of Authenticated Cell Cultures	qPCR	Semi-quantitative real-time PCR
FTDP-17	Frontotemporal dementia with parkinsonism linked to chromosome 17	ROS	Reactive oxygen species
GGT	Globular glial tauopathies	SB	SB431542
GWA	Genome-wide association	SEM	Standard error of the mean
hESC	Human embryoid stem cell	smNPC	Small molecule neural precursor cell
HipSci	Human Induced Pluripotent Stem Cell Initiative	SN	Substantia nigra
HRP	Horseradish peroxidase	SNP	Single nucleotide polymorphism
HTS	High-throughput screening	TBS	Tris-buffered saline
iPSC	Induced pluripotent stem cell	TBS-T	TBS containing 0.05% Tween®
KSR	Knockout serum replacement	TDP-43	Transactivation response DNA binding protein 43
LB	Lewy body	Thia	Thiazovivin
LBD	Lewy body disorder	UTC	Untreated control
MAPT	Microtubule-associated protein TAU	vaFTD	Variant frontotemporal dementia
MBD	Microtubule-binding domain		
M-PER™	Mammalian Protein Extraction Reagent		

1. Introduction and theoretical background

The hallmarks of neurodegenerative diseases are deposits of pathologically altered proteins in the human brain, the progressive loss of cell function and, eventually, neuronal cell death. The broad range of neurodegenerative diseases can be classified via their clinical symptoms (such as movement disorder and cognitive decline), the affected brain regions (e.g. frontotemporal degeneration) or the main protein that is found in the brain depositions (such as TAU) (Kovacs and Budka, 2010). Since clinical appearance rarely occurs in pure syndromes but rather as a mixture of different symptoms, the final diagnosis is only possible when histological and neuropathological evaluation of brain inclusions is carried out at autopsy (Dugger and Dickson, 2017). The most common proteins involved in neurodegenerative disorders are AMYLOID- β , TAU, α -SYNUCLEIN and transactivation response DNA-binding protein 43 (TDP-43). The diseases that these proteins are associated with are accordingly being classified as amyloidosis, tauopathies, synucleinopathies and TDP-43 proteinopathies, respectively (Kovacs et al., 2010).

Although the proteins mentioned above differ in their function, size and structure, they share the principal mechanism of protein aggregation. First, abnormal, misfolded, or overexpressed protein monomers form small oligomers which can aggregate further into bigger oligomers until protofibrils are formed. Upon reaching a certain size, mature fibrils can form larger filaments primarily with a β -sheet structure (Lee et al., 2007). The resulting deposits are categorized as plaques, tangles or threads. *In vitro* and *in vivo* models strongly suggest that protein pathology can be propagated from cell to cell throughout connected brain regions (Brettschneider et al., 2015). Although different proteins accumulate in the different diseases, biochemical processes contributing to neuronal damage and cell death are similar in all known proteinopathies to date. These processes include oxidative stress, impaired mitochondrial function, dysregulation of neuroinflammation, proteotoxic stress and impaired ubiquitin-proteasomal and autophagosomal/lysosomal systems (Jellinger, 2010).

In the following, the theoretical background of tauopathies and synucleinopathies as well as the proteins being involved are described in more detail. Additionally, the role of induced pluripotent stem cells as model systems in the research field of neurodegenerative diseases, specifically tauopathies, is illuminated.

1.1. Tauopathies

1.1.1. Classification of tauopathies

Tauopathies are characterized by aggregates of the TAU protein in the brain. Tauopathies can be divided into primary and secondary tauopathies depending on whether TAU is seen as the main driving force of the disease or only as a minor player (Spillantini and Goedert, 2013). Primary tauopathies are for example progressive supranuclear palsy and corticobasal degeneration. The most commonly known secondary tauopathy is Alzheimer's disease (the primary protein here appears to be AMYLOID- β) (Selkoe and Hardy, 2016).

Tauopathies can be further classified according to which TAU isoform, created via alternative splicing, is predominantly found in brain deposits (Goedert and Jakes, 1990). Inclusion or exclusion of exon 10 results in TAU isoforms with either three (3R TAU) or four (4R TAU) microtubule-binding repeats (Goedert et al., 1989b). Thus, tauopathies can be divided into 3R, 4R and 3R/4R tauopathies, depending on the ratio of TAU isoforms present in the brain inclusions (Rösler et al., 2019; Sergeant et al., 2005). Another classification of primary tauopathies are the familial forms of frontotemporal dementia with parkinsonism linked to chromosome 17. Details on the different tauopathies are described below.

3R tauopathies

The prototypical 3R tauopathy is Pick's disease (PiD), with characteristic histological features of so-called "Pick bodies" (Figure 1.1I). These spherical inclusions mainly consisting of 3R TAU are found in the cytoplasm of neurons in the limbic and neocortical regions (Dickson, 1998). Furthermore, 3R TAU positive inclusions can also occur in glia cells (Figure 1.1J). Clinically, PiD often presents with behavioral variant frontotemporal dementia (bvFTD) but can also cause primary progressive aphasia and corticobasal syndrome (Kovacs et al., 2013).

4R tauopathies

Progressive supranuclear palsy (PSP) is considered an atypical Parkinson syndrome displaying vertical gaze palsy and early falls/postural instability (Steele et al., 1964). On a histological level, PSP is characterized by globose 4R TAU inclusions in neurons, oligodendrocytic "coiled bodies" and "tufted astrocytes" (Figure 1.1A and B) (Dickson et al., 2010; Williams and Lees, 2009). Although corticobasal degeneration (CBD) shares some neuropathological features with PSP, like 4R TAU positive neuronal lesions and "coiled bodies", they differ for example in their astroglia pathology. While PSP displays tufted astrocytes, CBD exhibits astrocytic plaques (Figure 1.1C). Another characteristic of CBD are ballooned cortical neurons (Figure 1.1D) (Dickson et al., 2002). Clinical manifestations are, among others, progressive asymmetrical apraxia and often Parkinson symptoms. Additional 4R tauopathies

are argyrophilic grain disease (AGD) and globular glial tauopathies (GGT) (Ahmed et al., 2013; Tolnay and Clavaguera, 2004).

3R/4R tauopathies

In primary age-related tauopathies (PART), intracellular neurofibrillary tangles (NFTs) composed of 3R and 4R TAU in equal ratios have been observed mainly in the medial temporal lobe (Figure 1.1K) (Crary et al., 2014). Another 3R/4R tauopathy is chronic traumatic encephalopathy (CTE) which manifests after chronic repetitive head injuries and displays NFT pathology in the superficial cortical layer that spreads to the medial temporal lobe in later stages (McKee et al., 2009; McKee et al., 2013). Next to primary tauopathies, there are some disorders with a secondary mixed 3R/4R TAU pathology. A histological hallmark in Alzheimer's disease (AD), for example, are NFTs that occur next to primary extracellular AMYLOID- β plaque pathology (Goedert et al., 2006). Another example is the geographically isolated secondary tauopathy in the pacific region that clinically presents as amyotrophic lateral sclerosis and/or parkinsonism with dementia (ALS-PDC). Here, the 3R/4R pathology occurs together with TDP-43 accumulation in the low motor neurons (Figure 1.1L) (Steele and McGeer, 2008).

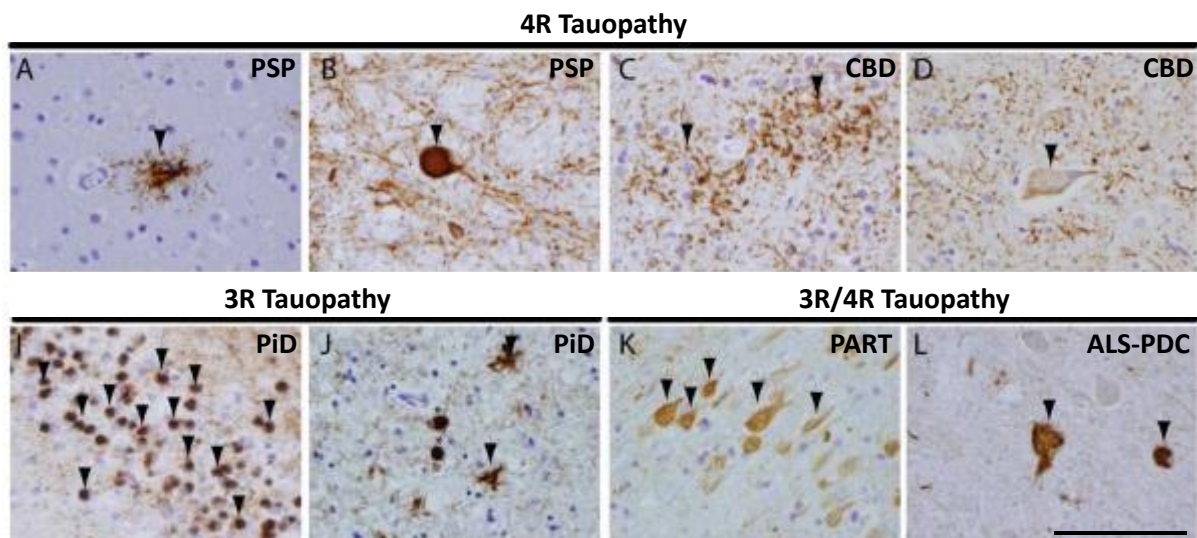


Figure 1.1: Histopathological features of tauopathy subtypes. Arrows indicate characteristic immunoreactive TAU inclusions for 4R (A-D), 3R (I-J) and 3R/4R (K-L) tauopathies. (A) shows a typical tufted astrocyte in the mid-frontal cortex in progressive supranuclear palsy (PSP) were as (B) displays a globose neuronal TAU tangle in the midbrain. For corticobasal degeneration (CBD), astrocytic plaques (C) and ballooned neurons (D) are characteristic. (I) shows typical spherical “Pick bodies” in the 3R tauopathy Pick’s disease (PiD) additional to the glial TAU inclusions visible in (J). (K) shows characteristic neurofibrillary tangles which can be found in primary age-related tauopathies (PART). In a rare form of amyotrophic lateral sclerosis and parkinsonism with dementia (ALS-PDC), TAU tangles are present in the spinal cord (L). scale bar=100 μ m [adapted from (Irwin, 2016)].

Frontotemporal dementia with parkinsonism linked to chromosome 17

In 1998, the first mutations in the *MAPT* gene coding for the TAU protein (located on chromosome 17) were described to cause frontotemporal dementia with parkinsonism (Hutton et al., 1998; Poorkaj et al., 1998; Spillantini et al., 1998). Since then, over 50 mutations have been associated with frontotemporal dementia with parkinsonism linked to chromosome 17 (FTDP-17) (Ghetti et al., 2015). These mutations are located in the exons as well as in the introns and can be classified as missense mutations that alter the TAU protein sequence, or splicing mutations which influence the alternative splicing of exon 10 and therefore change the isoform ratio of 3R and 4R TAU (Figure 1.2) (Goedert, 2005). Studies have shown that mutant forms of TAU can have a reduced binding affinity to microtubules resulting in decreased microtubule stability and increased amounts of free, unbound TAU (e.g. V337M, R406W and Δ 152T in Figure 1.2) (Hasegawa et al., 1998; Hong et al., 1998). Additionally, a number of missense mutations enhance the ability of TAU to aggregate, thus promoting TAU pathology such as P301L and P301S (Goedert et al., 1999; Nacharaju et al., 1999).

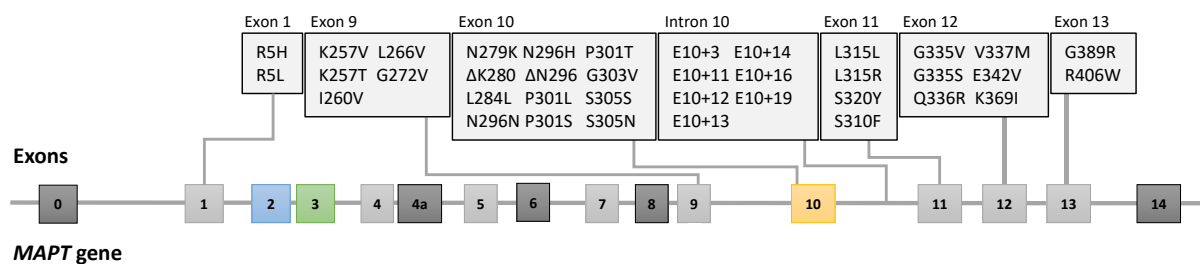


Figure 1.2: Mutations in the *MAPT* gene. Missense and silent mutations are mostly found in the exons 1, 9, 10, 11, 12 and 13 and in intron 10. Colored exons (blue, green and yellow) are subject to alternative splicing [modified based on (Brunden et al., 2009)].

Most mutations that influence the alternative splicing of *TAU* mRNA are either intronic mutations in intron 10 or missense mutations in exon 10 (N279K, L284L, Δ N296, N296N, N296H, S305N and S305S) (D'Souza et al., 1999; Hutton et al., 1998). These mutations mainly alter the splicing process by disrupting an inhibitory mRNA stem loop structure at the end of exon 10 and the beginning of the following intron. This causes an increased inclusion of exon 10 and thus higher levels of the 4R TAU isoform (Liu and Gong, 2008). Additionally, there are also some mutations that decrease the inclusion of exon 10, leading to higher 3R TAU levels (e.g. Δ K280) (D'Souza and Schellenberg, 2005). Although the dominant clinical manifestation of FTDP-17 is frontotemporal dementia, the mutations can cause a variety of clinical phenotypes including PSP, CBD, PiD and AD disorders (Guo et al., 2017).

1.1.2. TAU protein – structure, function and role in neurodegenerative diseases

The TAU protein was firstly isolated and described in 1975 as a microtubule assembly factor (Weingarten et al., 1975). This microtubule-associated protein TAU (*MAPT*) is encoded by the *MAPT* gene which is located on chromosome 17q21 (Neve et al., 1986).

Since TAU is a microtubule-associated protein it is mainly found in the axons of neurons where it binds and stabilizes microtubules (Trojanowski et al., 1989). To a lesser extent, TAU is also present in somatodendritic compartments (Tashiro et al., 1997). Additionally, it can also be found in oligodendrocytes and astrocytes (Klein et al., 2002) and even occurs in kidney and lung tissue (Gu et al., 1996).

Structure and function

The *MAPT* gene consists of 16 exons. By alternative splicing of the mRNA, six main TAU isoforms are created (Figure 1.3A) (Goedert and Jakes, 1990). Exons 2 and 3 code for a 29-amino acid long sequence near the amino-terminal end of the protein. Depending if none (0N), one (1N) or two (2N) of these N-terminal inserts are included, the respective TAU isoforms (0N, 1N or 2N) are translated (Goedert et al., 1989a). Exons 9, 10, 11 and 12 harbor microtubule-binding domains (MBDs) which are four highly conserved and imperfect repeats that are 30 to 31 amino acids long.

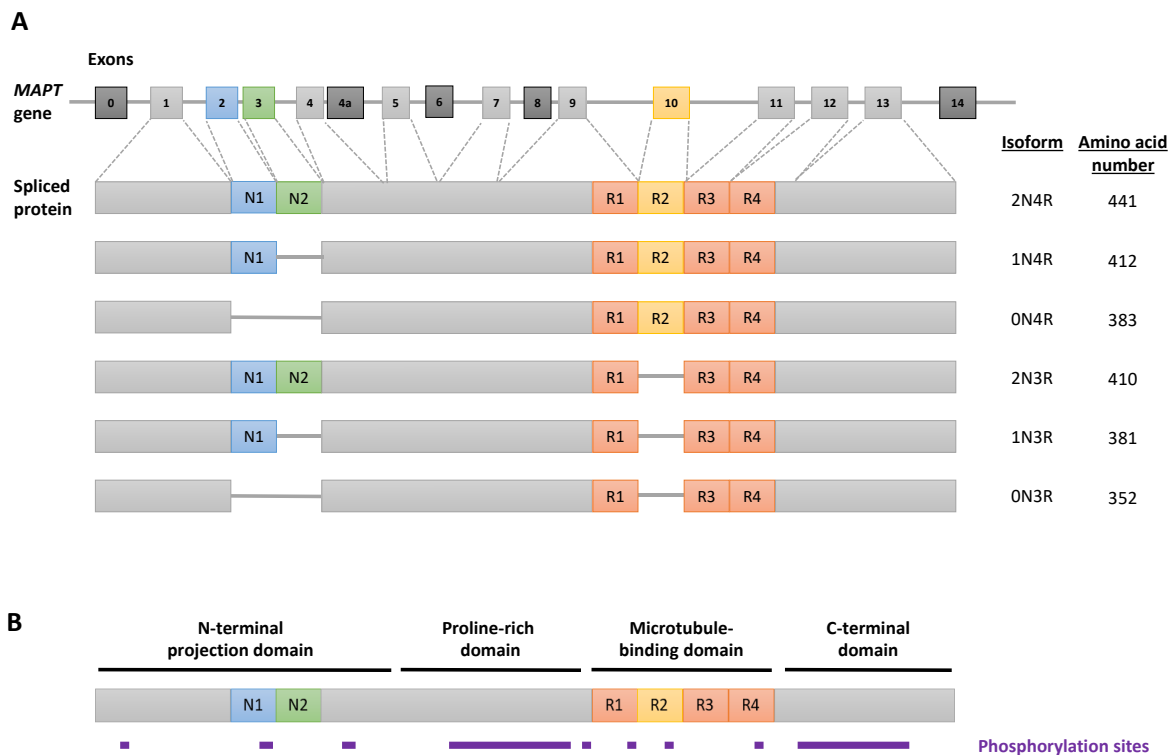


Figure 1.3: The human *MAPT* gene and the isoforms of the TAU protein. (A) The *MAPT* gene consists of 16 exons, of which eight are constitutively expressed in the TAU protein (Exon 1, 4, 5, 7, 9, 11, 12 and 13). Exons 0 and 14 are part of the 5' and 3' untranslated region, respectively, while the exons 4a, 6 and 8 are only transcribed in the peripheral nervous system. Exons 2 and 3 are alternatively spliced to create three TAU isoforms that contain either no, one or two N-terminal repeats (0N, 1N, or 2N). Inclusion or exclusion of exon 10 results in TAU isoforms with three or four repeat domains near the carboxyl-end (C-terminal) termed 3R or 4R TAU, thus resulting in a total of six TAU isoforms expressed in the adult human brain termed 0N3R, 1N3R, 2N3R, 0N4R, 1N4R and 2N4R. **(B)** The TAU protein can be divided into four different domains according to its biochemical properties. The N-terminal projection domain, the proline-rich domain, the microtubule-binding domain and the C-terminal tail. Phosphorylation is the predominant posttranslational modification with phosphorylation sites (purple) enriched in the flanking regions of the microtubule-binding domains [based on (Guo et al., 2017; Wang and Mandelkow, 2016)].

Alternative splicing of exon 10 creates TAU isoforms with either 3 or 4 MBDs thus termed 3R or 4R TAU, respectively (Goedert et al., 1989b). In combination with the inclusion or exclusion of exon 2 and 3, the TAU protein displays six isoforms in adult neurons: 0N3R, 1N3R, 2N3R, 0N4R, 1N4R and 2N4R. The abundance of the different isoforms changes over human development. In the fetal brain only the 0N3R and thus the shortest isoform, is present, while in the adult brain the 3R and 4R forms are equally abundant. The majority of the TAU protein (57%) in the adult brain contains one N-terminal insert (1N3R and 1N4R), whereas 37% contain 0N variants (0N3R, 0N4R). The 2N isoforms (2N3R and 2N4R) are underrepresented, making up only 9% of the total TAU protein (Goedert and Jakes, 1990).

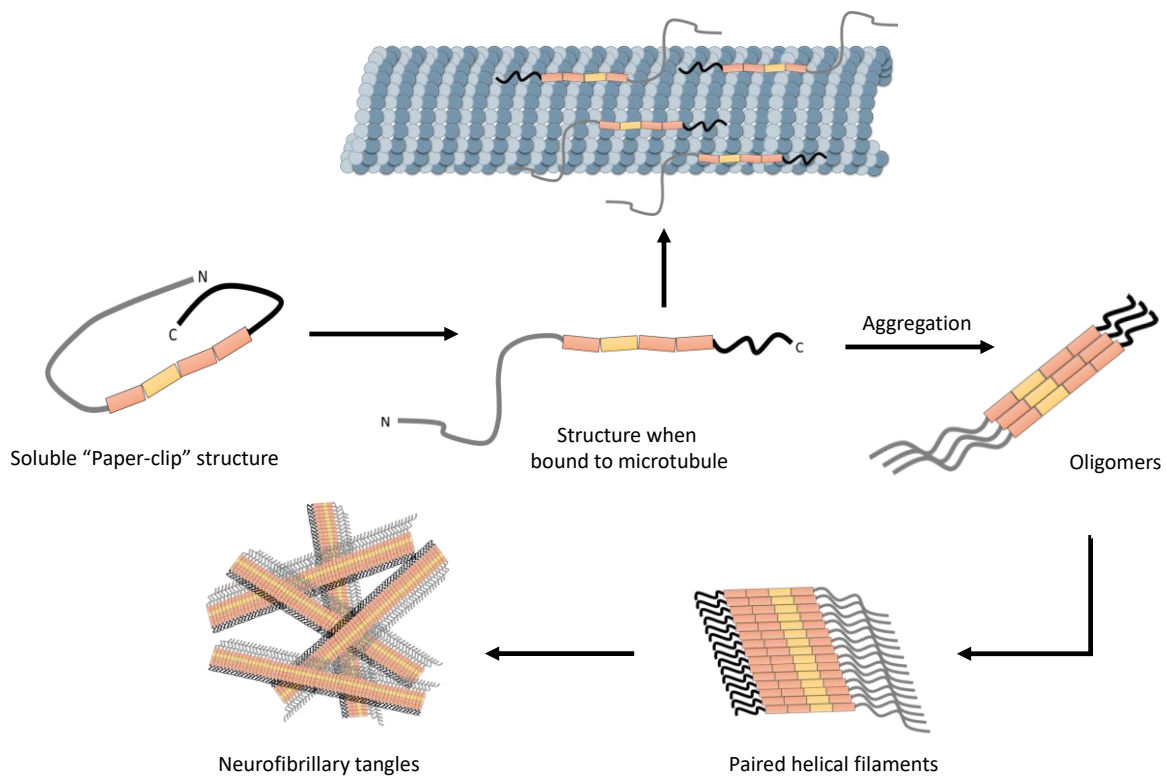


Figure 1.4: Structure and function of TAU. TAU is a water-soluble protein with a small amount of secondary structure that forms a paper-clip-like structure when unbound in the cytoplasm. When bound to a microtubule, this structure changes and the N-terminus projects away from the microtubule while the microtubule binding domains (MBD, displayed in orange and yellow) and the C-terminus are bound. The MBDs form the core of the fibrils when TAU starts to aggregate. At first, only small oligomers form, which grow to paired helical filaments (PHF). PHF in turn ultimately deposit as neurofibrillary tangles in the brain and are the characteristic pathology of tauopathies [based on (Guo et al., 2017)].

TAU is a highly water-soluble protein due to its low proportion of hydrophobic residues (Jeganathan et al., 2008). Divided by biochemical property, TAU comprises four structurally different domains (Figure 1.3B) (Mandelkow et al., 1996):

- (1) the acidic N-terminal projection domain (amino acids 1-150),
- (2) the proline-rich domain (amino acids 151-243),
- (3) the MBDs (244-369) and
- (4) the C-terminal tail (370-441).

TAU is a natively unfolded protein with a small amount of secondary structure with few short and transient elements such as β -sheets in the microtubule-binding domains (Mukrasch et al., 2009). These β -sheet structures have been described as the main drivers of the abnormal self-assembly (aggregation) of TAU. In diseased brains when TAU aggregates into paired helical filaments, the MBDs build the core of the structure (Figure 1.4) (Crowther et al., 1989). In healthy brains, free TAU in the cytoplasm has the tendency to form a paper-clip-like structure in which the N- and C-terminal ends fold towards the repeat domains. This loose association of the protein ends is broken when TAU binds to a microtubule and the N-terminus projects away from the microtubules (Figure 1.4) (Jeganathan et al., 2006).

With 85 possible phosphorylation sites (45 serine, 35 threonine and five tyrosine residues available), phosphorylation is the major posttranslational modification of the TAU protein and is an important regulator of its physiological function (Hanger et al., 2009). The phosphorylation sites are especially enriched in the flanking regions of the MBDs (Figure 1.3B). Phosphorylation of these sites and of serine residues directly located in the repeat domains reduces the binding affinity of TAU for microtubules (Drewes et al., 1995). This mechanism regulates TAU association with and dissociation from microtubules and thus microtubule stability (Sengupta et al., 1998). Abnormal phosphorylation or hyperphosphorylation of TAU can therefore interfere with its physiological function (Hoover et al., 2010). In AD patients and patients with other tauopathies, abnormal hyperphosphorylation is observed especially in paired helical filaments (PHF) (Grundke-Iqbal et al., 1986) and in accordance with these findings, hyperphosphorylated TAU is known to have a higher self-aggregation propensity (Köpke et al., 1993). Although phosphorylation is the most common posttranslational modification, TAU is also known to be acetylated (Irwin et al., 2012), methylated (Funk et al., 2014), glycosylated (Ledesma et al., 1994), polyaminated, glycosylated (Wang et al., 1996), nitrated (Reyes et al., 2008) or ubiquitinated (Cripps et al., 2006). Even SUMOylation (Dorval and Fraser, 2006), isomerization (Miyasaka et al., 2005) and oxidation (Landino et al., 2004) have been described. All these modifications can be present under both physiological and pathological conditions. Acetylation at specific lysine sides for example has been found in post-mortem brains of AD, PiD, FTLD-17 and PSP patients (Irwin et al., 2013; Min et al., 2015). How this and other posttranslational modifications may influence or contribute to disease-causing mechanisms remains to be investigated.

In addition to regulating microtubule dynamics (Janning et al., 2014), other functions of TAU have been proposed over the years. TAU has been described to regulate axonal transport by interacting with motor proteins like dynein and kinesin (Magnani et al., 2007; Stamer et al., 2002). Apart from its localization and function in axons, TAU is present in small amounts in the dendrites of neurites. Here, it has been suggested that TAU is involved in synaptic plasticity and localization of postsynaptic components (Ittner et al., 2010; Mondragón-Rodríguez et al., 2012). TAU can also regulate signaling

pathways by acting as a scaffolding protein for kinases (Lee et al., 1998). TAU is also found in the nucleus, where it is able to bind to DNA and RNA and may play a role in protecting genomic DNA, cytoplasmic RNA and nuclear RNA from cellular stress (e.g. hyperthermic and oxidative stress) (Sultan et al., 2011; Violet et al., 2014).

Role in neurodegenerative diseases

The main characteristic of tauopathies is TAU aggregation. Monomeric TAU is able to form β -sheet structures through interaction of their MBDs (von Bergen et al., 2000). Like other amyloid-forming proteins, TAU fibrilization follows a nucleation/elongation mechanism with nucleation as the rate-limiting step (Lee et al., 2007). Under physiological conditions, nucleation does not occur spontaneously (Kuret et al., 2005) but can be induced with anionic compounds (such as heparin), post-translational modifications that reduce the overall positive charge (such as hyperphosphorylation) and preformed seeds (such as seeds from patients' brains) (Alonso et al., 1996; Goedert et al., 1996; Peeraer et al., 2015). In the elongation phase, TAU oligomers form small primary fibrils which grow into larger PHF that can be found in NFT (Figure 1.4) (Barghorn and Mandelkow, 2002).

How TAU pathology influences cell toxicity and neuronal loss is still under debate. One possible contribution to neurotoxicity can be a toxic loss of function. In this scenario due to hyperphosphorylation and thus detachment from the microtubule, soluble TAU aggregates and is no longer able to fulfill its physiological function (Zhang et al., 2005). Experiments in mice have shown that some TAU functions can be compensated for by other microtubule-associated proteins such as MAP1A (Lei et al., 2014). Therefore, toxic loss of function might be conferred by the interruption of more recently described functions of TAU such as axonal transport, synaptic plasticity and DNA protection (see section above) (Wang and Mandelkow, 2016). In the past, the dominant opinion was that NTF would exert a toxic gain of function, since NFT distribution in the brain correlates with severity of clinical symptoms in tauopathies (Wang and Mandelkow, 2016). Recent findings, however, suggest that NFTs themselves are rather inert and sometimes their formation is even considered a protective mechanism (Cowan and Mudher, 2013). The focus for toxic TAU species is now shifted towards soluble oligomers which are suggested to contribute to loss of membrane function, mitochondrial and synaptic dysfunction and impairment of axonal transport (Flach et al., 2012; Lasagna-Reeves et al., 2011; Morfini et al., 2009). Although increased TAU oligomer levels could be detected in AD and PSP patients' brains, the exact role oligomers play in neurotoxicity remains under debate (Gerson et al., 2014).

1.1.3. The *MAPT* gene and its haplotypes

In 1997 a polymorphic dinucleotide marker between exon 9 and 10 of the *MAPT* gene coding for TAU was associated by Conrad et al. with the tauopathy PSP (Conrad et al., 1997). Baker et al. confirmed these findings two years later but described additional single nucleotide polymorphisms (SNP) located in the *MAPT* gene. Further analysis revealed a complete linkage disequilibrium of these polymorphisms, thus defining two extended haplotypes (the H1 and H2 haplotypes) spanning the whole *MAPT* gene (Baker et al., 1999). In the following years, the *MAPT* haplotype was, step-by-step, extended beyond the *TAU* gene (Ezquerro et al., 1999; Pastor et al., 2002). Pittman et al. defined the outer edges of the linkage disequilibrium in 2004 thus identifying an approximately 2 Mb long haplotype region on chromosome 17q21 including several other genes aside from *MAPT* (Figure 1.5) (Pittman et al., 2004). One characteristic of the H2 haplotype is a nearly 1 Mb long inversion, which includes the *MAPT* gene.

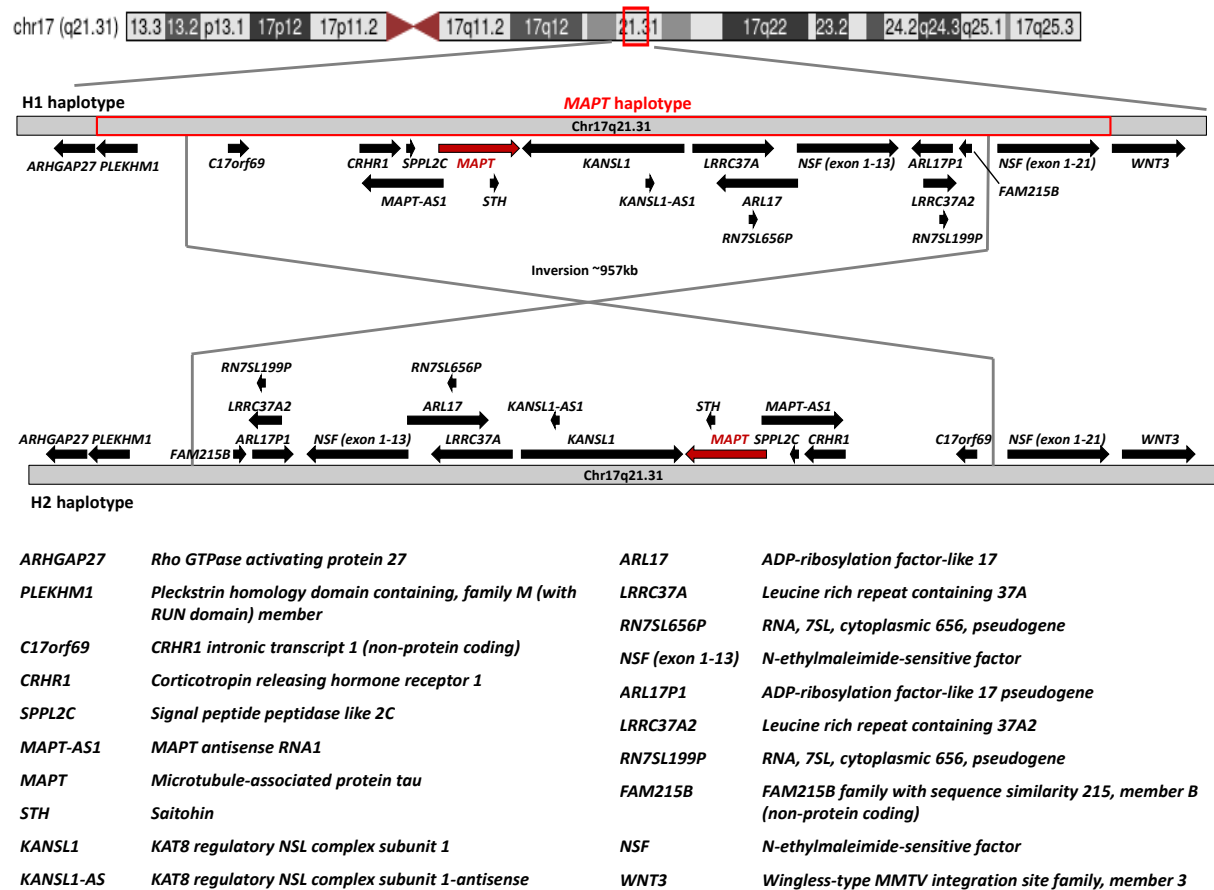


Figure 1.5: Structure of the *MAPT* haplotypes H1 and H2. The *MAPT* haplotype is located on chromosome 17q21.31. It spans a region of approximately 2 Mb with multiple genes (red box) including the *MAPT* gene (red arrow). The H2 haplotype is defined by a nearly 1 Mb big inversion polymorphism (grey lines). Black arrows indicate location of genes on the plus (arrows point to the right) or minus strand (arrows point to the left). The lengths of the arrows indicate the approximate lengths of genes. Chromosome 17 illustration and gene location information was taken from [http://genome-euro.ucsc.edu/index.html], [based on (Boettger et al., 2012; Bowles et al., 2019; Caffrey and Wade-Martins, 2007)].

Interestingly, the frequency with which the haplotypes occur in populations all over the world differs strongly. The H2 haplotype is largely confined to European cohorts. Here, it is present in a frequency of about 20%. In African and Asian populations, the H2 haplotype is almost absent (Stefansson et al., 2005).

Since its first discovery by Conrad et al. (Conrad et al., 1997), the H1 haplotype has been repeatedly associated with a higher risk of developing PSP in Caucasian cohorts. Over the years, this genetic association was also found for CBD and AD (Kouri et al., 2015; Myers et al., 2005). Surprisingly, genome-wide association (GWA) studies also identified the *MAPT* haplotype as a major risk factor for the classic synucleinopathy Parkinson's disease (PD) (Table 1.1) (Pascale et al., 2016). Additionally, Vuono et al. reported a connection between the rate of cognitive decline and *MAPT* haplotype in Huntington's disease (Vuono et al., 2015).

Table 1.1: Studies identifying *MAPT* haplotype as risk factor for neurodegenerative diseases

Disease	Odds ratio	P-value	Number of study subjects	Source
PSP	5.5	1.5×10^{-116}	4,611	(Höglinger et al., 2011)
CBD	3.7	1.4×10^{-12}	3,463	(Kouri et al., 2015)
AD	1.5	9.0×10^{-3}	612	(Myers et al., 2005)
PD	1.7	2.0×10^{-3}	378	(Pascale et al., 2016)

After defining the boundaries of the *MAPT* haplotype, Pittman et al. further fine-mapped the H1 haplotype (Pittman et al., 2005). By identifying five SNPs that only occur in the H1 haplotype, they proposed a classification of H1 sub-haplotypes (Figure 1.6 and Table 1.2).

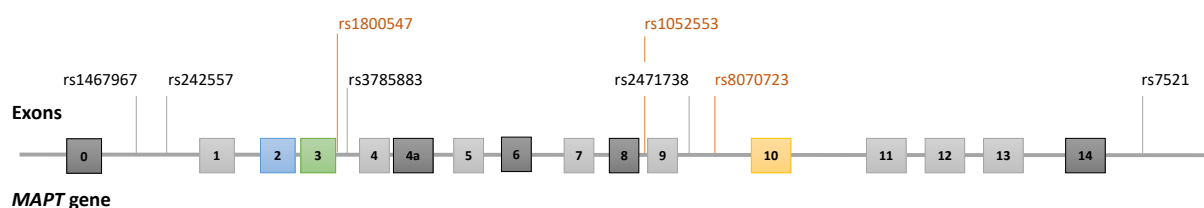


Figure 1.6: *MAPT* gene with haplotype-defining SNPs. 13 haplotype-defining SNPs have been described, most of them in the intronic regions of the *MAPT* gene. Three of those SNPs have been used to identify the *MAPT* genotype of cell lines purchased for this project (orange). Five SNPs that divide the H1 haplotype into sub-haplotypes are indicated in black. [Based on (Pittman et al., 2005; Wray and Hardy, 2010; Zabetian et al., 2007)].

Table 1.2: Sub-haplotypes-defining SNPs in *MAPT* gene

Sub-haplotypes	rs1467967	rs242557	rs3785883	rs2471738	rs8070723	rs7521
H1b	G/G	G/G	G/G	C/C	A/A	A/A
H1c	A/A	A/A	G/G	T/T	A/A	G/G
H1d	A/A	A/A	G/G	C/C	A/A	A/A
H1e	A/A	G/G	G/G	C/C	A/A	A/A

In what manner these sub-haplotypes may influence the H1 haplotype as a risk factor remains unclear. Some studies only link a sub-haplotype (e.g. the H1c haplotype) to a disease rather than the whole H1 locus (Ezquerro et al., 2011; Majounie et al., 2013; Zabetian et al., 2007; Zhang et al., 2017). By what mechanism the *MAPT* haplotype influences the risk for developing a sporadic neurodegenerative disease is still under investigation. Although the haplotype affects several genes, the main focus lies on the *MAPT* gene coding for the TAU protein, which is known to play a crucial role in neurodegenerative disorders (see also Chapter 1.1.2). None of the haplotype-defining SNPs described above alter the amino acid sequence of TAU. A mutated TAU is therefore excluded (Kwok et al., 2004). Since the SNPs are mainly found in intronic regions, they could influence the overall transcription efficiency and thus increase or decrease *TAU* mRNA levels over time which could lead to a change in protein levels. Another possibility could be a shift in the alternative splicing of the mRNA resulting in altered levels of TAU isoforms (Pittman et al., 2006). In fact, different studies have shown both modes of action: change in overall TAU levels or individual TAU isoform levels. These studies, however, are unclear as to whether both events occur simultaneously or only one exclusively. Using a Luciferase reporter assay in neuroblastoma cell lines, two groups reported a higher transcription efficiency from the H1 haplotype due to SNPs in the promotor region (Kwok et al., 2004; Myers et al., 2007). A higher overall *MAPT* expression on the mRNA level in H1 groups has also been shown in human brains (de Jong et al., 2012; Valenca et al., 2016). Other studies have not found a general increase in *MAPT* transcript in the investigated brain regions (Caffrey et al., 2006; Trabzuni et al., 2012). Interestingly, Myer et al. reported a higher total *MAPT* expression only for the sub-haplotype H1c as compared to all other genotypes (Myers et al., 2007). When investigating the different splice variants of the *MAPT* transcript, several groups found differences in the amount of certain *MAPT* isoforms between the haplotype groups. In human brains and neuroblastoma cell lines the H2 haplotype was associated with a higher level of exon 3 inclusion in *MAPT* mRNA resulting in more 2N isoforms of *TAU* (Caffrey et al., 2008; Trabzuni et al., 2012). The H1 haplotype on the other hand was connected to increased levels of transcripts containing exon 10 (i.e. 4R *TAU* isoforms) (Caffrey et al., 2006; Majounie et al., 2013). These studies argue that the H1 haplotype could convey a risk for neurodegeneration by (1) either increasing the amount of TAU protein in the brain over years, thus increasing the chances that TAU reaches a

threshold level for aggregation or (2) the level of 4R TAU isoforms (which are known to be more prone to aggregation) is increased in H1 carriers (Zhong et al., 2012). Correspondingly, the reported increase of 2N TAU isoforms for the H2 haplotype might lower disease risk since the addition of the second N-terminal insert decreases the aggregation propensity of TAU (especially in combination with a 3R background) (Zhong et al., 2012). All in all, the evidence suggests differential *MAPT* expression on an mRNA level between H1 and H2 carriers, although different studies offer conflicting results.

1.2. Synucleinopathies

1.2.1. Classification of synucleinopathies

Apart from tauopathies, a second major class of neurodegenerative diseases are synucleinopathies. They are defined by inclusions in the brain mainly consisting of the protein α -SYNUCLEIN (Figure 1.7). These inclusions are referred to as Lewy bodies (LBs). Depending on the type of aggregate and the location in the brain, synucleinopathies can be divided into two major subgroups: (1) Lewy body disorders (LBD) and (2) multiple system atrophy (MSA). The first category includes PD, PD with dementia and dementia with Lewy bodies (DLB). Here LBs are mainly found in the neuronal cytoplasm and filamentous α -SYNUCLEIN aggregates are additionally present in the neurites (“Lewy neurites”) (Spillantini et al., 1997). LBDs can present with clinical features such as dementia, parkinsonism and autonomic dysfunctions as well as sleep disorders and psychiatric features. In contrast, protein inclusions present in MSA are located in glia cells, mostly in oligodendrocytes and are called glial cytoplasmic inclusions (Lantos, 1998). MSA can be further divided into two clinical subtypes: (1) The parkinsonism-dominant MSA-P and (2) the cerebellar symptom-predominant MSA-C. They mainly differ in clinical symptoms and affected brain regions (striatonigral in MSA-P versus olivopontocerebellar degeneration in MSA-C) but have similar protein pathology (Fanciulli and Wenning, 2015; Jellinger, 2014).

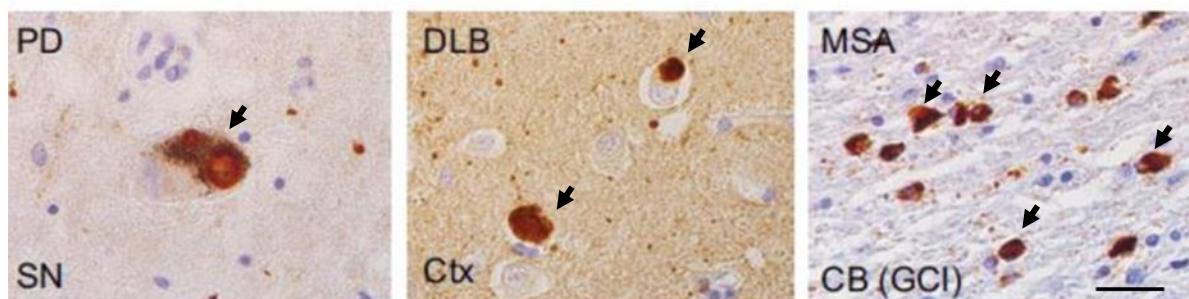


Figure 1.7: Characteristic α -SYNUCLEIN inclusions in different synucleinopathies. The first two pictures show Lewy bodies (black arrows) in the substantia nigra (SN) of Parkinson’s disease (PD) patients and in the cortex (Ctx) of patients with dementia with Lewy body (DLB). The third picture shows glial cytoplasmic inclusion (GCI) (black arrows) in the cerebellum (CB) of multiple system atrophy (MSA) patients. Scale bar: 25 μ m [adapted from (Peng et al., 2018)].

1.2.2. α -SYNUCLEIN protein – structure, function and role in neurodegenerative diseases

α -SYNUCLEIN was first described in 1988 by Maroteaux et al. and named due to its localization to synapses and nuclei (Maroteaux et al., 1988). In 1997, α -SYNUCLEIN was associated with neurodegeneration when it was identified as a major component of LBs (Spillantini et al., 1997) and a PD-causing mutation in the α -SYNUCLEIN coding gene *SNCA* was discovered (Polymeropoulos et al., 1997).

α -SYNUCLEIN is a small 140 amino acid protein consisting of three functional domains (Uversky, 2003):

- (1) the N-terminal region with four imperfect KTKEGV motif repeats,
- (2) the non-amyloid component (NAC) domain and
- (3) the highly acidic and negatively charged C-terminal region.

α -SYNUCLEIN can be found in its soluble cytoplasmic form or bound to membranes with a high curvature such as vesicles (Fortin et al., 2004). Membrane binding is mainly conferred by the N-terminal domain which forms a α -helical secondary structure, while the C-terminal domain remains unstructured and acts as an interaction site for other proteins and as a site for posttranslational modifications (Eliezer et al., 2001). The highly hydrophobic NAC domain is the main contributor to the tendency of α -SYNUCLEIN towards aggregation (Giasson et al., 2001).

The full functions of α -SYNUCLEIN remain under debate. There is evidence for its involvement in synaptic vesicular regulation because of its interaction with vesicular membranes. α -SYNUCLEIN, however, has also been shown to interact with other organelles such as mitochondria, the endoplasmic reticulum and the Golgi apparatus (Colla et al., 2012; Nakamura et al., 2011).

Although the vast majority of synucleinopathies are sporadic, there are some mutations in the *SNCA* gene that directly contribute to the development of neurodegenerative diseases, such as the missense point mutations A30P and A53T that cause familial PD (Krüger et al., 1998; Polymeropoulos et al., 1997) and E64K in familial DLB (Zarranz et al., 2004). Additionally, duplications and triplications of the *SNCA* gene have been found to cause an increase in α -SYNUCLEIN expression that confers to a higher risk for LBDs (Chartier-Harlin et al., 2004; Hofer et al., 2005). Apart from mutations, SNPs in intronic and exonic regions of *SNCA* have been described to increase the risk for synucleinopathies (Campêlo and Silva, 2017; Fuchs et al., 2008). Interestingly a dinucleotide microsatellite, *Rep1*, near the 5'UTR promoter region has also been linked to an increased risk for PD, potentially by influencing α -SYNUCLEIN expression (Chiba-Falek and Nussbaum, 2001).

1.3. The interplay of TAU and α -SYNUCLEIN in neurodegenerative diseases

Although neurodegenerative diseases are classified first via their clinical manifestations and later via autopsy according to their neuropathology, there are overlaps between the disorders. These overlaps are especially common between tauopathies and synucleinopathies and occur in the clinical presentations as well as in protein pathology. For example, in addition to AMYLOID- β and TAU pathology, LBs are found at a higher frequency in sporadic AD brains than in controls (Arai et al., 2001; Hamilton, 2000). LBs are also found in some clinical cases of PSP where TAU and α -SYNUCLEIN have been reported to colocalize in some neurons (Mori et al., 2002). This colocalization can also be observed in LBs of patients with synucleinopathies like DLB. When DLB diagnosis overlapped with Alzheimer-type pathology, up to 40% of LBs were positive for both TAU and α -SYNUCLEIN (Iseki et al., 2003; Ishizawa et al., 2003). Additionally, NFT and LB pathologies often coexist in the same brain (Jellinger, 2011). Since both TAU and α -SYNUCLEIN are amyloid-forming proteins that undergo a similar fibrillization process in disease, their joined aggregation in a cell-free *in vitro* assay was studied (Giasson et al., 2003). It was shown that TAU and α -SYNUCLEIN can induce the aggregation of one another below threshold levels of self-fibrillization (Lee et al., 2004; Nonaka et al., 2010).

Additionally, genetic studies have revealed a relation between tauopathies and synucleinopathies. The *MAPT* H1 haplotype has been identified as the second major risk factor for PD (Lill et al., 2012; Pascale et al., 2016). Since the *MAPT* gene encodes TAU and not α -SYNUCLEIN, exactly how the H1 haplotype confers PD risk remains unclear.

1.4. Cell culture models for neurodegenerative diseases

1.4.1. iPSC-derived neuronal cell models

Over the last few years, a novel cell culture model has revolutionized neurobiological research. In 2006, Yamanaka and Takahashi discovered that the introduction of four embryonic transcription factors Oct3/4, Sox2, c-Myc and Klf4 into differentiated cells can reverse their differentiation status back to a pluripotent state (Löhle et al., 2012; Takahashi et al., 2007). These so called induced pluripotent stem cells (iPSCs) can then be differentiated into any other cell type (Wray, 2017). Since iPSCs are primarily generated from mature fibroblasts, they circumvent the ethical controversies of using human embryoid stem cells (hESCs) as a source for pluripotency and are especially valuable in the field of neurobiology where the access to primary human neurons is very limited (Chamberlain et al., 2008; Koechling et al., 2010; Schwarz and Schwarz, 2010). Several protocols have been established to differentiate iPSCs into neurons and other brain cells (Tao and Zhang, 2016). Neural fate induction can

be achieved via the commonly used dual SMAD¹ inhibition pathway method which was established by Chambers et al. and uses SMAD signaling inhibitors Noggin and SB431542 to induce neuroectodermal lineage fate (in later protocols recombinant Noggin is replaced by the small molecule dorsomorphin) (Chambers et al., 2009; Derynck et al., 1998; Reinhardt et al., 2013). Further differentiation into different neuronal subtypes is achieved by either inhibiting or inducing specific signaling pathways (Brafman and Willert, 2017; Hu et al., 2010; Kim et al., 2014; Kirkeby et al., 2012; Shi et al., 2012).

Although iPSC models are a great opportunity for high-throughput screening (HTS) in a biologically relevant human neuronal cell model, most of the established protocols for iPSC-derived neurons in practice lack the high reproducibility and simplicity that are mandatory for HTS. Existing protocols often require splitting during the differentiation process as well as an extensive differentiation time and result in a highly variable and heterogeneous neuronal culture (Volpato et al., 2018). In 2013, Reinhardt et al. established a protocol that involves the generation of small molecule neural precursor cells (smNPC) as an intermediate step in the differentiation process (Reinhardt et al., 2013). smNPCs have many advantages:

- (1) they can quickly and robustly be expanded to generate large numbers of cells,
- (2) they can be kept in culture for numerous passages and can be frozen for stock generation but most importantly
- (3) they are able to differentiate into different neuronal lineages with high efficiency.

For the generation of smNPCs, neural induction is achieved by dual SMAD inhibition together with embryoid body (EB) formation. Here, the iPSCs are transferred in a suspension culture dish and are allowed to form floating aggregates (Eiraku et al., 2008). The neuroectoderm fate is stimulated by addition of the small molecules SB431542, dorsomorphin, CHIR99021 and purmorphamine. When the formed EBs are manually disrupted and plated on Matrigel[®], they form colonies of neural epithelial cells which can be split enzymatically and expanded for multiple passages. By the addition of different compounds, smNPCs can be differentiated into ventral and posterior CNS lineages like midbrain neurons and motor neurons as well as down a neural crest fate to mesenchymal cells (Reinhardt et al., 2013).

Recently, another approach that reduces variability and differentiation time has been established. Zhang et al. demonstrated a rapid and very efficient induction of neuronal differentiation by forced expression of a single transcription factor (Zhang et al., 2013). iPSCs were transduced with a lentiviral vector harboring the transcription factor *NEUROGENIN2* (*NGN2*) under a constitutive promoter. The

¹ SMADs are a family of proteins that function as signal transducers for receptors of the transforming growth factor beta superfamily, which regulate cell proliferation and differentiation (Derynck et al. 1998).

induced overexpression of *NGN2* resulted in a rapid conversion of iPSCs into a neuronal phenotype with a mature morphology in less than a week and with a high efficiency. The obtained neurons express high levels of cortical markers *Brn2*, *Cux2* and *FoxG1* as well as the GABA_A receptor and vGlut2 (Zhang et al., 2013).

1.4.2. iPSC models for tauopathies

Although iPSCs have proven to be a valuable tool in the research of TAU-related diseases, one of the drawbacks is that they represent a fetal state of neuronal development. Differentiated iPSC-derived neurons express a variety of mature neuronal markers, but overcoming the developmental regulation of the alternative splicing of TAU remains challenging (Fong et al., 2013; Miguel et al., 2019; Nakamura et al., 2019; Silva et al., 2016). The pre-natal brain expresses only the smallest, fetal form of TAU (ON3R) and the switch to expression of all six isoforms and an equal 3R and 4R TAU ratio only occurs postnatally (see also Chapter 1.1.2) (Goedert and Jakes, 1990). Therefore, only extensive differentiation periods of one year result in the expression of four TAU isoforms (ON3R, ON4R, 1N3R and 1N4R) on the protein level in iPSC-derived neurons (Sposito et al., 2015). More recent protocols like the *NGN2* overexpression and 3D-culturing methods accelerate time to differentiation and maturity (Imamura et al., 2016; Miguel et al., 2019; Zhang et al., 2013). Despite their limitations, iPSC models have proven suitable for investigating effects of missense and intronic mutations in the *MAPT* gene that cause FTLD-17. Studies have shown that the introduction of splicing mutations via gene editing or the generation of iPSC-derived neurons from mutation carriers results in an earlier expression of 4R TAU during neuronal differentiation and higher 4R TAU levels compared to control cell lines (Garcia-Leon et al., 2018; Imamura et al., 2016; Verheyen et al., 2018). Additionally, some groups have reported that mutations that alter the amino acid sequence of TAU and not the splicing process, do not lead to an increase in 4R TAU levels (Ehrlich et al., 2015; Iovino et al., 2015). These findings underline the value of iPSC models in the field of TAU-related diseases and show their usefulness for modeling certain aspects of disease phenotypes. Furthermore, several studies reported pathological differences aside from TAU isoform expression levels in iPSC-derived neurons from patients with FTLD-17 mutations as compared to cells from healthy controls (Birnbaum et al., 2018; Esteras et al., 2017; Imamura et al., 2016).

The vast majority of cases of tauopathies are, however, sporadic and are not caused by mutations in a single gene. Therefore, there is an urgent need for human cell models to investigate the mechanisms of sporadic diseases. For numerous tauopathies, the *MAPT* haplotype has been identified as a major risk factor (see Chapter 1.1.3) and is therefore an interesting candidate for disease modeling. So far, studies using heterozygous H1/H2 neuroblastoma cell lines have investigated *TAU* expression from the different alleles with an allele-specific expression assay and have found differential expression of *TAU*

isoforms when comparing the H1 and H2 alleles (Caffrey et al., 2008; Caffrey et al., 2006) . Recently, Beevers et al. were able to partially reproduce their findings from neuroblastoma cells with H1/H2 heterozygous iPSC lines (Beevers et al., 2017). So far, a systematic comparison of homozygous H1 and H2 iPSC lines is missing.

1.5. Aims of this thesis

The H1 *MAPT* haplotype has repeatedly been identified as a major risk factor for developing neurodegenerative diseases. However, the mechanisms through which this haplotype conveys the increased risk remain largely unknown. Previous studies have investigated the TAU expression in human brains carrying the H1 or H2 *MAPT* haplotype and in heterozygous cell models. The results continue to be inconclusive. So far, a systematic comparison of homozygous H1 and H2 iPSC lines has not been made. This study aimed to close that gap by using eight cell lines with either the H1/H1 or H2/H2 *MAPT* genotype to identify *MAPT* haplotype-dependent differences. These eight human iPSC lines were differentiated for 30 days into neurons and compared with a focus on the following questions:

1. Do all eight cell lines differentiate into neurons in an efficient and comparable manner and does differentiation yield similar quantities of neuronal subtypes across cell lines?
2. Are there differences in neuronal differentiation between the *MAPT* haplotype groups within the examined time frame of 30 days?
3. Do cell lines with different *MAPT* haplotypes differ in their TAU expression profile over the differentiation period of 30 days?
4. Do cell lines with different *MAPT* haplotypes express different levels of α -SYNUCLEIN on an mRNA or protein level within the examined time frame?
5. Are cell lines with the H1 haplotype more vulnerable to external stressors like oxidative stress and toxin treatment?

After displaying the employed material and methods in Chapter 2, the main findings of this work are presented in Chapter 3. First, the generation and differentiation of iPSC-derived neurons is assessed followed by the analysis of TAU and α -SYNUCLEIN expression in the differentiated neurons. Finally, the vulnerability of the different neurons to external stress is evaluated. These results are further discussed in Chapter 4 and Chapter 5 summarizes the thesis and gives a brief outlook on possibilities for future work.

2. Material and methods

This chapter presents the applied material and methods starting with the identification and selection of the used iPSC lines and their differentiation into neurons (Chapter 2.1). Chapter 2.2 displays the analytical methods that were used to identify *MAPT* haplotype-dependent differences followed by the statistical methods employed for data analysis in Chapter 2.3.

2.1. Cell line identification and cell differentiation

2.1.1. Identification and selection of iPSC lines

Cell lines from the Human Induced Pluripotent Stem Cell Initiative (HiPSci) of the European Collection of Authenticated Cell Cultures (ECACC) were stratified regarding their *MAPT* haplotype². Three haplotype defining SNPs (rs1800547, rs8070723 and rs1052553) were chosen to search the openly accessible genome sequencing data of healthy control individuals. Commercially available cell lines with the respective *MAPT* haplotype were identified and matched for donor sex and age, as well as iPSC passage number and pluripotency scores. The following eight lines (four H1/H1 and four H2/H2 lines) were purchased (see Table 2.1).

Table 2.1: Purchased cell lines

Cell line name	Catalogue number	<i>MAPT</i> haplotype	Donor age	Donor sex	PPS*	nPPS**	Passage number
HPSI1013i-yemz_1	77650060	H1/H1	70-74	Male	29,15	1,41	21
HPSI0913i-diku_1	77650088	H1/H1	60-64	Female	28,09	1,26	28
HPSI0614i-lepk_1	77650367	H1/H1	60-64	Female	29,90	1,30	13
HPSI0115i-melw_2	77650564	H1/H1	60-64	Male	22,83	1,30	20
HPSI0115i-zihe_1	77650561	H2/H2	75-79	Female	24,11	1,23	19
HPSI0614i-uilk_2	77650606	H2/H2	55-59	Male	8,5	1,50	14
HPSI0114i-zapk_3	77650156	H2/H2	60-64	Male	34,18	1,30	22
HPSI1113i-qolg_1	77650145	H2/H2	35-39	Male	54,55	0,86	21

* Pluripotency score; ** Novel pluripotency score

For future reference, only the four-letter code at the end of each cell line name will be used (e.g. yemz for HPSI1013i-yemz_1). A material transfer agreement was signed for all cell lines by DZNE and its collaborating partners on this project.

² See <https://www.phe-culturecollections.org.uk/products/celllines/ipsc/search.jsp>.

2.1.2. Genotyping

During the project, the chosen cell lines were genotyped for additional SNPs in the *MAPT* gene, as well as for SNPs in the *SNCA* gene coding the α -SYNUCLEIN protein. To analyze the genotyping array results for imputed and phased genotypes, available for each cell line at the HipSci website³, the freely available software GenomeBrowse from Golden Helix (Bozeman, MT, USA) was used and SNP genotypes of all cell lines were identified. The examination of the microsatellite *Rep1* near the promotor start site of the *SNCA* gene was performed in two steps. First, the GenomeBrowse software was used to read the GATK haplotype calls from the whole genome sequencing (also available on the HipSci website) and the region of interest was genotyped. Next, the whole microsatellite sequence was identified by viewing the raw reads of the whole genome sequencing data with the UCSC Browser⁴.

2.1.3. Cell culture

This thesis aimed to compare eight different iPSC lines to identify *MAPT* haplotype-dependent phenotypes which could be used in the future for a compound or drug screen in an HTS approach. Therefore, the selected iPSC culture model needed to fit the following criteria:

- (1) high proliferation rate to obtain enough starting material for HTS in a short time,
- (2) stability of expanding cell types,
- (3) a reproducible neuronal phenotype and
- (4) a short differentiation time.

As part of the project, a cooperation partner in Tübingen established a combined protocol of smNPC generation and *NGN2* overexpression which fulfill these criteria (Dhingra et al., 2020). Consequently, the iPSC lines were converted into smNPCs in a first step, which are more stable (less prone to spontaneous, unwanted differentiation) and easier to maintain compared to iPSCs. In a second step, the smNPCs were stably transduced with *NGN2* so that rapid neural differentiation was achieved with high efficiency and high reproducibility by *NGN2* overexpression (see Figure 2.1).

³ See <https://www.hipsci.org/lines>.

⁴ See <http://genome-euro.ucsc.edu/index.html>.

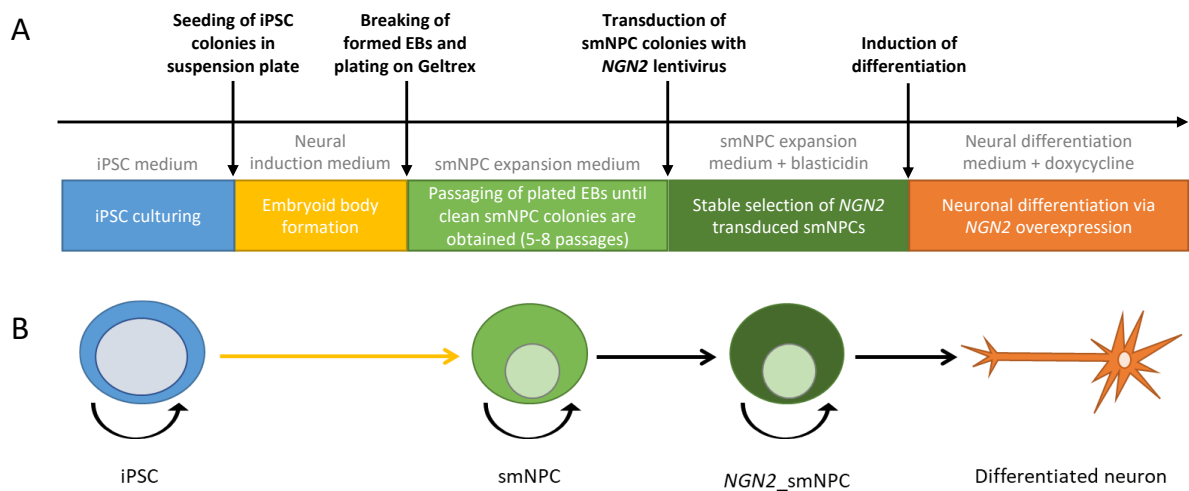


Figure 2.1: Overview of the differentiation protocol employed in this thesis. (A) Induced pluripotent stem cell (iPSC) colonies are cultured in iPSC medium until they are detached and seeded in a suspension plate for embryoid body (EB) formation. Here, the medium is changed to neural induction medium. When EBs are plated on Geltrex after 6 days, cells are cultured in small molecule neural precursor cell (smNPC) expansion medium until clean smNPC colonies are obtained. After five to eight passages, pure smNPC colonies can be transduced with *NGN2*-lentivirus. Stably transduced *NGN2*_smNPC are received by antibody selection with blasticidin and can be differentiated into neurons by induction of *NGN2* overexpression via doxycyclin. **(B)** Populations of iPSCs, smNPCs and *NGN2*_smNPCs can be expanded for numerous passages or can be frozen for stock generation as indicated by round arrows until *NGN2*_smNPC are finally differentiated into neurons [modified from (Strauß et al., 2021)].

iPSC culture and smNPC generation

The acquired HipSci iPSC lines were thawed and plated on Matrigel®-coated (Corning, New York, USA) culture vessels in Essential 8™ Flex medium (Thermo Scientific, Waltham, USA) supplemented with Rock-inhibitor thiazovivin (Thia; Merck Millipore, Burlington, USA) for better cell survival after thawing. The next day, the medium was changed to remove Thia. Clean iPSC colonies were split using gentle cell dissociation reagent (Stemcell Technologies, Vancouver, Canada), while colonies exhibiting features of spontaneous differentiation were passaged using ReLeSR™ (Stemcell). After expanding the thawed cells, at least ten vials of each cell line were frozen to generate a master cell bank.

Next, iPSCs were converted into smNPC using EB formation following a protocol from Dhingra et al (Dhingra et al., 2020). Pure iPSC colonies were detached and transferred into a low binding 6-well suspension plate that contained neural induction medium (Figure 2.2). For the first 2 days, the medium was composed of 78% DMEM/F12 medium, 20% knockout serum replacement, 1% non-essential amino acids, 1% GlutaMax™ (Life Technologies, Carlsbad, USA) and 0.1% β-mercaptoethanol (Sigma Aldrich, St. Louis, USA) and was supplemented with 10 μM dorsomorphin (DOR; Abcam, Cambridge, UK), 10 μM SB431542 (SB; selleckchem, Houston, USA), 0.5 μM purmorphamine (PMA; Biomol, Hamburg, Germany), 3 μM CHIR99021 (CHIR; Tocris, Bristol, UK) and 2 μM Thia (Millipore, Billerica, USA). For the next 2 days, the medium was replaced by N2B27 medium containing 48.425% DMEM/F12 medium, 48% Neurobasal™ Medium, 0.5% N-2 supplement, 1% B-27™ supplement

without Vitamin A (Life Technologies), 0.025% insulin (Sigma Aldrich), 0.5% non-essential amino acids, 1% GlutaMax™, 1% penicillin/streptavidin (Life Technologies) and 0.05% β-mercaptoethanol with the addition of 10 μM DOR, 10 μM SB, 0.5 μM PMA and 3 μM CHIR. For the last 2 days, the medium was replaced with smNPC expansion medium consisting of the above described N2B27 medium supplemented with 0.5 μM PMA, 3 μM CHIR and 64 μg/ml ascorbic acid (AA; Th. Geyer, Renningen, Germany). After 6 days in the suspension plate, the formed EBs were mechanically disrupted with a 1 ml filter tip and the obtained fragments were plated in Geltrex™-coated 6-well plates. Neural rosette-like structures formed and cells were passaged with Accutase® (Sigma Aldrich) after reaching 80% confluency. From then on, cells were cultured in smNPC expansion medium and passaged every 5-7 days until the culture contained compact, clean smNPC colonies (7-8 passages).

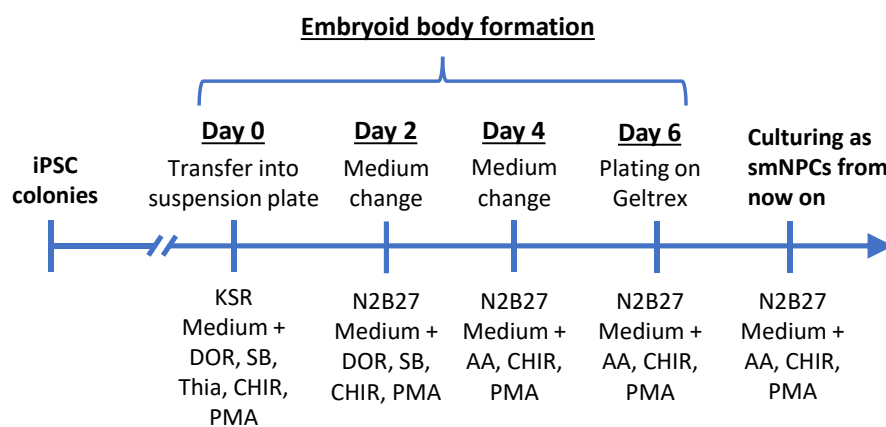


Figure 2.2: Scheme of the procedure to convert induced pluripotent stem cells (iPSCs) into small molecule neural precursor cells (smNPC). Detached iPSC colonies were transferred into a suspension plate and were grown over 6 days to form embryoid bodies. Every 2 days the medium was changed and certain small molecules were included or excluded. At day 6, the embryoid bodies were disrupted by pipetting and were plated on Geltrex™ in the final smNPC medium. From now on, the cells were cultured as smNPCs and were passaged several times to produce clean smNPC colonies. KSR: knockout serum replacement, DOR: dorsomorphin, SB: SB431542, Thia: thiazovivin, CHIR: CHIR99021, PMA: purmorphamine, AA: ascorbic acid.

Differentiation into neurons

For fast and robust differentiation of smNPCs into neurons, cells were transduced with an inducible lentivirus expression construct for the human transcription factor *NGN2* (pLV_TRET_hNgn2_UBC_Blast_T2A_rtTA3) (Menden et al., 2021). In addition to *NGN2* under the control of a tetracycline operator, the vector contains a blasticidin resistance gene to allow for selection of cells with stable integration. For transduction, smNPCs were plated in a 12-well plate at a density of 40,000 cell/cm². The medium was replaced with fresh medium containing 1 μM Thia the next day, an hour before the virus addition. 24 h after lentivirus treatment, cells were washed and the medium was refreshed. When cells reached a confluency of 70%, they were passaged and the antibiotic selection for stable integration of the *NGN2* vector was initiated. Cells were treated for

15 days with 15 µg/ml blasticidin (Invivogen, San Diego, USA). After the selection step, cells were cryopreserved to create master and working cell stocks.

*NGN2*_smNPCs were differentiated in multi-well plates coated first with 100 µg/ml poly-L-ornithine (Sigma Aldrich) and then with 10 µg/ml laminin (Sigma Aldrich). For differentiation, cells were directly seeded in *NGN2* induction medium composed of N2B27 medium supplemented with 2.5 µg/ml doxycycline (Sigma Aldrich) and 2 µM DAPT (Cayman, Ellsworth, USA). After the first 3 days of differentiation, the medium was completely removed and replaced with differentiation medium consisting of N2B27 medium supplemented with 2.5 g/ml doxycycline, 10 µM DAPT, 10 ng/ml BDNF, 10 ng/ml GDNF, 10 ng/ml NT-3 (Peprotech, Princeton, USA) and 0.5 µg/ml laminin. From day 6 onwards, half of the medium was refreshed every 3 days with differentiation medium without doxycycline and DAPT. Cells were differentiated for 0, 5, 10, 15, 30 and 60 days and then harvested, fixed, or used to generate the according readout (Figure 2.3).

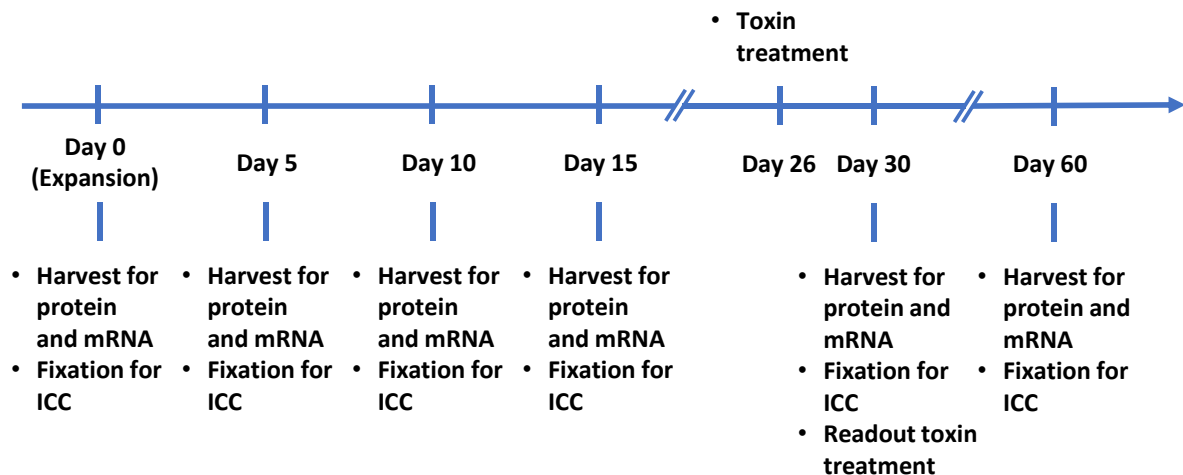


Figure 2.3: Experimental timeline. Cells were seeded for differentiation in different cell culture plate formats. Cells were harvested or fixed after 5, 10, 15, 30 and 60 days of differentiation. Additionally, cells were harvested and fixed in expansion as a day 0 reference. Obtained cell samples were used for protein and mRNA extraction for Western blot and qPCR analysis. Fixed cells were stained for immunocytochemistry (ICC). For the toxin treatment, cells were treated at day 26 of differentiation for 4 days and the readout was performed at day 30 of differentiation [modified from (Strauß et al., 2021)].

2.2. Analytical methods

2.2.1. Immunocytochemistry

For immunostaining, cells were seeded on cover slips in a 48-well plate at a density of 30,000 cells/cm². Cells were fixed with 4% paraformaldehyde (Roth, Karlsruhe, Germany) after several differentiation periods (Figure 2.3) for 10 min at room temperature. After fixation, cells were permeabilized for immunocytochemistry with 0.2% triton-X in phosphate-buffered saline (PBS). Cells were washed twice with PBS and then blocked in 1% bovine serum albumin (BSA), 2% horse and 2% goat serum and 0.05%

Tween® in PBS for at least one hour. Primary antibody solutions were prepared by dilution in blocking solution and cells were incubated in these solutions overnight at 4°C. Thereafter, the cells were washed twice with PBS containing 0.2% Tween® (PBS-T) before the secondary antibodies (also diluted in blocking solution) were applied for two hours. Cells were washed again twice with PBS-T before incubation with DAPI (Thermo Fisher, Waltham, USA) for 10 min (1:1000 in PBS). After washing with PBS, the cover slips were fixed on object slides with fluorescent mounting medium (Agilent Technologies, Santa Clara, CA, USA). The primary antibodies used are listed in Table 2.2 and fluorescent secondary antibodies from Thermo Scientific conjugated to Alexa Fluor™ dye 488 or 594 were used.

Microscopy was carried out with a Leica DMI6000B microscope (Leica Microsystems, Wetzlar, Germany) using a 40x air objective. The obtained images were analyzed and processed with ImageJ software (Schindelin et al. 2012, Schindelin et al. 2015). Brightness and contrast were set to the same values in all images of the same staining and the Cell Counter tool in the ImageJ software was used to quantify cell numbers.

Table 2.2: Antibodies used in immunocytochemistry

Antibody	Clone	Species	Dilution	Source
MAP2	Clone HM-2	Mouse	1:500	Abcam (ab11267)
MAP2ab	AP20	Mouse	1:500	Merck (MAB378)
NESTIN	Polyclonal	Rabbit	1:500	Abcam (ab82375)
GFAP	2.2B10	Rat	1:1000	Life Tech (130300)
GABA	Polyclonal	Rabbit	1:1000	Sigma-Aldrich (A2052)
SMI-312	SMI-312	Mouse	1:1000	Abcam (ab24574)
SYNAPSIN	D12G5	Rabbit	1:500	Cell Signaling (52975)
GEPHYRIN	Polyclonal	Rabbit	1:1000	Abcam ab32206
Total TAU	TAU-12	Mouse	1:500	Merck (MAB2241)
3R TAU (RD3)	Clone 8E6/C11	Mouse	1:500	Millipore (05-803)
4R-TAU (RD4)	Clone 1E1/A6	Mouse	1:100	Millipore (05-804)
α-SYNCLEIN	14H2L1	Rabbit	1:500	Invitrogen (701085)
β-3-TUBULIN	D71G9	Rabbit	1:500	Cell Signaling (5568S)

2.2.2. Semi-quantitative real-time PCR

For semi-quantitative real-time PCR (qPCR), cells were seeded in a 6-well plate at a cell density of 50,000 cells/cm² and were harvested at different time points (Figure 2.3) with RLT lysis buffer from the RNeasy plus kit (Qiagen, Hilden, Germany). Cell lysates were homogenized via vortexing and frozen at -80°C until further processing. After thawing, the samples were brought to room temperature and mRNA was isolated using the RNeasy plus kit according to the manufacturer's instructions. In brief,

samples in RLT buffer were transferred to a genomic DNA eliminator spin column and centrifuged for 30 s at 10,000 rpm. One sample volume of 70% ethanol was added to the flow-through and mixed by pipetting. The solution was then transferred to an RNeasy spin column and centrifuged for 15 s at 10,000 rpm. The flow-through was discarded and the bound mRNA in the column was washed with 700 μ l RW1 buffer by centrifugation. Next, two washing steps with 500 μ l RPE buffer were performed followed by centrifugation. During washing, the collection tube was changed every other step to increase mRNA purity. After the final RPE buffer wash the spin column was centrifuged for 1 min at 10,000 rpm to dry the membrane and remove traces of buffer. To elute the mRNA, the spin column was placed in a microfuge tube and 30 μ l of RNase-free water was added directly to the membrane and centrifugation was carried out at 10,000 rpm for 1 min. The mRNA concentration was measured with a NanoDrop.

Complementary DNA (cDNA) was prepared via reverse transcription using 500 ng mRNA per reaction with the iScript kit (Bio-Rad Laboratories, Hercules, Ca) according to the manufacturer's protocol. For the qPCR reaction the following material was used: 5 ng of complementary cDNA, 0.2 μ M forward and reverse primers together with SYBR green select qPCR supermix (Thermo Fisher). For the qPCR reaction the StepOne Plus system was used (Applied Biosystems, Waltham, MA) with the following protocol: 2 min at 50°C, 2 min at 95°C and 40 cycles of 15 s at 95°C and 60 s at 60°C with additional recording of the melting curve. Since not all samples could be run on the same plate, for each plate and gene of interest/internal control gene, a standard dilution curve was included. The cDNA standard serial dilution was prepared by first pooling 5 μ l cDNA from all samples and then diluting four times by a factor of five in water. Using the C_t values of the serial dilution, a linear regression curve was generated and the relative mRNA expression levels of samples on each plate could be calculated. This way, inter-plate reaction differences were accounted for. The primers and their sequences are listed in Table 2.3. As internal controls expression of three housekeeping genes were measured (*UBQLN1*, *PSMC1* and *GPBP1*) to normalize measurements for the genes of interest.

Table 2.3: Primers used for qPCR

Target	Forward primer	Reverse primer
<i>PMSC1</i>	CACACTCAGTGCCGGTAAAA	GTAGACACGATGGCATGATTGT
<i>UBQLN1</i>	TGCAGGTCTGAGTAGCTTGG	AACTGTCTCATCAGGTCAGGAT
<i>GPBP1</i>	ATCATTGGTCTTCAACCTTCC	ATCCTCAGTTAAGGGAGCACA
Total TAU	CGTCCCTGGCGGAGGAAATA	CCCGTGGTCTGTCTTGCTT
3R TAU	AGGCGGGAAGGTGCAAATAG	CCTGGCCACCTCCTGGTTTATG
4R TAU	GCCCATGCCAGACCTGAAGA	CCTCCCGGGACGTGTTTATG
α -SYNUCLEIN	AAGAGGGTGTCTCTATGTAGGC	GCTCCTCCAACATTTGTCACTT
<i>SOX2</i>	AGTCTCCAAGCGACGAAAA	GCAAGAAGCCTCTCCTTGAA

2.2.3. Western blot

For protein expression analysis, cells were seeded in 6-well plates at a density of 50.000 cells/cm² and were harvested at different time points (Figure 2.3) with Mammalian Protein Extraction Reagent (M-PER™) lysis buffer (Thermo Fisher) containing protease inhibitors (cOmplete, Roche Basel, Switzerland) and phosphatase inhibitors (phoSTOP, Roche). After incubation on ice for 15 min, samples were frozen at -80°C for at least one hour to facilitate lysis of cells. Next, samples were thawed and homogenized by pipetting and then incubated again on ice for 15 min. After centrifugation at 13,000 rpm for 30 min, the supernatant containing the M-PER™-soluble protein fraction was removed and transferred into a fresh tube. Protein concentrations were measured using a BCA protein assay kit (Thermo Fisher) and calculated with a BSA standard curve.

The insoluble protein remained in the cell pellet and was extracted with sarkosyl. The pellet was washed once with M-PER™ buffer and centrifuged at 45,000 rpm for 1 h at 4°C. After discarding the supernatant, sarkosyl-buffer was added (1% sarkosyl, 10 mM Tris-HCl, 150 mM NaCl, 5 mM EDTA) and the pellet was disrupted by pipetting up and down and vortexing. Samples were incubated at room temperature with agitation at 700 rpm and then again centrifuged at 45,000 rpm for 1 h at room temperature. The supernatant (sarkosyl-soluble fraction) was collected as the insoluble protein fraction and the protein concentration was measured as described above.

Before gel electrophoresis, samples containing 20 µg protein were denatured by boiling (95°C for 5 min) with XT-buffer (for Western blots for 4R TAU detection, 60 µg protein was needed). Samples were loaded on 10% Bis-Tris Criterion™ polyacrylamide gels (Bio-Rad Laboratories) and run at 150 V for 70 min with MES buffer. Protein transfer to a 0.2 µm polyvinylidene difluoride (PVDF) membrane was performed using transfer buffer containing 20% methanol and a semidry blotting system (Trans-Blot Turbo Transfer System, Bio-Rad Laboratories) using the following protocol: 40 min at 1 A and 25 V. The membrane was fixed with 0.4% paraformaldehyde for 20 min after the transfer and then washed with PBS. Blocking of the membrane was carried out with 5% skimmed milk (Sigma-Aldrich) in tris-buffered saline (TBS) with 0.05% Tween® (Sigma-Aldrich) (TBS-T) for one hour at room temperature. Primary antibodies were diluted in 1% BSA in TBS-T and incubated with the blot overnight at 4°C. After washing the next day with TBS-T, the secondary horseradish peroxidase (HRP)-conjugated antibodies (diluted in 5% skimmed milk in TBS-T) were added for 1-2 hours at room temperature. Clarity Western ECL Substrate (Bio-Rad Laboratories) or femto ECL (Thermo Fisher) was used to develop the HRP signal and blots were imaged with an Odyssey® Fc imaging system (LI-COR Biotechnology, Lincoln, Netherlands). Analysis of captured images was performed with the Image Studio™ Software from LI-COR. Primary antibodies used for Western blotting can be found in Table 2.4, secondary antibodies were the

following: HRP-coupled anti-mouse IgG (1:2500, Vector Laboratories, Burlingame, CA) and anti-rabbit IgG (1:5000, Vector Laboratories).

To probe with new antibodies, the membrane was briefly washed with TBS-T and then incubated in stripping buffer containing β -mercaptoethanol for 20-30 min at 50°C. Before blocking again with milk, the membrane was washed thoroughly with deionized water to remove residual β -mercaptoethanol, followed by a 30 min wash with TBS-T. The probing of the membrane with new primary and secondary antibodies, as well as blot development, was performed as described above.

Table 2.4: Antibodies used for Western blot

Antibody	Clone	Species	Dilution	Source
Total TAU	Polyclonal	Rabbit	1:3000	Agilent Dako (CAC-TIP-4RT-P01)
Total TAU	Clone TAU-5	Mouse	1:1000	Millipore (MAB361)
3R TAU (RD3)	Clone 8E6/C11	Mouse	1:1000	Millipore (05-803)
4R TAU (RD4)	Clone 1E1/A6	Mouse	1:300	Millipore (05-804)
Phospho-TAU (Ser202, Thr205)	Clone AT8	Mouse	1:1000	Life Tech (MN1020)
Phosphor-TAU (Thr231)	Clone AT180	Mouse	1:1000	Life Tech (MN1040)
MC1		Mouse	1:250	Gift from Peter Davies
α -SYNUCLEIN (AB1)	Polyclonal	Rabbit	1:500	Cell signaling (2642S)
α -SYNUCLEIN (AB2)	Syn211	Mouse	1:500	Invitrogen (MA5-12272)
β -3-TUBULIN	D71G9	Rabbit	1:500	Cell signaling (5568S)
GAPDH	6C5	Mouse	1:200	Santa Cruz (sc-32233)

Intercalibration protein standards were generated and run together with the samples of interest on every blot. Thus, signals from samples could be normalized to signals from the protein standard and values could be compared between Western blots. To create the protein standards, a few microliters from samples at all time points were pooled. M-PERTM-soluble and sarkosyl-soluble samples were pooled separately and the respective protein standard was used with the corresponding samples. For every time point at least three biological replicates for each cell line were generated and analyzed by Western blot.

2.2.4. Cell survival without antioxidants

N2B27 medium (described in Chapter 2.1.3) was prepared using B-27TM supplement without antioxidants (Life Technologies) to investigate the survival of neurons differentiating in medium without antioxidants. Cells were cultured for three weeks in expansion medium containing N2B27 without antioxidants to wash out antioxidants before differentiation. In parallel, cells were also cultured in expansion medium containing N2B27 with antioxidants. For differentiation, cells were

seeded in a 96-well plate at a density of 20,000 cells/well. Differentiation medium was also prepared from N2B27 medium with and without antioxidants and cells were differentiated under parallel conditions. Cell viability was assessed at different time points (day 8, day 10, day 13 and day 15) with the fluorescent dye calcein red-orange which stains viable cells (ThermoFisher). A final calcein concentration of 250 nM was added to the medium and the cells were incubated at 37°C for 30 min. Thereafter, the medium was completely removed and replaced by PBS. The fluorescence intensity was measured with a CLARIOstar® microplate reader from BMG Labtech at an excitation wavelength of 577 nm and emission wavelength of 620 nm. Every cell line had their own control with cells expanded and differentiated in medium with antioxidants, which was used for normalization.

2.2.5. Toxin treatment

For treatment with the mitochondrial inhibitor annonacin, cells were seeded in a clear 96-well plate at a density of 20,000 cells/well. After 26 days of differentiation, the cells were treated with the respective toxin. Annonacin was diluted from a 1 mM stock solution in dimethyl sulfoxide (DMSO) to a final concentration of 800 nM in fresh differentiation medium which was added to the cells. Neurons were further cultivated for 4 days without medium change. On day 4 of treatment, cell viability was measured with the calcein-red-orange assay and metabolic activity was assessed using the MTT (3-[4,5-dimethylthiazol-2-yl]-2,5 diphenyl tetrazolium bromide) assay. The calcein staining was carried out as describe above (Chapter 2.2.4). After measurement of calcein, cells were incubated in 500 ng/ml MTT solution for an hour at 37°C, thereafter the solution was removed and the plate was frozen at -80°C for at least an hour. For cell lysis, the plate was thawed and the formed formazan was dissolved in DMSO. The absorbance of the solution was measured at 570 nm with a CLARIOstar® plate reader from BMG Labtech. For normalization, each cell line had their own untreated control to rule out signal differences due to, for example, differences in cell density.

2.3. Statistical analysis

For statistical data analyses the GraphPad Prism 9.1.0 software⁵ for Windows (GraphPad Software, San Diego, California USA) was used. Pooled cell line data for the *MAPT* haplotype groups were represented as mean \pm standard error of the mean (SEM) of n=4 cell lines for each haplotype. Data displaying individual cell lines are represented as mean \pm SEM of independent experiments. For analysis of *MAPT* haplotype groups over the differentiation periods, 2-way analysis of variance (ANOVA) followed by a post-hoc Tukey's test or Sidak's test was performed. For all other analyses, an unpaired t-test was used. Specifications are given in each figure legend.

⁵ See www.graphpad.com.

3. Results

The following chapter describes the results of the experimental part of this thesis. In a first step, the generation of *NGN2*_smNPCs from iPSC lines is documented by bright field images of the different conversion stages (Chapter 3.1), followed by their differentiation into neurons with the respective characterization of all cell lines (Chapter 3.2). In a second step, the expression of the disease-relevant proteins TAU and α -SYNUCLEIN was analyzed and compared between the two haplotype groups and is presented in Chapter 3.3 and 3.4, respectively. Finally, Chapter 3.5 presents the vulnerability of the differentiated neurons when they are exposed to external stressors like oxidative stress and toxins.

3.1. Generation of *NGN2*_smNPCs from iPSC lines

The purchased iPSCs were treated as described in Chapter 2.1.3 to generate a cell stock. Thereafter, all cell lines were converted into smNPCs via EB formation and dual SMAD inhibition. The whole process is schematically shown in Figure 3.1A.

Bright field pictures (1) to (8) in Figure 3.1B document the conversion process from iPSCs over smNPCs to differentiated neurons. First, clean iPSC colonies (1) were detached and seeded in neural induction medium to form EBs (2). When EBs showed signs of neuroectoderm patterning at day 6 (3), they were disrupted mechanically and seeded on GeltrexTM where they formed neural rosette-like structures (4). From then on, cells were passaged by single cell detachment with Accutase[®] and selected for smNPCs by neuronal expansion medium until pure smNPC cultures were obtained, visible by compact colonies and well-defined colony edges (5,6). smNPCs were further treated with the *NGN2*-lentivirus and selected via antibiotic resistance for stable vector integration. Cells were cryopreserved at this time point to generate a master and working cell bank. *NGN2*_smNPCs could be differentiated via induction of *NGN2* overexpression through doxycycline-supplemented differentiation medium. Merely one day after initiation of the differentiation protocol, cells began to form processes (7) and three days later a clear neuronal morphology and a growing neuronal network was visible (8).

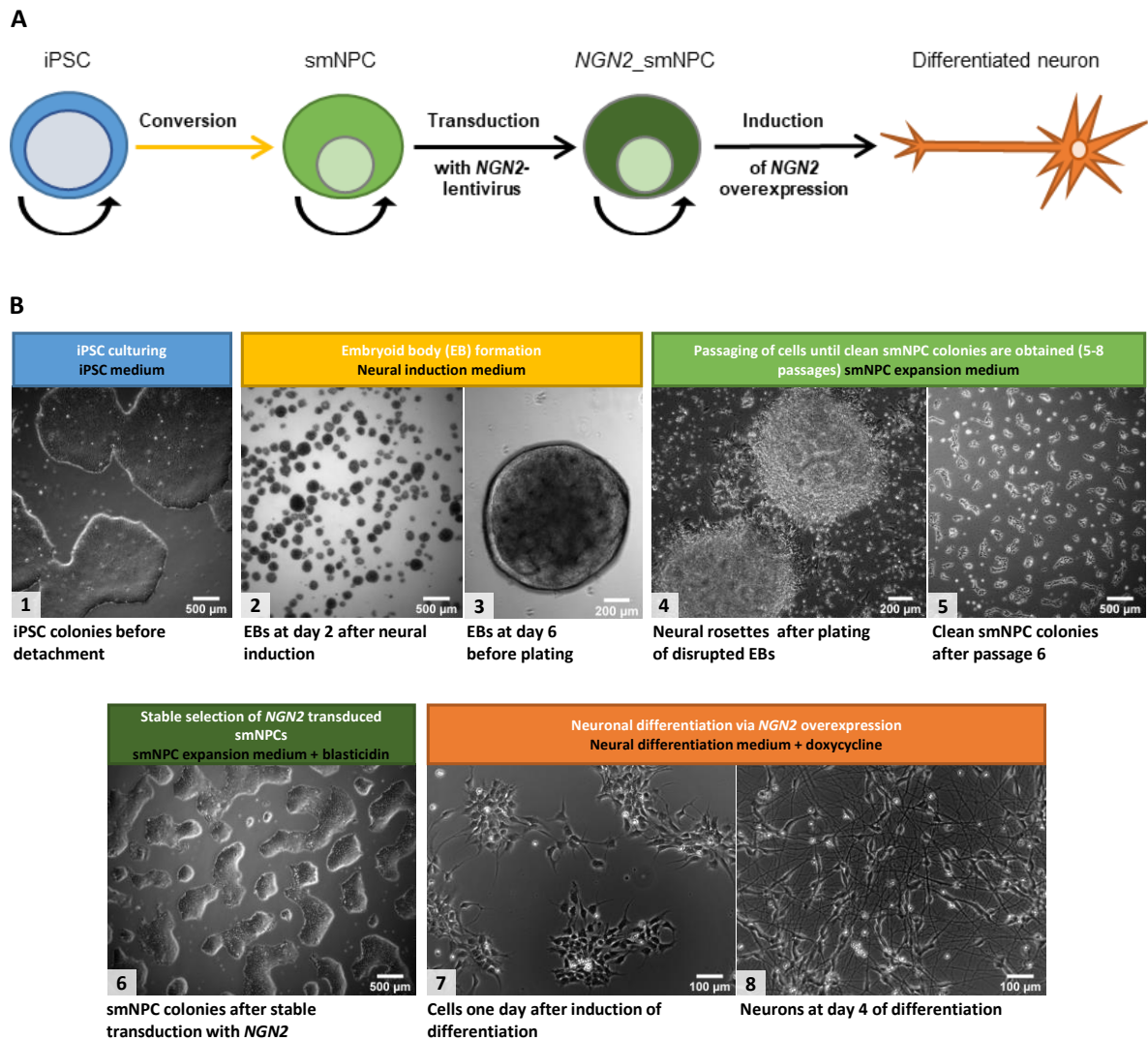


Figure 3.1: Conversion of iPSC lines into *NGN2*_smNPCs. (A) Schematic protocol overview. First, iPSCs were converted into smNPCs via embryoid body (EB) formation and then transduced with *NGN2*-lentivirus to generate *NGN2*_smNPCs. Upon *NGN2* overexpression, these cells can be differentiated into neurons. Round arrows indicate expandable cell populations, which can be frozen for stock generation. (B) Conversion and differentiation process with representative bright field pictures. Pure iPSC colonies (1) were detached and seeded in neural induction medium to form EBs (2). At day 6, when neuroectoderm patterning is visible (3), EBs were disrupted and plated on Geltrex™ (4). Cells were further passaged by single cell dissociation until clean smNPC colonies were obtained (5). smNPCs were then transduced with *NGN2*-lentivirus and stable integration was selected for by antibody resistance (6). When plated in neural differentiation medium containing doxycycline, overexpression of *NGN2* was triggered. Cells showed signs of neuronal processes the next day (7) and three days later, a clear neuronal morphology and a growing neuronal network was visible (8) [modified from (Strauß et al., 2021)].

3.2. Differentiation and characterization of *NGN2*_smNPC lines

To evaluate cellular differentiation upon the induction of *NGN2* overexpression, all cell lines were fixed or harvested at different time points (5, 10, 15, 30 and 60 days). Expanding cells were used as a day 0 reference (see also Figure 2.3).

First, cell survival at day 30 and day 60 of the differentiation period was compared to identify suitable samples for further characterization (Chapter 3.2.1). Characterization of neurons was done by cell marker expression analysis applying qPCR and Western blot (Chapter 3.2.2) as well as immunocytochemistry (Chapter 3.2.3 and 3.2.4).

3.2.1. Evaluation of cell survival at day 30 and 60 of differentiation

Cells were cultured for 30 days without any visible effects on cell viability. With extended culturing, however, cells were prone to detachment and showed signs of a disintegrated and fragmented neuronal network. Therefore, cell viability of cell samples after 30 and 60 days of differentiation was assessed through the examination of nuclei morphology via DAPI staining (Figure 3.2A and B). 30-day old cells showed primarily viable, uncondensed cell nuclei together with a strong neuronal staining of the dendritic marker MAP2, demonstrating a mature neuronal morphology with an extended dendritic tree (Figure 3.2A).

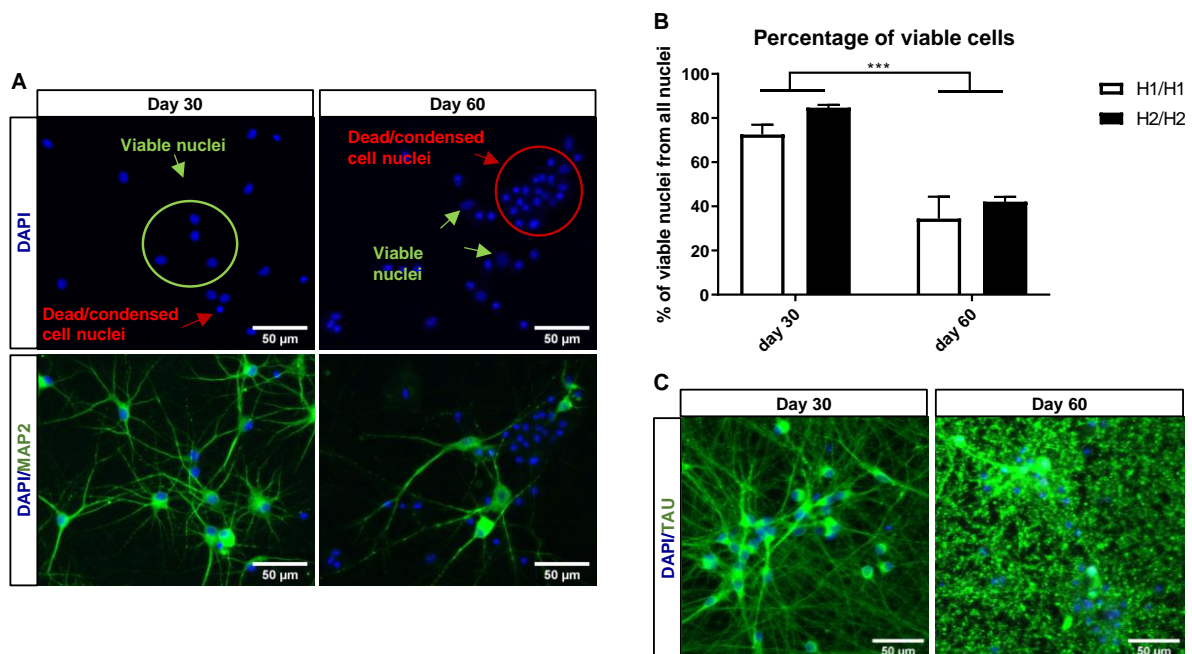


Figure 3.2: Evaluation of cell survival at day 30 and day 60 of differentiation. (A) DNA marker DAPI showed several condensed nuclei at day 60 which lack staining for the dendritic marker MAP2 and were indicative of apoptotic cells. In comparison, 30-day old cells displayed very few condensed nuclei and numerous MAP2 positive cells. (B) Quantification of viable nuclei versus all nuclei revealed a 50% reduction in viability. Data are represented as mean \pm SEM of $n=4$ cell lines for each haplotype group. 2-way ANOVA was performed. *** $p < 0.001$. (C) Immunostaining with neuronal marker TAU showed a healthy and mature neuronal network at day 30, while at day 60 most of the network was degraded.

After a differentiation time of 60 days, however, numerous condensed nuclei were visible and only a few MAP2 positive cells with uncondensed nuclei remained. Quantification of viable nuclei revealed a reduction of living cells by approximately 50%: cell viability dropped from 79% at day 30 to 38% at day 60 (Figure 3.2B). There was no significant difference in cell viability between cell lines of the H1/H1 or H2/H2 haplotype. Additionally, staining with the neuronal marker TAU showed a dense neuronal network at day 30 of differentiation which was largely degraded at day 60 (Figure 3.2C).

As a result of this evaluation, samples from 60-day old cells were excluded from further analysis since the number of viable cells did not match the requirements of this study.

3.2.2. Evaluation of differentiation via *SOX2* and β -3-TUBULIN expression

In a next step, expression of the neural stem cell marker *SOX2* and the neuronal marker β -3-TUBULIN were measured to verify efficient differentiation of all cell lines into neurons. Results for the 30-day differentiation period are presented in Figure 3.3. In the absence of *NGN2* overexpression, proliferating cells expressed high levels of *SOX2* (day 0) which were strongly and significantly reduced upon differentiation (Figure 3.3A). At day 5 of differentiation, *SOX2* expression was downregulated by approximately 60% and decreased further as the 30-day differentiation continued. Complementary to these findings, the neuronal protein β -3-TUBULIN was weakly expressed in expanding cells. When differentiation was induced, however, protein levels greatly increased after 5 days (Figure 3.3B). For the remaining 30-day differentiation period, β -3-TUBULIN level stayed stable. There were no differences in the expression levels of *SOX2* and β -3-TUBULIN between H1/H1 and H2/H2 cell lines, indicating a comparable differentiation rate for both haplotype groups.

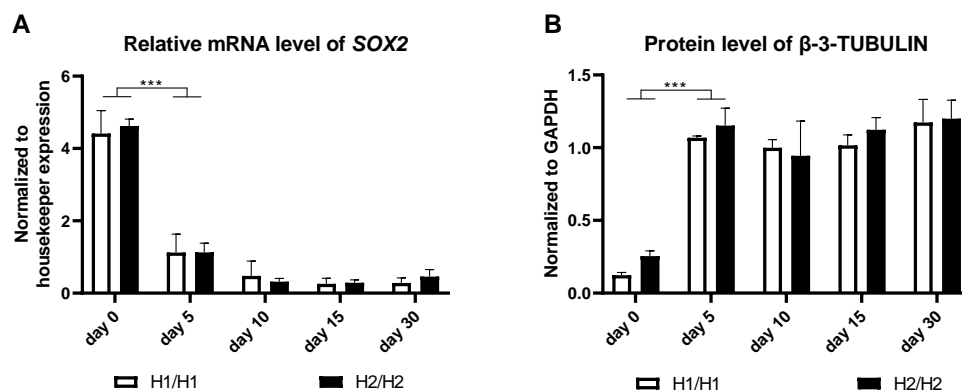


Figure 3.3: Expression of *SOX2* and β -3-TUBULIN over a differentiation period of 30 days. (A) mRNA level of the neural stem cell marker *SOX2* was strongly downregulated upon differentiation. (B) Protein levels of the neuronal marker β -3-TUBULIN were strongly upregulated upon differentiation. Data are represented as mean \pm SEM of $n=4$ cell lines for each haplotype group. 2-way ANOVA followed by Tukey's test was performed. * $p < 0.001$. No significant difference for any marker was detectable between haplotype groups.**

3.2.3. Identification and quantification of cell types during differentiation via immunocytochemistry

All cell lines were characterized via immunocytochemistry to quantify cell types that are present in the cell culture over a differentiation period of 30 days (Figure 3.4). First, cells were stained for the neural progenitor marker NESTIN, the neuronal and dendritic marker MAP2 and the glial marker GFAP at the different time points (see quantification in Figure 3.4A and representative fluorescence images in Figure 3.5 and Figure 3.6). Thereafter, the neuronal population was analyzed in more detail by staining for the neurotransmitter GABA and the cortical marker BRN2 (see Figure 3.4B and C for quantification and Figure 3.7 and Figure 3.8 for representative fluorescence images).

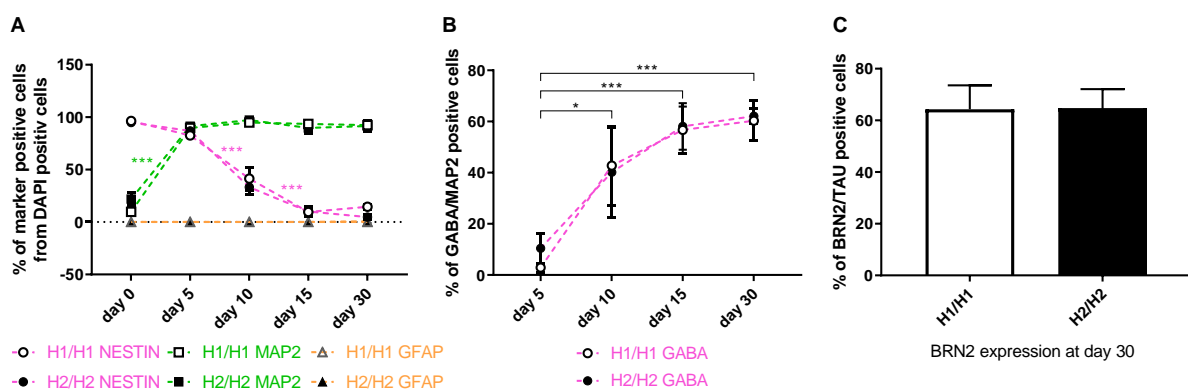


Figure 3.4 Quantification of cell types over a differentiation period of 30 days. (A) Quantification of stained cells positive for the dendritic marker MAP2, the neural progenitor marker NESTIN and the glial marker GFAP over a differentiation period of 30 days. While the percentage of NESTIN positive cells decreased from 96 to 10%, MAP2 expression increased significantly upon differentiation from 16 to 92%. With under 1% at day 30, glia cells were nearly absent from the cell culture. Data are represented as mean \pm SEM of $n=4$ cell lines for each haplotype group. 2-way ANOVA followed by Tukey's test was performed. *** $p<0.001$ (B) The percentage of GABAergic (GABA positive) cells from total neurons (MAP2 positive cells) increased over the differentiation period from 7% at day 5 to 61% at day 30. Data are represented as mean \pm SEM of $n=4$ cell lines for each haplotype group. 2-way ANOVA followed by Tukey's test was performed. * $p<0.05$, *** $p<0.001$ (C) 65% of mature neurons (TAU positive) express a marker for cortical layer 2/3 neurons (BRN2) at day 30 of differentiation. Data are represented as mean \pm SEM of $n=4$ cell lines for each haplotype group. Unpaired t-test was performed. No significant difference for any marker was detectable between haplotype groups [modified from (Strauß et al., 2021)].

Graph A in Figure 3.4 illustrates the development of NESTIN and MAP2 expression over the differentiation period of 30 days. Before differentiation (day 0), the majority of dividing cells showed an intensive NESTIN staining (96%), while only a few cells were MAP2 positive (15%) (see also Figure 3.5A). 5 days after induction of differentiation, neuronal processes started to form and MAP2 expression was upregulated in nearly all cells (91%). NESTIN was still strongly expressed (85% of cells) at day 5, meaning that most cells at this time point were double positive for both markers. Later into the differentiation, the percentage of NESTIN positive cells decreased significantly, first to 37% at day 10 and then to 10% at day 15. MAP2 expressing cells remained at around 92% from day 5 onwards throughout the whole 30-day differentiation period.

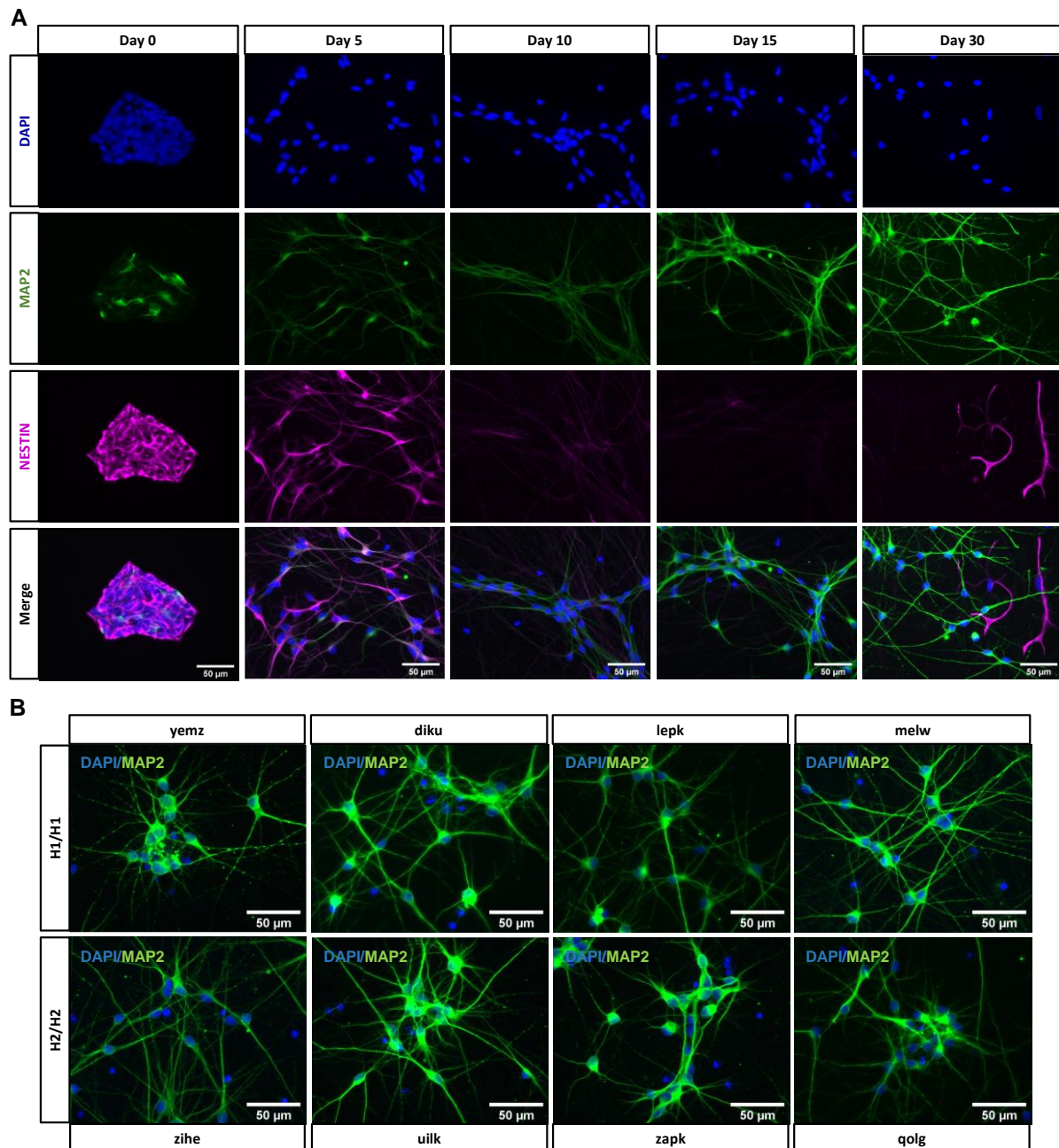


Figure 3.5: Immunostaining at different time points of differentiation with neural progenitor marker NESTIN and dendritic marker MAP2. (A) Staining with MAP2 and NESTIN. At day 0 before differentiation induction, nearly all cells strongly expressed the neural precursor marker NESTIN, while only a few were positive for the neuronal marker MAP2. In the early days of differentiation (5 days), most cells were double positive for both markers. While MAP2 staining increased from day 5 onwards, expression of NESTIN decreased over time. At day 30, the remaining NESTIN positive cells were MAP2 negative and displayed a non-neuronal morphology. (B) MAP2 staining for all cell lines at day 30 of differentiation showed comparable staining pattern and cell morphology amongst all cell lines [modified from (Strauß et al., 2021)].

At day 30, 10% of NESTIN positive cells remained in the culture. In contrast to the early phase of differentiation, NESTIN positive cells were MAP2 negative and displayed a non-neuronal morphology in later stages of differentiation. This result indicates that a small percentage of cells insufficiently differentiated into neurons and remained in their neural precursor state. Overall, *NGN2*_smNPCs differentiated quickly and efficiently into neurons upon *NGN2* overexpression as shown by

immunostaining with NESTIN and MAP2. Although there were some minor differences between cell lines regarding the percentage of MAP2 and NESTIN positive cells, there were no significant haplotype-dependent differences.

Figure 3.5B (MAP2 staining) additionally shows that all cell lines displayed similar neuronal cell morphology after 30 days of differentiation.

Next, cells were stained with the dendritic marker MAP2 and the glial marker GFAP (Figure 3.6). Over the entire 30-day differentiation period there was no expression of GFAP in any cell line (except one), indicating the absence of glial cells in the culture. Only one cell line (qolg H2/H2), displayed GFAP positive cells with astrocyte morphology at day 30 of differentiation (cell line presented in Figure 3.6). The percentage of glial cells, however, remained low at 3%. The overall percentage of astrocytes was therefore neglectable (below 1%) and without a significant difference between the *MAPT* haplotype groups (see Figure 3.4A for quantification).

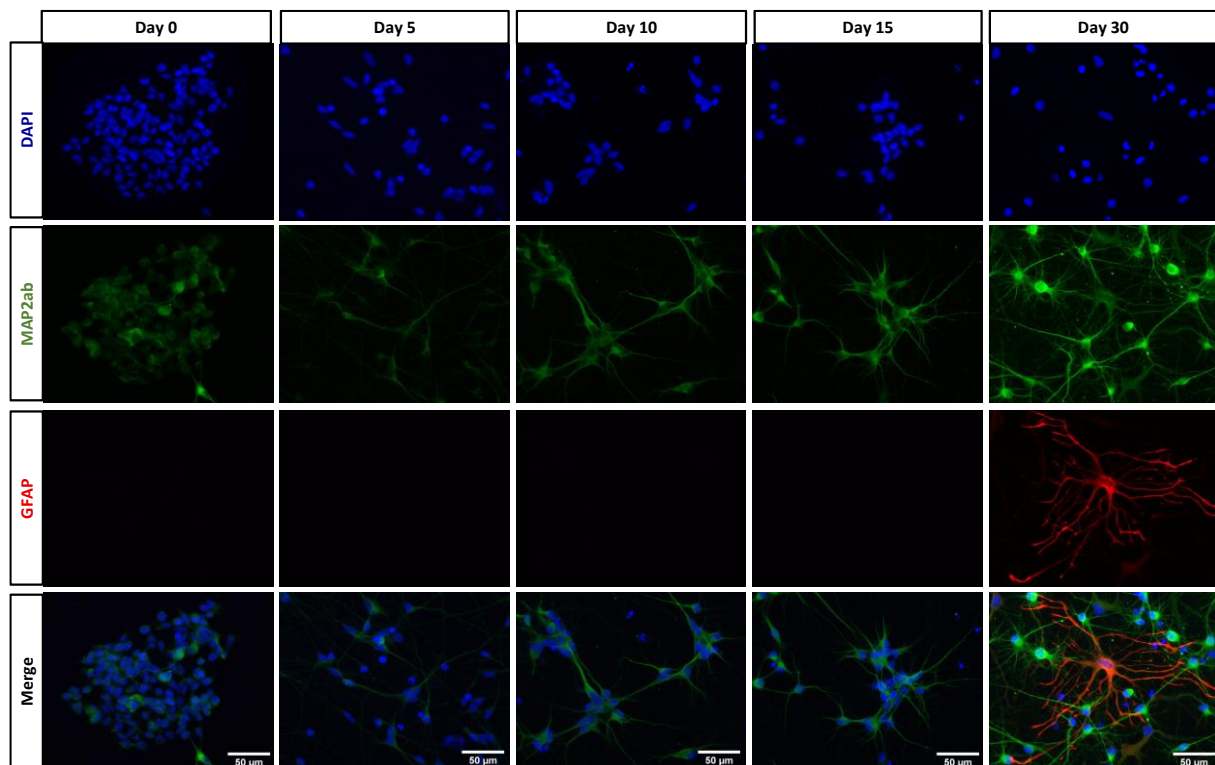


Figure 3.6: Immunostaining at different time points of differentiation with glial marker GFAP. Staining with MAP2 and GFAP showed no visible expression of GFAP from day 0 to day 15, while expression of MAP2 is present from day 0 onwards and increased over time. At day 30, in the displayed cell line (qolg), there were some GFAP positive cells detectable that displayed an astrocytic morphology [modified from (Strauß et al., 2021)].

When Zhang et al. first described the differentiation of iPSCs into neurons via *NGN2* overexpression, they reported expression of cortical and GABAergic markers in the obtained neurons (Zhang et al., 2013). To further specify the neuronal cell population that is present in the culture, an additional immunostaining for the neurotransmitter GABA and the cortical marker BRN2 was performed. To

evaluate the percentage of GABA positive cells within the total neuronal population, cells were co-stained with MAP2 (see quantification in Figure 3.4B and fluorescence images in Figure 3.7A).

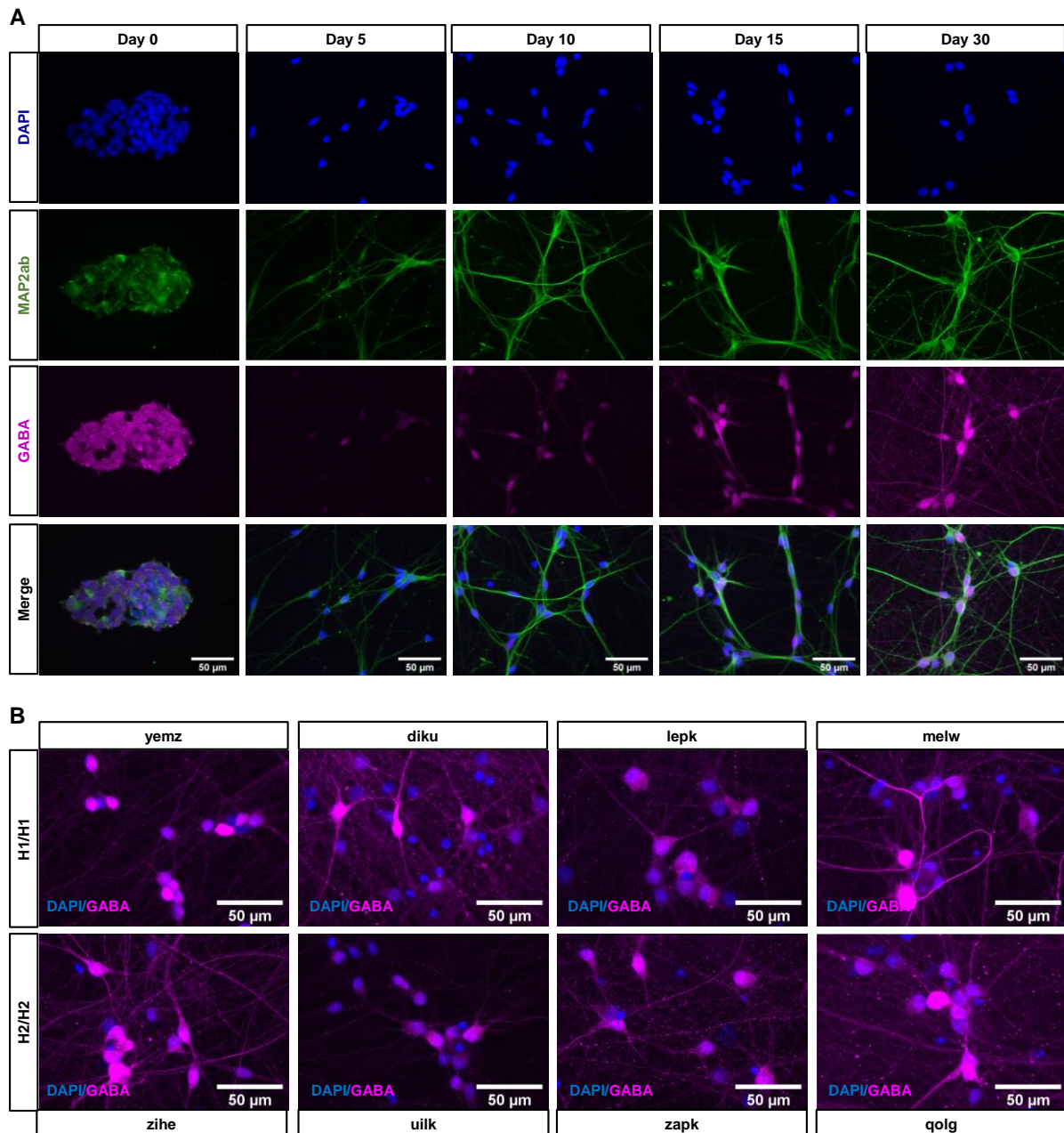


Figure 3.7: Immunostaining for the neurotransmitter GABA. (A) Immunostaining for GABA and MAP2. At day 5 of differentiation only a few neurons (MAP2 positive cells) showed a weak GABA signal. Over the differentiation period, the number of GABAergic cells increased. From day 15 onwards, the signal intensified and the distribution of the neurotransmitter in the cells changed. Until day 15 of differentiation the signal was mainly located in or close to the soma, at day 30, however, GABA was visible throughout the network of neuronal processes. **(B)** After 30 days of differentiation some cell lines differed in the intensity of the GABA signal along the neuronal network as well as in the soma. This difference did not manifest between the *MAPT* haplotype groups but was instead visible between cell lines of one haplotype [modified from (Strauß et al., 2021)].

The fluorescence images show a strong unspecific staining in proliferating smNPCs with the GABA antibody. Therefore, day 0 was excluded from quantitative analysis. After day 5 of differentiation a weak GABA signal was visible in 7% of cells. The expression level of GABA increased with longer periods of differentiation. At day 10, an average of 40% of cells were GABA positive with high variability between cell lines. GABA expression was further upregulated until day 15 of differentiation to 57% GABA positive cells. The percentage of GABA positive cells only slightly increased to 61% at day 30. Over the 30-day differentiation period, the GABA staining signal intensity increased and its distribution in the cell changed as well. Early in differentiation, the signal was rather localised in the soma and soma-near processes (Figure 3.7A). Figure 3.7B shows GABA staining of all cell lines at day 30. At this time point, GABA expression was visible along axons and within the whole neuronal network. Although the percentage of GABAergic neurons ranged from 41% (diku H1/H1) to 78% (yemz H1/H1) between cell lines at day 30, there was no statistical difference between the haplotype groups. Figure 3.7B also shows prominent differences in the intensity of GABA signal along the neuronal network as well as in the cell soma. These differences, however, were equally distributed between H1/H1 and H2/H2 groups.

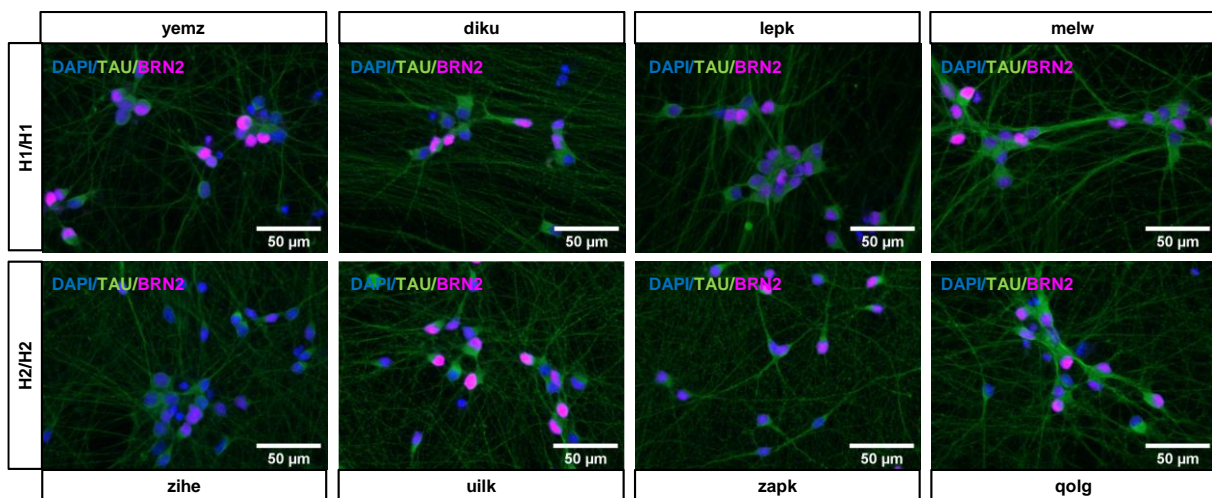


Figure 3.8: Immunostaining for the cortical marker BRN2 and neuronal marker TAU at day 30 of differentiation. Both markers displayed a comparable staining pattern across all cell lines [modified from (Strauß et al., 2021)].

Finally, cells were stained with the marker BRN2 for cortical layer 2/3 neurons (see Figure 3.4C for quantification and Figure 3.8 for fluorescence images). BRN2 staining was unspecific in proliferating cells and early differentiating neurons. Therefore, BRN2 staining was assessed only at day 30 of differentiation, in combination with TAU staining, to ensure neuronal maturity of cells. At this time point, an average of 65% of cells were positive for BRN2 in both cell line haplotype groups (see Figure 3.4C). All cell lines showed a comparable staining pattern for both the cortical marker BRN2 and the neuronal marker TAU at day 30 of differentiation (Figure 3.8).

3.2.4. Further characterization of differentiated neurons

One representative cell line was stained with additional neuronal markers to further evaluate cellular differentiation over the 30-day period.

Figure 3.9A shows immunostaining for the neurofilament marker SMI-312 and the microtubule marker β -3-TUBULIN, both visualizing the axons of neurons. After the first 5 days of differentiation, the cells developed long, visible axons, although the network was still sparse. At day 10, the network was notably denser as shown by both markers. The network further matured until day 30 of differentiation.

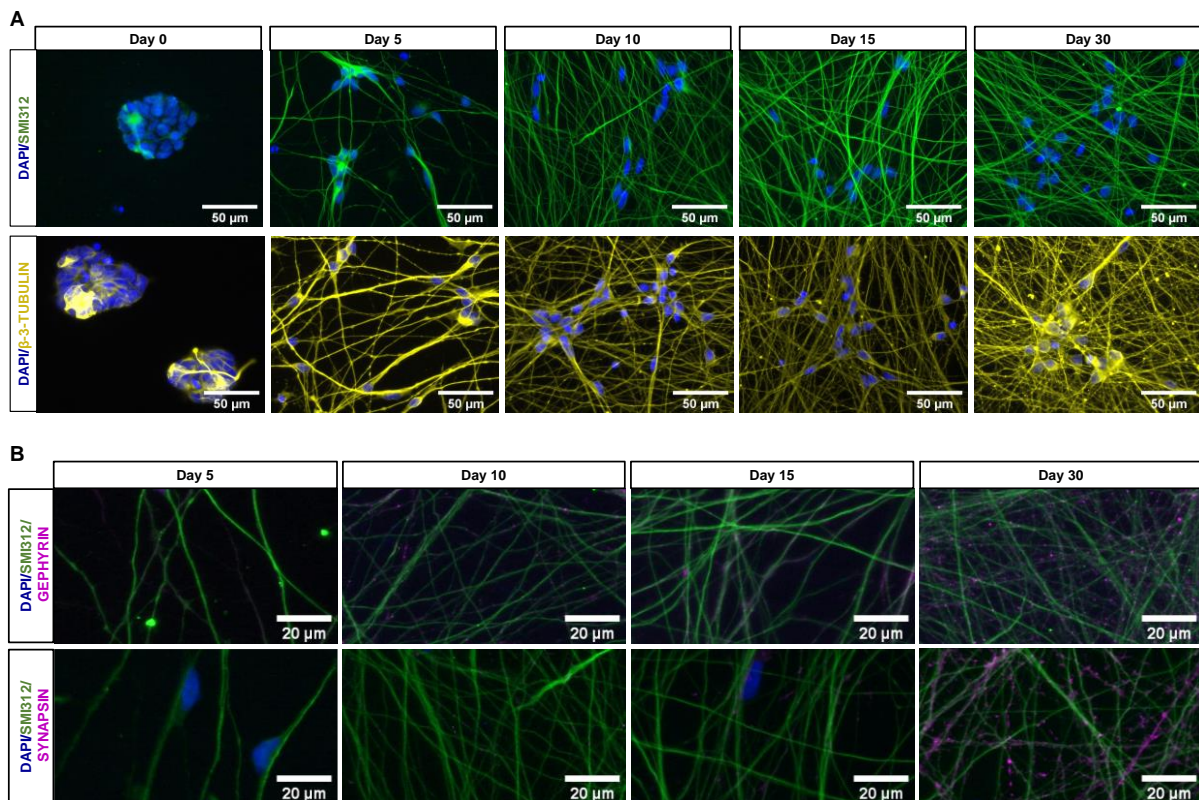


Figure 3.9: Immunostaining for additional neuronal markers. (A) Staining with the axonal markers SMI-312 (neurofilaments) and β -3-TUBULIN (microtubules) showed a sparse neuronal network at day 5 of differentiation. The network density increased over longer differentiation periods and resulted in a mature neuronal network at 30 days, as indicated by staining patterns for both markers. (B) The postsynaptic marker GEPHYRIN and presynaptic marker SYNAPSIN were not visible along axons at day 5 of differentiation. At day 10 and 15, some sporadic synaptic dots were visible for the marker GEPHYRIN, while presynaptic sites were faintly visible only from day 15 onwards. At day 30 of differentiation, both markers showed that there was a dense distribution of synapses along the axons [modified from (Strauß et al., 2021)].

Cell maturity was evaluated by examining the presence of synapses (Figure 3.9B). The markers GEPHYRIN for postsynaptic proteins and SYNAPSIN for presynaptic proteins were used together with a SMI-312 staining to visualize the localisation of the synapses along axons. 5 days of differentiation was not sufficient to visualize synapses along the neuronal network. On day 10 and 15 however, some scattered postsynaptic dots were visible on some axons, while presynaptic protein was only detectable

from day 15 onwards. At day 30 of differentiation both pre-and post-synapses are distributed densely along the neuronal network.

3.3. TAU expression in differentiated neurons with homozygous H1 or H2 *MAPT* haplotypes

When considering possible mechanisms through which the *MAPT* haplotype could convey elevated risk for tauopathies, the *MAPT* gene coding for the TAU protein is of special interest for comprehensive investigations. Indeed, some groups have found differences in TAU expression between H1 and H2 carriers in cell models as well as in patients; however, mainly at the mRNA level (Caffrey et al., 2006; Kwok et al., 2004; Myers et al., 2007). Therefore, in this work, expression of TAU at the protein level was studied in the cell lines in addition to the mRNA level. Methods include immunofluorescent and qPCR analysis of TAU (Chapter 3.3.1), Western blot (Chapter 3.3.2) and genotyping (Chapter 3.3.3).

3.3.1. Immunofluorescent and qPCR analysis of TAU

First, TAU protein expression was visualized via immunocytochemistry over the 30-day differentiation period by staining for total TAU, as well as for 3R and 4R TAU (Figure 3.10A). Total TAU and 3R TAU staining was visible from day 5 (total TAU) or day 10 (3R TAU) onwards and showed a growing and maturing neuronal network over time. Both antibodies displayed a similar staining pattern with signals in the soma as well as in the axons of neurons. The 4R TAU isoform, on the other hand, was only detectable via immunostaining after 30 days. The signal remained weak and was mainly visible in the soma.

At day 30 of differentiation, all cell lines were stained with a pan TAU antibody (Figure 3.10B). Although all cell lines exhibited a dense neuronal network, TAU signal intensity or distribution differed between some of the cell lines. The H1/H1 cell line yemz, for example, displayed strong staining in the soma but weaker TAU signal along the axons, while the H1/H1 cell line diku presented with even TAU staining throughout the whole cell. These staining differences were, however, found in both *MAPT* haplotype groups and were not haplotype dependent. Overall, the neuronal networks in all cell lines looked comparable.

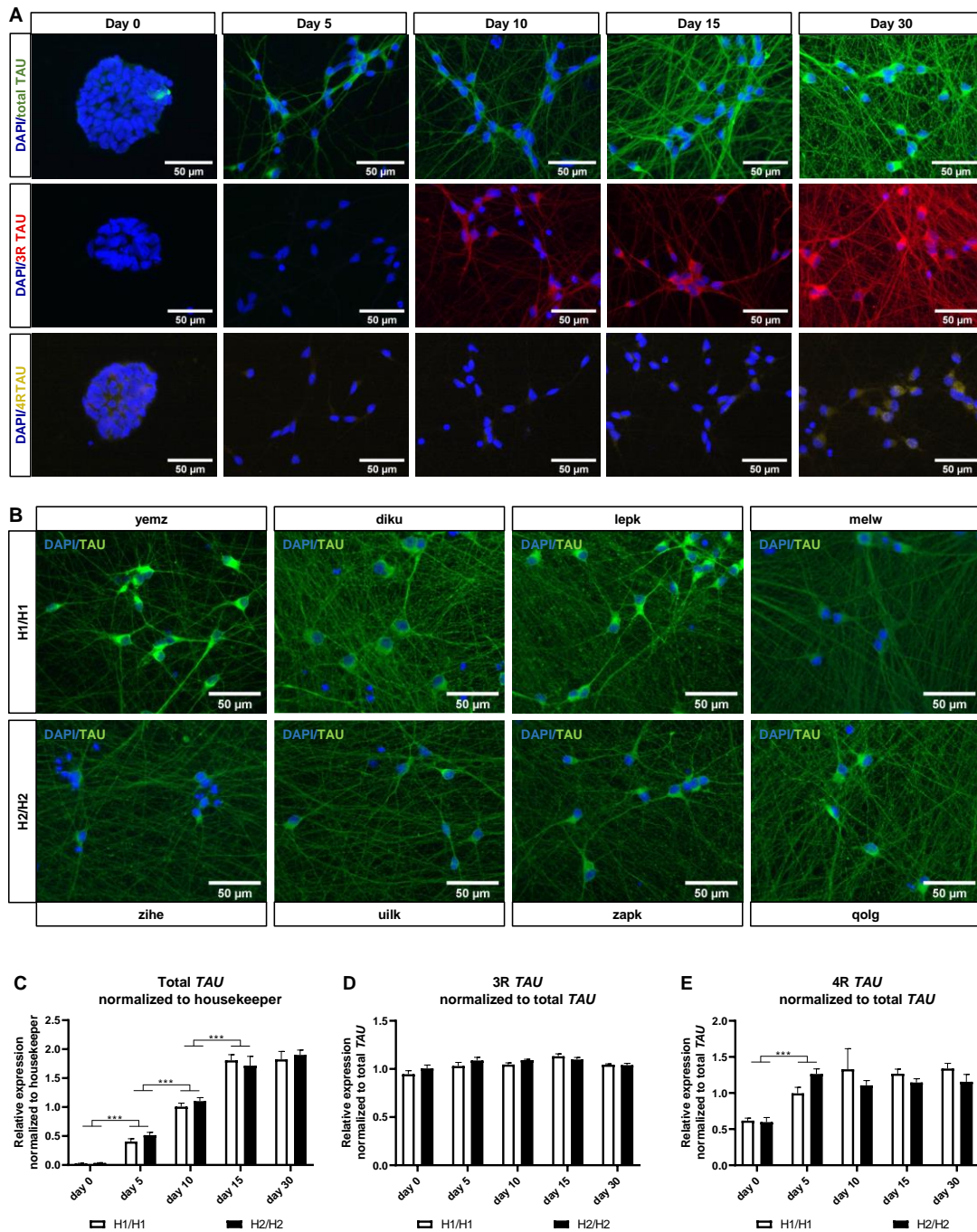


Figure 3.10: Immunofluorescent and qPCR analysis of TAU and its isoforms. (A) Immunostaining for total TAU, 3R TAU and 4R TAU over a differentiation period of 30 days. Total TAU and 3R TAU staining was visible from day 5 and 10 onwards, respectively, showing a growing and maturing neuronal network during the differentiation period. The 4R TAU isoform, however, was only detectable after day 30 of differentiation. The signal was weak and mainly visible in the soma. **(B)** TAU staining at day 30 of differentiation revealed differences in TAU signal intensity between cell lines, but the neuronal networks in general looked similar and there were no differences visible between the haplotype groups. **(C-E)** qPCR data for total *TAU*, 3R *TAU* and 4R *TAU*. Total *TAU* levels normalized to housekeeping genes increased significantly with differentiation time until day 15 and then remain stable. 3R and 4R *TAU* data was normalized to total *TAU* levels. 3R *TAU* mRNA levels did not change over the differentiation period, while 4R *TAU* levels increased significantly from day 0 to day 5 relative to total *TAU*. No expression differences could be detected between H1/H1 and H2/H2 haplotype groups. Data are represented as mean \pm SEM of $n=4$ cell lines for each haplotype group. 2-way ANOVA followed by Tukey's test was performed. *** $p < 0.001$ [modified from (Strauß et al., 2021)].

mRNA levels of *TAU* were investigated with qPCR using primers specific for total *TAU*, or the 3R *TAU* and 4R *TAU* isoforms (see Figure 3.10C-E). After normalizing total *TAU* data to housekeeping genes, a significant increase in mRNA levels from day 0 to day 15 of differentiation could be observed (Figure 3.10C). From day 15 to day 30, total *TAU* mRNA levels remained unchanged. 3R and 4R *TAU* data were normalized to total *TAU* levels to assess changes in isoform expression independent from overall *TAU* levels (Figure 3.10D and E). The 3R *TAU* level stayed unchanged over time, while, on the other hand, 4R *TAU* increased significantly from day 0 to day 5. This indicates an upregulation of the 4R isoform when neuronal differentiation is induced. For the remaining differentiation period, 4R expression remained unchanged. No differences in expression levels of total *TAU* or any isoforms were detected between the H1/H1 and H2/H2 haplotype groups, illustrated as white and black bars, respectively.

3.3.2. Protein analysis of TAU via Western blot

After assessing *TAU* mRNA levels in the cell lines, multiple antibodies were used to study the expression of TAU protein at different time points in the soluble as well as in the insoluble protein fraction. Results of Western blot analysis are shown in Figure 3.11 and Figure 3.12. For total TAU levels, two different antibodies were used: a polyclonal TAU antibody from Dako and a monoclonal TAU-5 antibody from Millipore. The polyclonal antibody had a higher sensitivity, allowing for detection of TAU protein even in expanding cells (day 0). The monoclonal TAU antibody, TAU-5, only detected TAU protein in differentiating cells, starting at day 5. Both antibodies showed a continuous increase in TAU expression as differentiation proceeded with the highest levels detectable at day 30 of differentiation (Figure 3.11A and B).

The total TAU protein in the insoluble protein fraction showed, comparable to that in the soluble fraction, increasing levels with proceeding differentiation. Again, the Dako antibody detected TAU at day 0, while the TAU-5 antibody detected a signal only after 5 days of differentiation. For both antibodies, TAU levels stayed consistent from day 10 to day 15 but increased again until day 30 (Figure 3.11E and F). Comparing the H1/H1 and H2/H2 groups regarding their total TAU levels, no significant difference was detectable, neither in the soluble nor in the insoluble fraction.

In accordance with the mRNA analysis, 3R and 4R TAU Western blot data was normalized to total TAU to assess changes in isoform levels independent from overall TAU levels. While the 3R TAU level stayed constant during the differentiation period up until day 15, after which it significantly decreased up to day 30 (Figure 3.11C), the 4R TAU isoform was only weakly detectable from day 15 onwards (Figure 3.11D). This makes 3R TAU the predominant TAU isoform expressed in this cell model and during this time period. In accordance with this 3R TAU data which shows a decrease in expression from day 15 onwards, the 4R TAU level, although still weak, increased significantly between day 15 and day 30. 3R TAU levels remained stable over the whole differentiation period in the insoluble protein fraction,

while the 4R TAU isoform could not be detected (Figure 3.11G and H). There were no significant differences in TAU isoform expression between H1 and H2 cell lines in either soluble or insoluble fractions.

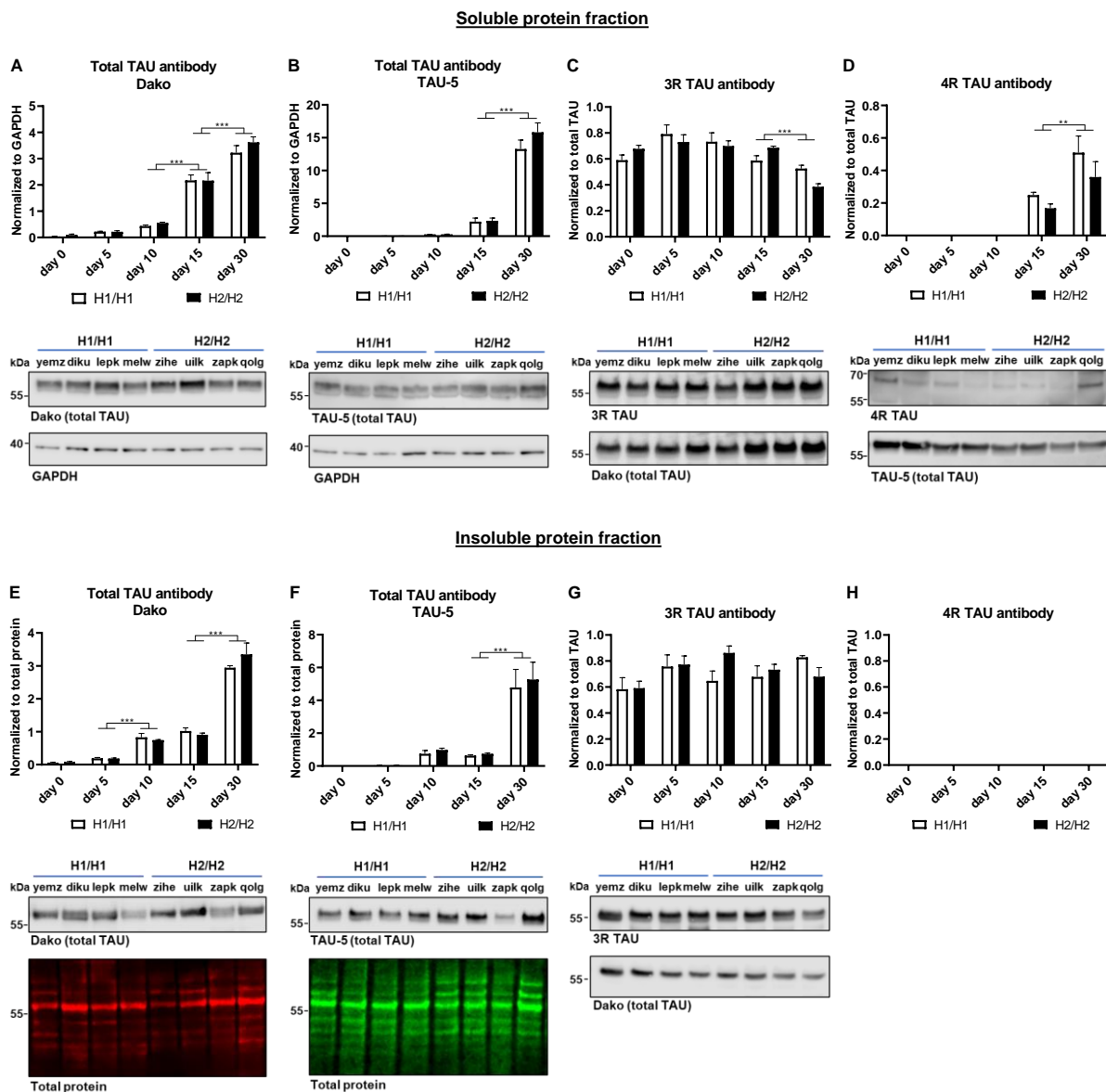


Figure 3.11: Western blot analysis with total TAU, 3R and 4R TAU antibodies over 30 days. (A-D) Western blot analysis of the soluble protein fraction. Total TAU levels were detected with Dako and TAU-5 antibodies (A and B) and data was normalized to GAPDH. Total TAU expression increased significantly as differentiation progressed, reaching its highest levels at day 30. (C and D) 3R and 4R TAU data was normalized to total TAU levels. 3R TAU expression stayed constant until day 15 and then decreased significantly, while 4R TAU was only detectable from day 15 onwards and increased significantly up to day 30. (E-H) Western blot analysis of insoluble protein fraction. Total TAU levels were detected with Dako and TAU-5 antibodies (E and F) and data was normalized to total protein. Total TAU expression increased significantly with longer differentiation periods, reaching its highest levels at day 30. While 4R TAU (H) was not detectable, 3R TAU levels were normalized to total TAU levels (G) and remained unchanged over the differentiation period. No significant differences could be detected between H1/H1 and H2/H2 cell lines for any of the antibodies or fractions. Data are represented as mean \pm SEM of $n=4$ cell lines for each haplotype group. 2-way ANOVA followed by Tukey's test was performed. ** $p<0.01$, *** $p<0.001$. Displayed Western blot pictures are representative blots from day 30 of differentiation for the respective antibody [taken from (Strauß et al., 2021)].

Levels of phosphorylated TAU (p-TAU) were analyzed using two different p-TAU antibodies (Figure 3.12). The AT8 and the AT180 antibodies bind to different phosphorylated epitopes on the TAU protein, with AT8 binding phosphorylated Serine202 and Threonine205 and AT180 binding phosphorylated Threonine230. As with the TAU isoform expression analysis above, p-TAU signal was normalized to the total TAU signal. Both AT8 and AT180 clones showed an increase of p-TAU levels over time, indicating that with extended differentiation time more TAU becomes phosphorylated. With both p-TAU antibodies, a signal could only be detected in differentiating cells (day 5 onwards) and the highest p-TAU levels were found at day 30 of differentiation (Figure 3.12A and B). The p-TAU levels, however, did not differ significantly, when comparing the H1/H1 and H2/H2 haplotype groups at any time point.

Similar to the soluble fraction, there was no p-TAU signal detectable in the insoluble protein fraction from proliferating cells (Figure 3.12D and E). The earliest time point at which there was a weak p-TAU signal was day 5 of differentiation. In contrast to the soluble protein fraction (but in line with the total TAU results of the insoluble fraction), the p-TAU level stayed constant between day 10 and day 15 of differentiation. From day 15 to day 30 p-TAU level increased again. Although there was variability in p-TAU signal between cell lines, there was no *MAPT* haplotype-dependent difference.

In addition to the investigation of phosphorylated TAU, levels of conformationally changed TAU in the cell lines at different time points was studied (Figure 3.12C and F). This was assessed with the MC1 antibody that recognizes a disease-specific TAU conformational change dependent on the N-terminus and a sequence in the third microtubule-binding repeat (Jicha et al., 1997). In line with the Western blot results of the other antibodies, the MC1 signal in the soluble and insoluble protein fractions also increased during the differentiation period. The highest levels of MC1-positive TAU were measurable at day 30 of differentiation. Like the p-TAU antibodies, MC1-positive TAU was only detectable from day 5 onwards in the soluble protein fraction and from day 10 onwards in the insoluble protein fraction. In the soluble fraction, there was no significant difference in levels of conformationally-changed TAU detected with the MC1 antibody between H1 and H2 lines. The insoluble fractions from H2/H2 cell lines, however, had significantly higher levels of MC1-positive TAU at day 30 of differentiation than H1/H1 cell lines.

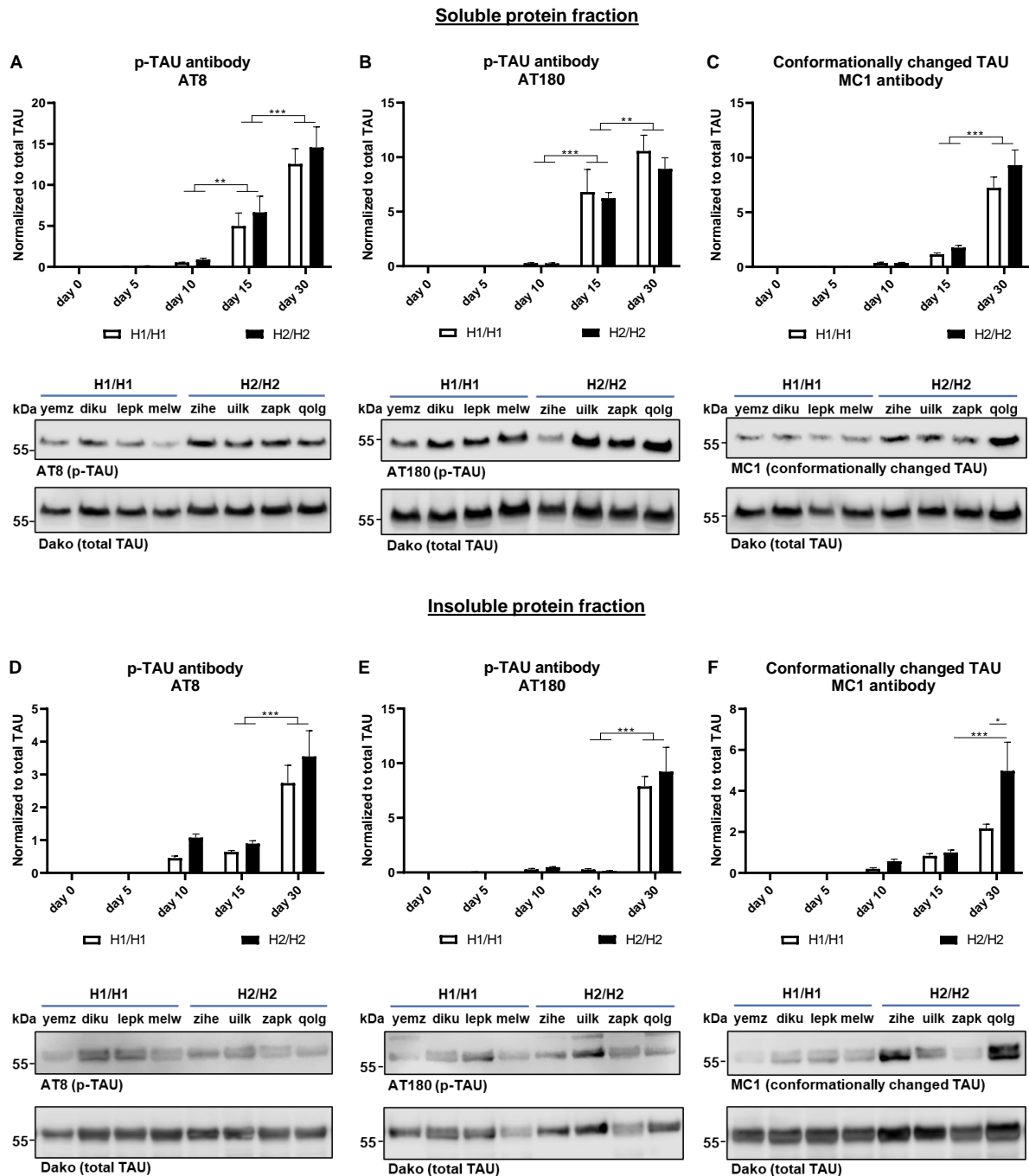


Figure 3.12: Western blots for phosphorylated and conformationally changed TAU. For assessment of phosphorylated TAU (p-TAU) levels, two antibodies were used: AT8 and A180. Conformationally changed TAU was detected with the MC1 antibody. Western blot data was normalized to total TAU levels for all three antibodies. (A-C) Western blot analysis of the soluble protein fraction. MC1, AT8 and A180 antibodies showed that p-TAU and conformationally changed TAU increased significantly with longer differentiation periods, reaching their highest levels at day 30. (D-E) Western blot analysis of the insoluble protein fraction. Once again MC1, AT8 and A180 antibodies showed that p-TAU and conformationally changed TAU increased significantly with longer differentiation periods, reaching their highest levels at day 30. For both fractions, no significant differences could be detected between H1/H1 and H2/H2 haplotype groups when using either of the two p-TAU antibodies. In the soluble fraction there was also no significant difference between H1 and H2 cells for the MC1 antibody. In the insoluble fraction, however, H2/H2 cell lines showed significantly higher levels of MC1-positive TAU at day 30 of differentiation than H1/H1 cells. Data are represented as mean \pm SEM of $n=4$ cell lines for each haplotype group. 2-way ANOVA followed by Tukey's or Sidak's test (MC1 Western blot) was performed. * $p<0.05$, *** $p<0.001$. Displayed Western blot pictures are representative blots from day 30 of differentiation for the respective antibody [taken from (Strauß et al., 2021)].

3.3.3. Genotyping for H1 sub-haplotypes

The H1 haplotype can further be divided into sub-haplotypes that have been described by Pittman et al. (see also Table 1.2) (Pittman et al., 2005). In some studies, an association of the H1 haplotype with a risk for neurodegenerative diseases could only be found for a sub-haplotype, for example the H1c haplotype (Ezquerra et al., 2011; Myers et al., 2005). Therefore, the H1/H1 cell lines were mapped regarding their H1 sub-haplotype genotype using the SNPs described in Chapter 1.1.3 and Table 1.2. The following Table 3.1 shows that none of the analyzed cell lines is homozygous for a sub-haplotype, therefore, a further examination was not performed.

Table 3.1: Genotyping of H1 cell lines for H1 sub-haplotypes-defining SNPs

Cell line	rs1467967	rs242557	rs3785883	rs2471738	rs8070723	rs7521
yemz	A/A	A/G	G/A	T/C	A/A	A/A
diku	A/A	A/A	G/G	C/T	A/A	G/G
lepik	A/A	A/A	G/G	T/C	A/A	G/A
melw	A/A	A/G	G/G	C/T	A/A	A/A

3.4. α -SYNUCLEIN expression in differentiated neurons with homozygous H1 or H2 *MAPT* haplotypes

3.4.1. Analysis of α -SYNUCLEIN expression on mRNA and protein level

In addition to being a major risk factor for some tauopathies, the H1 haplotype has been associated with an increased risk of PD (Di Battista et al., 2014; Ezquerra et al., 2011; Zabetian et al., 2007). Since PD is classified as a synucleinopathy with α -SYNUCLEIN being the primarily affected protein, not only the expression profile of TAU was studied in the cell model but also the expression levels of α -SYNUCLEIN.

First, α -SYNUCLEIN expression on the mRNA level was investigated using qPCR (Figure 3.13A). Over the differentiation period of 30 days, a steady increase in α -SYNUCLEIN mRNA levels were observed. When comparing the H1 and H2 *MAPT* haplotype groups, the H1/H1 cell lines expressed significantly more α -SYNUCLEIN than the H2/H2 cell lines – independent of the time point (2-way ANOVA $p=0.011$).

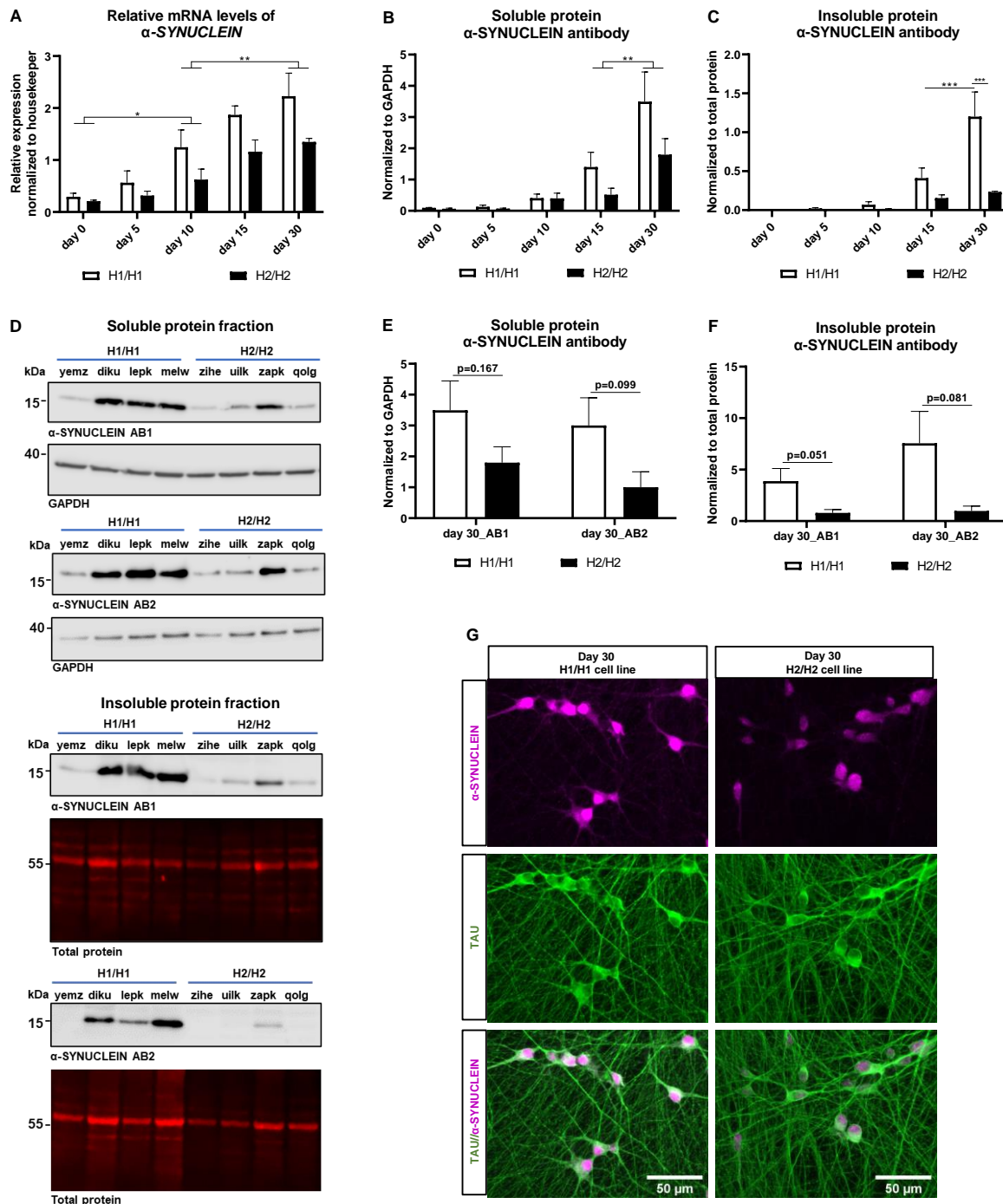


Figure 3.13: Analysis of α -SYNUCLEIN expression over time on protein and mRNA levels. (A) mRNA analysis with qPCR for α -SYNUCLEIN over a differentiation period of 30 days. α -SYNUCLEIN expression increased significantly and continuously over time. H1/H1 cell lines showed significantly higher α -SYNUCLEIN levels than H2/H2 cell lines independent of the differentiation time ($p=0.0011$). Data are represented as mean \pm SEM of $n=4$ cell lines for each haplotype group. 2-way ANOVA followed by Tukey's test was performed. * $p<0.05$, ** $p<0.01$. (B-C) Western blot analysis of soluble and insoluble protein fraction for α -SYNUCLEIN during a differentiation time of 30 days. α -SYNUCLEIN protein expression increased significantly over time in both fractions. Significantly higher α -SYNUCLEIN levels could be detected in the H1/H1 haplotype group compared to the H2/H2 haplotype group in both protein fractions. In the soluble protein fraction, this observation was independent of the differentiation time point ($p=0.036$). In the insoluble protein fraction, however, a statistically significant difference between H1 and H2 cells did not manifest until day 30 of differentiation. Data are represented as mean \pm SEM of $n=4$ cell lines for each haplotype group. 2-way ANOVA was performed followed by Tukey's or Sidak's test. ** $p<0.01$, *** $p<0.001$.

Figure 3.13 (continued): (D) Representative Western blots for two α -SYNUCLEIN antibodies (AB1 and AB2) for the soluble and the insoluble protein fraction at day 30 of differentiation. (E-F) Western blot analysis of soluble and insoluble protein with two different α -SYNUCLEIN antibodies (AB1 and AB2) in 30-day old cells could not detect a significant difference between H1/H1 and H2/H2 groups when testing with an unpaired t-test. Data are represented as mean \pm SEM of n=4 cell lines for each haplotype group. (G) Immunofluorescent staining of a representative H1/H1 and H2/H2 cell line for α -SYNUCLEIN and TAU at day 30. A stronger α -SYNUCLEIN signal in the H1 cells was visible compared to H2 cells, while TAU staining was comparable between the two cell lines [taken from (Strauß et al., 2021)].

For further examination, the α -SYNUCLEIN protein expression in soluble and insoluble protein fractions was analyzed via Western blot (Figure 3.13B and C). Similar to the mRNA data, α -SYNUCLEIN protein expression increased continuously with increasing differentiation period, both in the soluble as well as in the insoluble protein fraction. Additionally, significantly higher expression of α -SYNUCLEIN was detected in the H1/H1 cell lines as compared to H2/H2 lines. In the soluble protein fraction this observation was independent of the length of differentiation (2-way ANOVA $p=0.036$). In the insoluble protein fraction, however, a statistically significant difference between H1 and H2 groups did not manifest until day 30 of differentiation, although the tendency towards higher α -SYNUCLEIN levels in H1 cells was visible at earlier time points.

As there was a significant difference in α -SYNUCLEIN levels between haplotype groups in both fractions at day 30 of differentiation as well as the highest overall α -SYNUCLEIN expression, this time point was used to verify the Western blot results with a second α -SYNUCLEIN antibody (AB2). This AB2 could replicate the Western blot results from the first antibody (AB1) (Figure 3.13D-F). However, when testing the day 30 data from both antibodies with an unpaired t-test, no statistically significant difference was detected between the H1 and H2 haplotype groups for either antibody or protein fraction.

Finally, to visualize α -SYNUCLEIN protein expression differences between H1 and H2 cells, two representative cell lines with each *MAPT* genotype at day 30 of differentiation were selected and stained via immunocytochemistry (Figure 3.13G). In accordance with the results from qPCR and Western blot, the H1/H1 cell line displayed a stronger α -SYNUCLEIN signal than the H2/H2 cell line, while on the other hand, the TAU staining of the neuronal network is comparable between both cell lines.

3.4.2. α -SYNUCLEIN expression over time via immunocytochemistry

To visualize α -SYNUCLEIN expression and cellular localization during the 30-day differentiation period, one representative cell line was immunostained with an α -SYNUCLEIN antibody (Figure 3.14). While there was a strong signal in proliferating cells, this is most likely an unspecific signal, since it contradicts the Western blot results showing a lower α -SYNUCLEIN level at day 0 than in differentiating cells. After 5 days of differentiation, α -SYNUCLEIN expression was mainly located in the nucleus. In 10- and 15-

day old cells, the signal intensity increased and the cellular distribution of α -SYNUCLEIN started to change, localizing the protein not only in the nucleus but also in the soma. After 30 days of differentiation the signal intensity greatly increased, especially in the nucleus. Furthermore, at this point, α -SYNUCLEIN was now also distributed along the axons indicating a greater maturity of the cells since α -SYNUCLEIN is a synaptic protein.

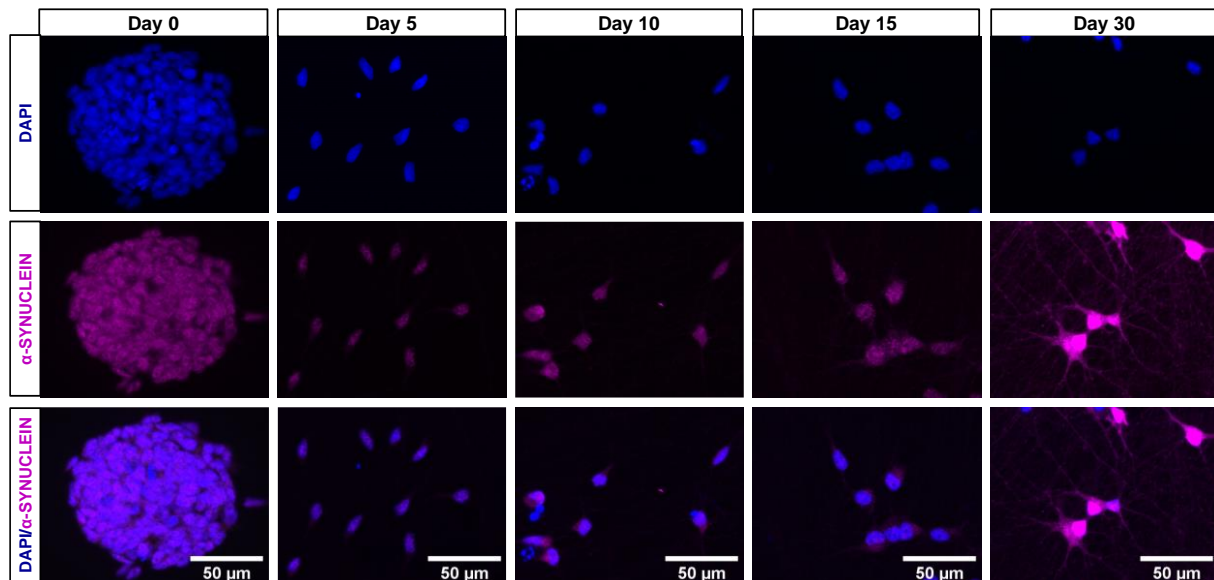


Figure 3.14: Immunostaining of α -SYNUCLEIN expression over 30 days. Cells expressed a weak mainly nuclear α -SYNUCLEIN signal at day 5 of differentiation. At day 10 and 15, signal intensity only slightly increased while the distribution of α -SYNUCLEIN expanded from the nucleus to the soma of the cells. In 30-day old cells, α -SYNUCLEIN staining was also visible along axons, while the staining intensity greatly increased in the nucleus and soma.

3.4.3. Genotyping of *SNCA* gene for disease conveying SNPs

The observed differences in α -SYNUCLEIN expression between H1 and H2 cell lines already at the mRNA level is an unexpected result. Although the *MAPT* genotype encompasses not only the *MAPT* gene coding for TAU but also several other genes, none of the genes thus far have been described to regulate α -SYNUCLEIN transcription. Therefore, the *SNCA* gene coding for α -SYNUCLEIN was investigated in all cell lines to rule out possible gene variations that could influence differential α -SYNUCLEIN expression.

Over the years, numerous SNPs in the *SNCA* gene, for example in the promotor region and the 3'-UTR, have been associated with a higher risk of developing synucleinopathies, potentially by changing α -SYNUCLEIN expression (Campêlo and Silva, 2017). Eight of the SNPs that have been described to increase PD risk and/or were associated with higher expression of α -SYNUCLEIN were selected (Table 3.2). The cell lines were genotyped for the selected SNPs (Table 3.3), to investigate whether the differential α -SYNUCLEIN expression between the cell line groups could be explained by SNPs in the *SNCA* gene.

Table 3.2: Location of SNPs on SNCA gene

5' UTR (promotor region)	Intron 4	3' UTR
rs2619363 (Winkler et al., 2007)	rs2736990 (McCarthy et al., 2011; Pan et al., 2013)	rs356165 (Cardo et al., 2012; Winkler et al., 2007)
rs2619364 (Winkler et al., 2007)		rs356219 (Linnertz et al., 2009; Mata et al., 2010)
rs2583988 (Winkler et al., 2007)		rs181489 (Elbaz et al., 2011)
<i>Rep1</i> (Chiba-Falek and Nussbaum, 2001; Cronin et al., 2009; Fuchs et al., 2008)		rs356182 (Cheng et al., 2016)

When grouping the cell lines according to their SNP genotypes in the *SNCA* gene, there was no association of any *SNCA* genotype with the expression pattern observed for the cell lines.

Table 3.3: Genotypes of cell lines for certain SNPs in SNCA gene

Cell line	rs2583988	rs2610364	rs2619363	rs356182	rs181489	rs356219	rs356165	rs2736990
yemz	C/T	A/G	G/T	G/A	T/C	G/A	G/A	G/A
diku	C/T	A/G	G/T	G/G	T/T	G/G	G/G	G/G
lepik	T/T	G/G	T/T	G/G	T/T	G/G	G/G	G/G
melw	C/T	A/G	G/T	G/A	T/C	G/A	G/A	G/A
zihe	C/C	A/A	G/G	G/A	T/C	G/A	G/A	G/A
uilk	C/C	A/A	G/G	A/A	C/C	A/A	A/A	A/A
zapk	C/C	A/A	G/G	A/A	C/C	A/A	A/A	A/A
qolg	C/C	A/A	G/G	A/A	C/C	A/A	A/A	A/A

In addition to SNPs, a complex, polymorphic microsatellite called *Rep1* (D4S3481) near the *SNCA* promotor region (approximately 10 kb upstream of the transcription start site) has been associated with enhanced risk for PD (Fuchs et al., 2008). The number of dinucleotide repeats in the microsatellite sequence can differ: (TC)₁₀₋₁₁(TT)₁(TC)₉₋₁₁(TA)₇₋₉(CA)₁₀₋₁₃. Depending on the length of the sequence, PCR products (when resolved by electrophoreses) run at 257 bp, 259 bp, 261 bp and 263 bp and this nomenclature is used when the *Rep1* genotypes are described (Chiba-Falek et al., 2003). Studies have shown that longer repeats in *Rep1* (261 and 263 bp) are associated with increased transcription of α -SYNUCLEIN (Cronin et al., 2009; Fuchs et al., 2008). Therefore, the *Rep1* repeat sequences of the cell lines were identified and cells were genotyped accordingly (Table 3.4). But again, when grouping the cell lines corresponding to their *Rep1* genotype, no expression pattern explaining the α -SYNUCLEIN expression data could be found.

Table 3.4: Sequence of *Rep1* microsatellite for the different cell lines

Cell line → genotype*	TC	TT	TC	TA	CA	Genotype according to length
Reference sequence → 0/0	10	1	10	8	10	259/259
yemz → 0/1	11	1	9	10	10	259/263
diku → 1/1	10/11	1	10	8	11/10	261/261
lepik → 0/1	11	1	11	7	10	259/261
melw → 0/1	11	1	11	7	10	259/261
zihe → 0/0	10	1	10	8	10	259/259
uilk → 1/1	10	1	10	8	11	261/261
zapk → 0/1	10	1	11	7	11	259/261
qolg → 0/1	10	1	10	8	11	259/261

* When sequence is different to reference sequence on only one allele, only this deviant sequence is listed in the table.

3.5. Vulnerability of differentiated neurons with homozygous H1 or H2 *MAPT* haplotypes to external stressors

In sporadic neurodegenerative diseases there is no apparent genetic mutation that is causal for the disease. Although several genetic risk factors have been identified to increase the risk for sporadic neurodegeneration (such as the *MAPT* haplotype), they are not enough to solely trigger neurodegenerative diseases but rather act in combination with other genetic variations and/or environmental factors. To investigate whether the *MAPT* haplotype could influence vulnerability to environmental factors, cell lines were exposed to external stressors like oxidative stress and toxins. Mimicking a physiological version of oxidative stress, cells were not treated with a reactive oxygen species (ROS) inducing reagent but were cultured, first in expansion and then during differentiation, in medium deprived of antioxidants. This way, the ROS generated during normal metabolic activity accumulated over time and caused oxidative stress. The cell damage due to accumulating ROS is a slow process compared to the treatment with toxins, the viability was therefore assessed over several days to capture the point of cell death (which could change between experiments). When cells were differentiated in medium without antioxidants, axons started to spontaneously degenerate after approximately 10 days of differentiation (Figure 3.15B). Although the variability between experiments and different cell lines was high, the cell viability measured with the calcein assay was significantly reduced to 50 % after 15 days of differentiation (Figure 3.15A). A significant difference in vulnerability to oxidative stress between H1/H1 and H2/H2 groups could, however, not be detected.

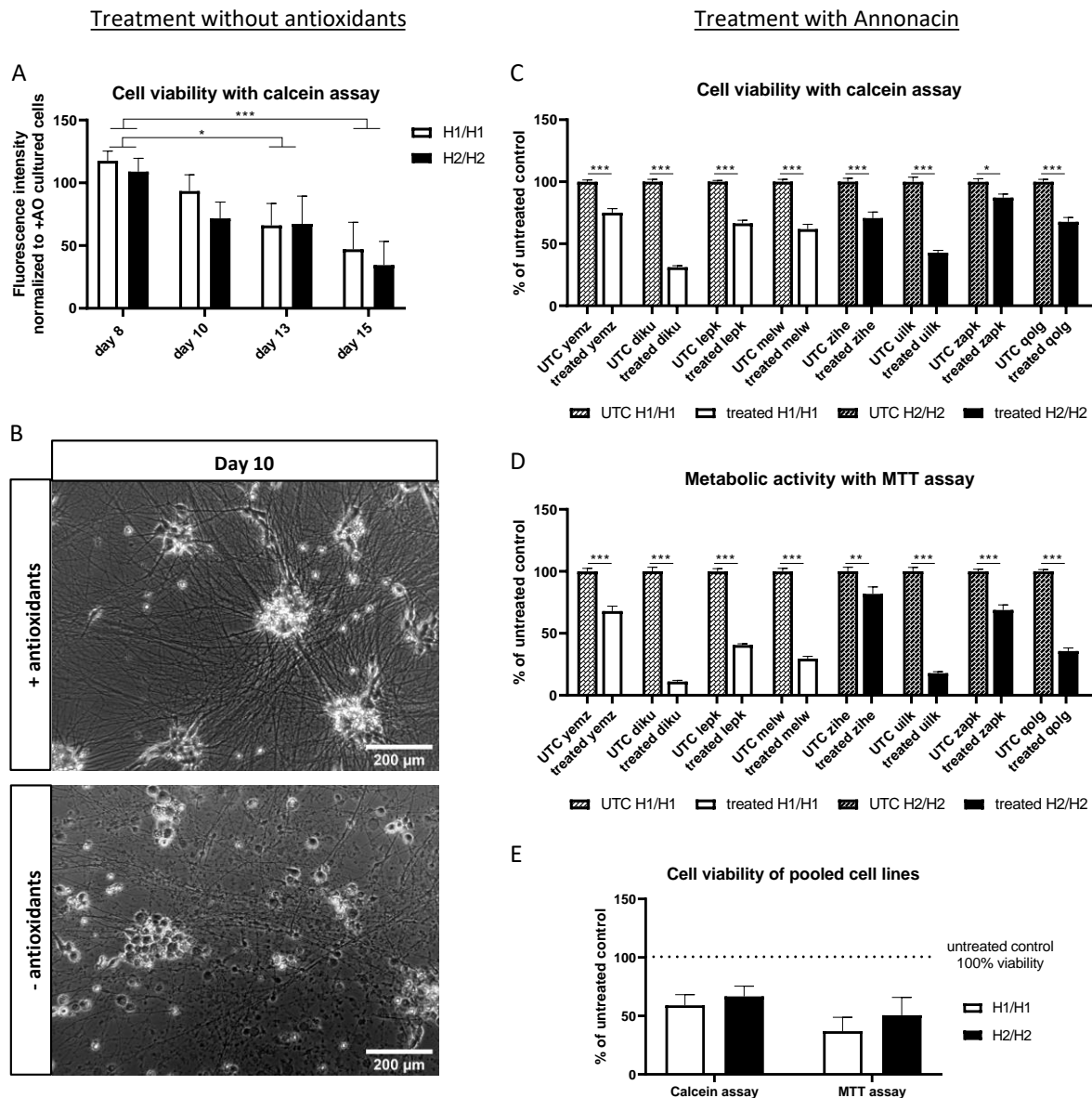


Figure 3.15: Treatment of cells with external stressors. (A-B) Cells were differentiated in medium without antioxidants (AO) and cell viability was assessed with calcein staining from day 8 to day 15 (A). Cell viability started to decrease from day 10 onwards and was reduced to 50 % at day 15. There were no significant differences in cell viability between cell lines with H1/H1 and H2/H2 haplotypes. Data are represented as mean \pm SEM of $n=4$ cell lines for each haplotype group. 2-way ANOVA followed by Tukey's was performed. * $p<0.05$, *** $p<0.001$. (B) At day 10, signs of degeneration were visible in cells cultured without antioxidants. (C-E) Cells were treated with the mitochondrial inhibitor annonacin for 4 days. Cell viability was analyzed with calcein staining (C) and metabolic activity with MTT assay (D). A 4-day treatment with annonacin reduced cell viability and mitochondrial activity significantly in all cell lines compared to untreated controls (UTC). Data are represented as mean \pm SEM of $n=8$ independent experiments per cell line. 2-way ANOVA followed by Sidak's test was performed. * $p<0.05$, ** $p<0.01$, *** $p<0.001$ (E) When cell lines were pooled into haplotype groups, no significant difference in cell viability or metabolic activity could be detected between H1/H1 and H2/H2 groups after annonacin treatment. Data are represented as mean \pm SEM of $n=4$ cell lines for each haplotype group. Unpaired t-test was performed [modified from (Strauß et al., 2021)].

To further investigate the susceptibility of the cell lines to environmental factors, the cells were treated with the mitochondrial inhibitor annonacin. This toxin has been described to cause atypical parkinsonism (Caparros-Lefebvre and Elbaz, 1999; Höglinger et al., 2005). At a differentiation time of 26 days, the cells were treated with 800 nM annonacin for 4 days. The cell viability was measured using the live-cell stain calcein at day 30 of differentiation while the mitochondrial activity was assessed with the MTT assay. 4 days of toxin treatment significantly reduced metabolic activity and cell viability in all cell lines (Figure 3.15C and D). The reduction in viability ranged between the cell lines from 30 to 80% and the reduction in mitochondrial activity showed even greater variability ranging from 10 to 80%. Percentage reduction in cell viability correlated with a similar level of reduction in metabolic activity. When the H1 and H2 *MAPT* haplotype groups were compared regarding their vulnerability to annonacin, a trend towards higher cell viability for H2/H2 cells was visible for both the calcein and MTT assays, although this difference did not reach statistical significance (Figure 3.15E).

4. Discussion

Sporadic tauopathies are one of the main challenges in modern neurobiological research, especially since the underlying mechanisms remain unclear. GWA studies have identified the *MAPT* haplotype as a major risk factor for neurodegenerative diseases, surprisingly not only for tauopathies such as CBD, PSP and AD but also for the synucleinopathy PD. How the H1 haplotype influences the risk for neurodegenerative disorders is, however, still under investigation. Studies in postmortem brain tissue have reported differential expression of *TAU* mRNA in H1/H1 carriers as compared to H2/H2 carriers (de Jong et al., 2012; Valenca et al., 2016). Additionally, experiments in heterozygous reporter cell lines such as neuroblastoma cell lines and iPSCs have found differential expression levels from the H1 allele as compared to H2 (Beevers et al., 2017; Caffrey et al., 2006; Kwok et al., 2004). So far, a systematic analysis of iPSCs with the two homozygous *MAPT* haplotypes, H1/H1 and H2/H2 has been missing in scientific literature. The analyses presented in this work aimed to close that gap.

The following sections discuss the results as presented in Chapter 3.

4.1. Cell differentiation and characterization

Since the development of the iPSC model, a number of differentiation protocols from iPSC to neurons have been established to model neurodegenerative diseases. The drawbacks of a direct differentiation are long differentiation times between 70 to 200 days or more (Garcia-Leon et al., 2018; Iovino et al., 2015; Silva et al., 2016; Sposito et al., 2015) and a great variability in the resulting neuronal cell population (Volpato et al., 2018). For a comparison of several cell lines with different genetic backgrounds, however, a minimal variability during the differentiation is essential. Therefore, an adapted technique from Zhang et al. was employed in this work that utilizes the overexpression of *NGN2* in iPSCs to induce a rapid differentiation into cortical layer 2/3 neurons (Zhang et al., 2013). To further increase robustness of the model, the iPSCs were first converted into smNPC before transfection with the *NGN2*-lentivirus as described by Dhingra et al. (Dhingra et al., 2020). smNPCs have the advantage of being neural progenitors that can be cryopreserved and expanded for numerous passages without changing their differentiation properties (Reinhardt et al., 2013).

Within 5 days of induction of *NGN2* overexpression in the obtained *NGN2*_smNPCs, all cell lines expressed important neuronal markers such as β -3-TUBULIN, MAP2 and TAU on a protein level and the percentage of the neuronal population (MAP2 positive cells) reached over 90%. Accordingly, the neural stem cell marker SOX2 was downregulated after 5 days of differentiation on the mRNA level. Additionally, the number of cells positive for the neural progenitor marker NESTIN decreased from day 10 onwards. These results indicate a switch in cell fate from neural stem cells to maturing neurons in

the first 10 days on the mRNA and protein levels. There were no significant differences between H1/H1 and H2/H2 cell lines in the expression of the above-named markers, indicating a comparable differentiation rate for both haplotype groups. The neurons further matured with a longer differentiation period, visible by the expression of synaptic proteins and the growing neuronal network. Electrophysiological properties of the cells, however, were not analyzed in this work. All eight cell lines displayed a comparable pattern in MAP2 staining at day 30 of differentiation, although, neurite length, growth cones and synapses have not been analyzed in detail. With glial cell numbers under 1% and neuronal numbers over 90%, the cell cultures consisted of a highly enriched neuronal population. Further characterization of the obtained neurons showed a comparable percentage of cortical and GABAergic neurons between the two haplotype groups.

Overall, the employed protocol used in this study allowed for a fast and robust differentiation that was suitable for the comparison of different cell lines.

Although the differentiation of iPSCs into enriched neuronal cultures is desirable when comparing several different cell lines, the cultures lack the complexity of the biological cell composition in the human brain which can be, for example, achieved with primary foetal human neural progenitor cells (Moon et al., 2016). The lack of glial cells might limit the differentiation time of the protocol to 30 days. The results show that without the support of non-neuronal cell populations, the number of viable cells decreased by 50% from day 30 to day 60 of differentiation. Since the cells already expressed a variety of important neuronal marker (such as MAP2, β -3-TUBULIN, TAU, SYNPASIN and GABA) at day 30 of differentiation, this differentiation period was considered acceptable for this study.

4.2. TAU expression in differentiated *NGN2*_smNPCs

4.2.1. TAU expression over the 30-day differentiation period

In the human brain, the expression of all six TAU isoforms is developmentally regulated and only occurs in the adult brain. Since iPSC-derived neurons mostly remain in an early developmental state, they predominantly express the foetal 0N3R TAU isoform (Fong et al., 2013; Miguel et al., 2019; Nakamura et al., 2019). This remains a major challenge for tauopathy modelling with iPSC. Direct differentiation protocols need at least 100 days until 4R TAU is detectable (Garcia-Leon et al., 2018; Iovino et al., 2015; Sposito et al., 2015). In the iPSC model used in this study, expression of 4R TAU protein is detected at day 15. Although 0N3R TAU is the predominant isoform expressed in this model, 3R TAU levels started to decrease between day 15 and day 30 of differentiation, while the 4R TAU isoform increased. This indicates a fast maturation of cells under *NGN2* overexpression.

The protein expression of 4R TAU was, however, still very low at day 30 of differentiation (visible in western blot and immunostaining at low signal intensity). It is therefore expected that a longer

differentiation period would increase the ratio of 4R TAU, ultimately leading to the developmental switch to equal levels of 3R and 4R isoforms as shown with other differentiation methods (Sposito et al., 2015). Unfortunately, a differentiation period exceeding 30 days with the protocol used here without an astrocyte co-culture was not possible due to drastic reduction in cell viability.

With a longer differentiation period and increased TAU expression, TAU levels in the insoluble protein fraction increased, indicating more aggregated TAU with the increasing age of the neurons. Furthermore, over time, more TAU became phosphorylated. Since p-TAU is known to have a reduced binding affinity to microtubules and a higher propensity to aggregate (Drewes et al., 1995; Köpke et al., 1993), higher p-TAU levels could be the reason why an increased level of TAU was found in the insoluble fraction with increasing differentiation time. This is also supported by increased p-TAU levels in the insoluble fraction.

4.2.2. TAU expression in homozygous H1 and H2 neurons

After the *MAPT* haplotype was connected to a greater risk of developing neurodegenerative disorders, several scientists have tried to elucidate the causal mechanisms. Since splicing mutations in the *MAPT* gene that alter the isoform ratio in patients are known to cause familial forms of tauopathies (Goedert, 2005), the most likely explanation for the H1 risk would be a change in TAU expression levels conveyed by the *MAPT* haplotype. When comparing the transcription efficiency of the H1 and the H2 promotor with a Luciferase reporter assay in neuroblastoma cells, Kwok et al. found a higher transcription efficiency from the H1 promotor (Kwok et al., 2004). Evaluation of mRNA expression levels in human brains showed also different levels in H1 and H2 patients, although different studies offer conflicting results: while higher *MAPT* expression in brains from H1/H1 patients have been reported in some studies (de Jong et al., 2012; Valenca et al., 2016), others could not find elevated total *MAPT* expression from H1 alleles (Caffrey et al., 2006; Trabzuni et al., 2012). Furthermore, another group only reported higher *MAPT* expression in patients carrying the H1 sub-haplotype H1c (Myers et al., 2007). Other studies describe a greater inclusion of exon 10 in the *MAPT* transcript (4R TAU isoform) from H1 alleles (Caffrey et al., 2006; Majounie et al., 2013; Myers et al., 2007). So far, only one group investigated the *MAPT* risk factor with an iPSC model and evaluated the allele-specific expression of the *MAPT* gene in heterozygous H1/H2 cells (Beevers et al., 2017). They reported a higher level of *MAPT* transcripts from the H1 allele, while the exon 10+ transcripts were not differentially expressed between the two alleles. Most studies so far have concentrated on *MAPT* expression on the mRNA level. Therefore, it remains uncertain what consequences differential mRNA expression has on TAU protein levels in the brain. The work presented here is the first systematic comparison of eight homozygous iPSC lines, four H1/H1 and four H2/H2, evaluating *MAPT* expression on a transcriptional as well as on a translational level.

In contrast to the findings of Beevers et al. in iPSC, significant expression differences between H1 and H2 cells regarding total mRNA *MAPT* transcript were not detected. Additionally, for the 3R and 4R *TAU* isoform, no significant differences were visible between the haplotype groups.

On the protein level, there was more variability in TAU expression between the cell lines than on the mRNA level (visible by higher SEM). It did not manifest itself, however, in a statistical difference between the haplotype groups either for total TAU protein or the 3R and 4R TAU isoforms. For the 4R TAU isoform, there was a visible trend towards higher expression in the H1 haplotype cell lines. This observation did not reach statistical significance, but the 4R TAU protein levels were still low at day 30 of differentiation. It might, therefore, be possible that this tendency would become significant after a longer differentiation period. Additionally, the inter-individual variance might limit the identification of haplotype-dependent differences considering the sample size of eight cell lines (four cell lines per haplotype).

Comparisons of phosphorylated TAU did not reveal a significant difference between the H1/H1 and the H2/H2 cell lines. This is true for the p-TAU levels in the soluble as well as in the insoluble protein fraction.

Interestingly, an investigation of conformationally altered TAU showed significantly higher levels of MC1-positive TAU in the insoluble protein fraction of the H2/H2 cells compared to H1/H1 at day 30 of differentiation. A study from Wider et al. supports this finding (Wider et al., 2012). Here, patients with AD and LBD, which are not primary tauopathies, were compared regarding their secondary TAU pathology like NFT. Surprisingly, H2 carriers were connected to a higher NFT burden than the H1 carriers. This examination encourages our observation of increased conformationally altered TAU in the insoluble fraction in H2/H2 cells and may indicate increased aggregation in this haplotype. Two further studies, however, could not find differences in TAU pathology (NFT and neuritic plaques) in patients with PD and DLB between H1 and H2 cases (Colom-Cadena et al., 2013; Robakis et al., 2016). Despite that, all three studies suggest that a higher *MAPT* transcription level in H1 brains as described by other groups does not necessarily translate into more TAU pathology in the brains of patients. Since the mechanism and role of TAU and TAU pathology in cell toxicity and neuronal loss is still under debate, this is not necessarily contradictory. Recent findings suggest that NFT themselves are rather inert and their formation is sometimes even considered a protective mechanism (Cowan and Mudher, 2013).

4.3. α -SYNUCLEIN expression in homozygous H1 and H2 neurons

The H1 haplotype has not only been connected to an increased risk for tauopathies but also for PD. Therefore, α -SYNUCLEIN levels were analyzed in the different cell lines in addition to the TAU

expression profile. Surprisingly, α -SYNUCLEIN expression levels were significantly higher in cells with the H1 haplotype compared to the H2 haplotype on an mRNA as well as on a protein level, independent of the time point. Interestingly, even in the insoluble fraction, H1/H1 showed increased α -SYNUCLEIN levels at day 30 of differentiation. The mechanism by which the H1 haplotype increases the risk for synucleinopathies remains unknown. As described in Chapter 1.3, TAU pathology can appear in synucleinopathies like PD and DLB as secondary pathology.

Two studies support the finding of higher α -SYNUCLEIN levels without a difference in TAU levels between H1 and H2 on a pathophysiological level (Colom-Cadena et al., 2013; Robakis et al., 2016). α -SYNUCLEIN pathology like LB count in the brain was significantly higher in patients with DLB or PD that were carriers of the H1/H1 genotype. TAU pathology like NFT, however, was not significantly different between H1 and H2 carriers. Wider et al. (already mentioned in Chapter 4.2.2) also identified an increased LB count in H1 carriers (here in patients with AD and DLB) but additionally reported a higher TAU pathology (NFT count) in the H2 haplotype (Wider et al., 2012). These results endorse the observation of a higher level of conformationally altered TAU in the insoluble fraction in H2/H2 group and increased α -SYNUCLEIN expression levels in H1/H1 cell lines in the model used in this study.

Since expression of α -SYNUCLEIN is elevated on the mRNA level, it is unclear how the H1 haplotype might affect the transcription. Considering the variation in α -SYNUCLEIN expression between cell lines within one haplotype group and the sample size of four cell lines per haplotype, another genetic factor independent of the *MAPT* haplotype could be responsible for the difference in α -SYNUCLEIN expression. Therefore, SNPs in the *SNCA* gene that are reportedly associated with increased risk for synucleinopathies and the microsatellite *Rep1* (Campêlo and Silva, 2017) were selected and cell lines were genotyped accordingly. The genotypes of the chosen variants, however, did not explain the described α -SYNUCLEIN expression pattern.

Next to *MAPT*, several other genes lie within the 2 Mb region of the *MAPT* haplotype. It is therefore possible that another gene from the haplotype is influencing α -SYNUCLEIN expression. de Jong et al. have reported that the expression of other genes apart from *MAPT* are affected by the H2 inversion polymorphism (de Jong et al., 2012). Although little is known about these other genes, none of them have so far been reported to regulate transcription of the *SNCA* gene.

4.4. Vulnerability of homozygous H1 and H2 neurons to external stressors

The risk of developing a neurodegenerative disease is not solely defined by the genetics of the individual but is rather an interplay between genetic and environmental factors. Because of the high energy demand and the high degree of mitochondrial energy production, neurons are especially exposed to oxidative stress (Moreira et al., 2005). Therefore, neuronal culture media is usually

supplemented with antioxidants to reduce the levels of ROS (Perry et al., 2004). One study proposed a differential antioxidant response in cells with different *MAPT* haplotypes: Wang et al. identified an antioxidant response element (ARE) in the intron 1 of the *MAPT* gene as a binding platform for the transcription factor NRF2 which is a key regulator of the cellular antioxidant response (Wang et al., 2016). The study linked a SNP in the ARE on the H2 haplotype to a stronger binding of NRF2 and a higher transcription level of *MAPT*. Higher transcription levels from the H2 allele have been detected by several groups for *MAPT* transcripts containing exon 3 (2N TAU isoforms) (Beevers et al., 2017; Caffrey et al., 2008; Trabzuni et al., 2012). Wang et al. proposed an upregulation of the more aggregation resistant 2N TAU isoforms up on oxidative stress in H2 haplotype (Wang et al., 2016). To test whether cells with a different *MAPT* haplotype background would differ in their vulnerability to oxidative stress, cells were cultured and differentiated in medium without antioxidants in this thesis. In contrast to a toxin treatment, the omission of antioxidants and thus the slow increase in oxidative stress mimics the influence of environmental factors in a more physiological way. This method has, however, the disadvantage that the exact time point of measurable cell toxicity or cell death can vary between experiments. Additionally, cell survival showed high variability between cell lines. Therefore, a significant difference in susceptibility to oxidative stress was not detected between haplotype groups. Furthermore, the proposed protection during oxidative stress by upregulation of the 2N TAU isoform in H2 cells, might not be applicable in this cell model, as here the 0N3R TAU isoform is predominantly expressed.

Treatment with the mitochondrial inhibitor annonacin is a more direct method to investigate vulnerability to external stressors. After its identification as a toxin that causes atypical parkinsonism (Caparros-Lefebvre and Elbaz, 1999; Höglinger et al., 2005), annonacin was shown to induce TAU pathology in cell culture models (Bruch et al., 2017; Escobar-Khondiker et al., 2007). Next to a general reduced viability until cell death, treated cells exhibited increased TAU protein expression, especially the 4R TAU isoform.

When cell lines were exposed to annonacin, all cells showed reduced viability and metabolism, as measured by calcein and MTT, after 4 days of treatment. The variation between cell lines independent of the *MAPT* haplotype was, however, high. Although a trend was visible, indicating slightly higher cell survival in the H2/H2 group, this did not reach statistical significance. For the treatment with annonacin and the readout, the maximum differentiation time of 30 days was chosen displaying the highest expression levels of total TAU and 4R TAU. A toxin treatment at an earlier point during differentiation might reduce the variability between cell lines as cells are more homogenous in the early differentiation phase. Less variability in the experimental set up might lead to the identification of significant differences in cell survival after annonacin treatment between *MAPT* haplotype groups.

5. Conclusion

This work presents a valuable tool of eight iPSC lines with either the H1 or the H2 *MAPT* haplotype, which can be differentiated into neurons in a fast and reproducible manner. This cell model can be used to identify *MAPT*-dependent phenotypes to elucidate the mechanisms of the H1 haplotype as a risk factor for tauopathies and other neurodegenerative diseases. The presented data demonstrate that all cell lines were efficiently differentiated into enriched neuronal cell populations within a considerably short differentiation period with the expression of 4R TAU protein after only 15 days. Systematic comparison showed a significant difference in the expression profile of disease relevant proteins between the two haplotype groups. Increased levels of conformationally-changed TAU are detectable in the insoluble fraction of H2 cells at day 30 of differentiation compared to H1 cells. The expression of α -SYNUCLEIN, however, was higher on the mRNA and protein levels independent of the differentiation time point in the H1/H1 group as compared to H2/H2.

There is variability between cell lines within the haplotype groups, especially on the protein level. To verify the presented results, it would therefore be desirable to acquire additional cell lines for each haplotype to increase the sample size and reduce inconsistencies within the haplotype groups. Additionally, if a co-culture with non-neuronal cells, like glial cells, were to be utilized, the differentiation period could potentially be extended without a massive reduction in cell viability. A longer differentiation period would increase the expression of 4R TAU and might reveal a haplotype-dependent difference for this TAU isoform.

So far, there are no approved therapies available to halt or slow down neurodegenerative disease progression. Therefore, there is an urgent need for the discovery of new therapeutic compounds (Rösler et al., 2020). The iPSC resource presented here could be a helpful tool for the identification of molecular targets for therapeutic drugs and candidates for therapeutic drug repositioning. The cell model is applicable for high-throughput approaches due to its ability to be used for fast and robust neuronal differentiation. The detection of *MAPT*-dependent phenotypes could be used in a high-throughput screen to identify possible drug candidates. Furthermore, after the first characterization and analysis of disease-relevant proteins, these cells can be used to investigate other disease relevant mechanism such as microtubule-associated organelle transport, mitochondrial function, or TAU uptake, seeding and aggregation processes. All in all, the established resource of eight cell lines is a valuable tool for future studies to elucidate the underlying mechanisms of the H1 risk factor.

List of publications

- Strauß, T.**, Marvian-Tayaranian, A., Sadikoglou, E., Dhingra, A., Wegner, F., Trümbach, D., Wurst, W., Heutink, P., Schwarz, S. C. and Höglinger, G. U., 2021. iPS Cell-Based Model for MAPT Haplotype as a Risk Factor for Human Tauopathies Identifies No Major Differences in TAU Expression. *Front. Cell Dev. Biol.* 9:726866, doi: [10.3389/fcell.2021.726866](https://doi.org/10.3389/fcell.2021.726866).
- Truong, D. J., Phlairaharn, T., Eßwein, B., Gruber, C., Tümen, D., Baligács, E., Armbrust, N., Vaccaro, F. L., Lederer, E. M., Beck, E. M., Geilenkeuser, J., Göppert, S., Krumwiede, L., Grätz, C., Raffl, G., Schwarz, D., Zirngibl, M., Živanić, M., Beyer, M., Körner, J. D., Santl, T., Evsyukov, V., **Strauß, T.**, Schwarz, S. C., Höglinger, G. U., Heutink, P., Doll, S., Conrad, M., Giesert, F., Wurst, W., Westmeyer, G. G., 2021. Non-invasive and high-throughput interrogation of exon-specific isoform expression. *Nat Cell Biol* 23, 652-663, doi:[10.1038/s41556-021-00678-x](https://doi.org/10.1038/s41556-021-00678-x).

Declaration of contribution

The generation of an iPSC stock and conversion of iPSC lines into NGN2_smNPCs was done with the valuable help of Ashutosh Dhingra and Dr. Eldem Sadikoglou, Department of Genome Biology of Neurodegenerative Diseases, German Center for Neurodegenerative Diseases (DZNE), 72076, Tübingen, Germany.

Proofreading of the thesis was done with the valuable help of Dr. Sigrid Schwarz. Department of Translational Neurodegeneration, German Center for Neurodegenerative Diseases (DZNE), 81377, Munich, German.

References

- Ahmed, Z., Bigio, E. H., Budka, H., Dickson, D. W., Ferrer, I., Ghetti, B., Giaccone, G., Hatanpaa, K. J., Holton, J. L., Josephs, K. A., Powers, J., Spina, S., Takahashi, H., White, C. L., 3rd, Revesz, T., Kovacs, G. G., 2013. Globular glial tauopathies (GGT): consensus recommendations. *Acta Neuropathol* 126, 537-544, doi:10.1007/s00401-013-1171-0.
- Alonso, A. C., Grundke-Iqbal, I., Iqbal, K., 1996. Alzheimer's disease hyperphosphorylated tau sequesters normal tau into tangles of filaments and disassembles microtubules. *Nat Med* 2, 783-7, doi:10.1038/nm0796-783.
- Arai, Y., Yamazaki, M., Mori, O., Muramatsu, H., Asano, G., Katayama, Y., 2001. Alpha-synuclein-positive structures in cases with sporadic Alzheimer's disease: morphology and its relationship to tau aggregation. *Brain Res* 888, 287-296, doi:10.1016/s0006-8993(00)03082-1.
- Baker, M., Litvan, I., Houlden, H., Adamson, J., Dickson, D., Perez-Tur, J., Hardy, J., Lynch, T., Bigio, E., Hutton, M., 1999. Association of an extended haplotype in the tau gene with progressive supranuclear palsy. *Hum Mol Genet* 8, 711-5, doi:10.1093/hmg/8.4.711.
- Barghorn, S., Mandelkow, E., 2002. Toward a unified scheme for the aggregation of tau into Alzheimer paired helical filaments. *Biochemistry* 41, 14885-96, doi:10.1021/bi026469j.
- Beevers, J. E., Lai, M. C., Collins, E., Booth, H. D. E., Zambon, F., Parkkinen, L., Vowles, J., Cowley, S. A., Wade-Martins, R., Caffrey, T. M., 2017. MAPT Genetic Variation and Neuronal Maturity Alter Isoform Expression Affecting Axonal Transport in iPSC-Derived Dopamine Neurons. *Stem Cell Reports*, doi:10.1016/j.stemcr.2017.06.005.
- Birnbaum, J. H., Wanner, D., Gietl, A. F., Saake, A., Kundig, T. M., Hock, C., Nitsch, R. M., Tackenberg, C., 2018. Oxidative stress and altered mitochondrial protein expression in the absence of amyloid-beta and tau pathology in iPSC-derived neurons from sporadic Alzheimer's disease patients. *Stem Cell Res* 27, 121-130, doi:10.1016/j.scr.2018.01.019.
- Boettger, L. M., Handsaker, R. E., Zody, M. C., McCarroll, S. A., 2012. Structural haplotypes and recent evolution of the human 17q21.31 region. *Nat Genet* 44, 881-5, doi:10.1038/ng.2334.
- Bowles, K., Pugh, D., Farrell, K., Han, N., TCW, J., Liu, Y., Liang, S., Qian, L., Bendl, J., Fullard, J., Renton, A., Casella, A., Iida, M., Bandres-Ciga, S., Gan-Or, Z., Heutink, P., Siitonen, A., Bertelsen, S., Karch, C., Frucht, S., Kopell, B., Peter, I., Park, Y., Crane, P., Kauwe, J., Boehme, K., Höglinger, G., group, P. w., Consortium, I. P. s. D. G., Consortium, P. S. P. G., Charney, A., Roussos, P., Wang, J., Poon, W., Raj, T., Crary, J., Goate, A., 2019. 17q21.31 sub-haplotypes underlying H1-associated risk for Parkinson's disease and progressive supranuclear palsy converge on altered glial regulation. *bioRxiv*, 860668, doi:10.1101/860668.
- Brafman, D., Willert, K., 2017. Wnt/ β -catenin signaling during early vertebrate neural development. *Dev Neurobiol* 77, 1239-1259, doi:10.1002/dneu.22517.
- Brettschneider, J., Del Tredici, K., Lee, V. M., Trojanowski, J. Q., 2015. Spreading of pathology in neurodegenerative diseases: a focus on human studies. *Nat Rev Neurosci* 16, 109-20, doi:10.1038/nrn3887.
- Bruch, J., Xu, H., Rosler, T. W., De Andrade, A., Kuhn, P. H., Lichtenthaler, S. F., Arzberger, T., Winklhofer, K. F., Müller, U., Höglinger, G. U., 2017. PERK activation mitigates tau pathology in vitro and in vivo. *EMBO Mol Med* 9, 371-384, doi:10.15252/emmm.201606664.
- Brunden, K. R., Trojanowski, J. Q., Lee, V. M., 2009. Advances in tau-focused drug discovery for Alzheimer's disease and related tauopathies. *Nat Rev Drug Discov* 8, 783-93, doi:10.1038/nrd2959.

- Caffrey, T. M., Wade-Martins, R., 2007. Functional MAPT haplotypes: bridging the gap between genotype and neuropathology. *Neurobiol Dis* 27, 1-10, doi:10.1016/j.nbd.2007.04.006.
- Caffrey, T. M., Joachim, C., Wade-Martins, R., 2008. Haplotype-specific expression of the N-terminal exons 2 and 3 at the human MAPT locus. *Neurobiol Aging* 29, 1923-9, doi:10.1016/j.neurobiolaging.2007.05.002.
- Caffrey, T. M., Joachim, C., Paracchini, S., Esiri, M. M., Wade-Martins, R., 2006. Haplotype-specific expression of exon 10 at the human MAPT locus. *Hum Mol Genet* 15, 3529-37, doi:10.1093/hmg/ddl429.
- Campêlo, C., Silva, R. H., 2017. Genetic Variants in SNCA and the Risk of Sporadic Parkinson's Disease and Clinical Outcomes: A Review. *Parkinsons Dis* 2017, 4318416, doi:10.1155/2017/4318416.
- Caparros-Lefebvre, D., Elbaz, A., 1999. Possible relation of atypical parkinsonism in the French West Indies with consumption of tropical plants: a case-control study. Caribbean Parkinsonism Study Group. *Lancet* 354, 281-6, doi:10.1016/s0140-6736(98)10166-6.
- Cardo, L. F., Coto, E., de Mena, L., Ribacoba, R., Lorenzo-Betancor, O., Pastor, P., Samaranch, L., Mata, I. F., Díaz, M., Moris, G., Menéndez, M., Corao, A. I., Alvarez, V., 2012. A search for SNCA 3' UTR variants identified SNP rs356165 as a determinant of disease risk and onset age in Parkinson's disease. *J Mol Neurosci* 47, 425-30, doi:10.1007/s12031-011-9669-1.
- Chamberlain, S. J., Li, X. J., Lalande, M., 2008. Induced pluripotent stem (iPS) cells as in vitro models of human neurogenetic disorders. *Neurogenetics* 9, 227-35, doi:10.1007/s10048-008-0147-z.
- Chambers, S. M., Fasano, C. A., Papapetrou, E. P., Tomishima, M., Sadelain, M., Studer, L., 2009. Highly efficient neural conversion of human ES and iPS cells by dual inhibition of SMAD signaling. *Nat Biotechnol* 27, 275-80, doi:10.1038/nbt.1529.
- Chartier-Harlin, M. C., Kachergus, J., Roumier, C., Mouroux, V., Douay, X., Lincoln, S., Levecque, C., Larvor, L., Andrieux, J., Hulihan, M., Waucquier, N., Defebvre, L., Amouyel, P., Farrer, M., Destée, A., 2004. Alpha-synuclein locus duplication as a cause of familial Parkinson's disease. *Lancet* 364, 1167-9, doi:10.1016/s0140-6736(04)17103-1.
- Cheng, L., Wang, L., Li, N. N., Yu, W. J., Sun, X. Y., Li, J. Y., Zhou, D., Peng, R., 2016. SNCA rs356182 variant increases risk of sporadic Parkinson's disease in ethnic Chinese. *J Neurol Sci* 368, 231-4, doi:10.1016/j.jns.2016.07.032.
- Chiba-Falek, O., Nussbaum, R. L., 2001. Effect of allelic variation at the NACP-Rep1 repeat upstream of the alpha-synuclein gene (SNCA) on transcription in a cell culture luciferase reporter system. *Hum Mol Genet* 10, 3101-9, doi:10.1093/hmg/10.26.3101.
- Chiba-Falek, O., Touchman, J. W., Nussbaum, R. L., 2003. Functional analysis of intra-allelic variation at NACP-Rep1 in the alpha-synuclein gene. *Hum Genet* 113, 426-31, doi:10.1007/s00439-003-1002-9.
- Colla, E., Coune, P., Liu, Y., Pletnikova, O., Troncoso, J. C., Iwatsubo, T., Schneider, B. L., Lee, M. K., 2012. Endoplasmic reticulum stress is important for the manifestations of α -synucleinopathy in vivo. *J Neurosci* 32, 3306-20, doi:10.1523/jneurosci.5367-11.2012.
- Colom-Cadena, M., Gelpi, E., Martí, M. J., Charif, S., Dols-Icardo, O., Blesa, R., Clarimón, J., Lleó, A., 2013. MAPT H1 haplotype is associated with enhanced α -synuclein deposition in dementia with Lewy bodies. *Neurobiol Aging* 34, 936-42, doi:10.1016/j.neurobiolaging.2012.06.015.
- Conrad, C., Andreadis, A., Trojanowski, J. Q., Dickson, D. W., Kang, D., Chen, X., Wiederholt, W., Hansen, L., Masliah, E., Thal, L. J., Katzman, R., Xia, Y., Saitoh, T., 1997. Genetic evidence for the involvement of tau in progressive supranuclear palsy. *Ann Neurol* 41, 277-81, doi:10.1002/ana.410410222.

- Cowan, C. M., Mudher, A., 2013. Are tau aggregates toxic or protective in tauopathies? *Front Neurol* 4, 114, doi:10.3389/fneur.2013.00114.
- Crary, J. F., Trojanowski, J. Q., Schneider, J. A., Abisambra, J. F., Abner, E. L., Alafuzoff, I., Arnold, S. E., Attems, J., Beach, T. G., Bigio, E. H., Cairns, N. J., Dickson, D. W., Gearing, M., Grinberg, L. T., Hof, P. R., Hyman, B. T., Jellinger, K., Jicha, G. A., Kovacs, G. G., Knopman, D. S., Kofler, J., Kukull, W. A., Mackenzie, I. R., Masliah, E., McKee, A., Montine, T. J., Murray, M. E., Neltner, J. H., Santa-Maria, I., Seeley, W. W., Serrano-Pozo, A., Shelanski, M. L., Stein, T., Takao, M., Thal, D. R., Toledo, J. B., Troncoso, J. C., Vonsattel, J. P., White, C. L., 3rd, Wisniewski, T., Woltjer, R. L., Yamada, M., Nelson, P. T., 2014. Primary age-related tauopathy (PART): a common pathology associated with human aging. *Acta Neuropathol* 128, 755-66, doi:10.1007/s00401-014-1349-0.
- Cripps, D., Thomas, S. N., Jeng, Y., Yang, F., Davies, P., Yang, A. J., 2006. Alzheimer disease-specific conformation of hyperphosphorylated paired helical filament-Tau is polyubiquitinated through Lys-48, Lys-11, and Lys-6 ubiquitin conjugation. *J Biol Chem* 281, 10825-38, doi:10.1074/jbc.M512786200.
- Cronin, K. D., Ge, D., Manninger, P., Linnertz, C., Rossoshek, A., Orrison, B. M., Bernard, D. J., El-Agnaf, O. M., Schlossmacher, M. G., Nussbaum, R. L., Chiba-Falek, O., 2009. Expansion of the Parkinson disease-associated SNCA-Rep1 allele upregulates human alpha-synuclein in transgenic mouse brain. *Hum Mol Genet* 18, 3274-85, doi:10.1093/hmg/ddp265.
- Crowther, T., Goedert, M., Wischik, C. M., 1989. The repeat region of microtubule-associated protein tau forms part of the core of the paired helical filament of Alzheimer's disease. *Ann Med* 21, 127-32, doi:10.3109/07853898909149199.
- D'Souza, I., Schellenberg, G. D., 2005. Regulation of tau isoform expression and dementia. *Biochim Biophys Acta* 1739, 104-15, doi:10.1016/j.bbadis.2004.08.009.
- D'Souza, I., Poorkaj, P., Hong, M., Nochlin, D., Lee, V. M., Bird, T. D., Schellenberg, G. D., 1999. Missense and silent tau gene mutations cause frontotemporal dementia with parkinsonism-chromosome 17 type, by affecting multiple alternative RNA splicing regulatory elements. *Proc Natl Acad Sci U S A* 96, 5598-603, doi:10.1073/pnas.96.10.5598.
- de Jong, S., Chepelev, I., Janson, E., Strengman, E., van den Berg, L. H., Veldink, J. H., Ophoff, R. A., 2012. Common inversion polymorphism at 17q21.31 affects expression of multiple genes in tissue-specific manner. *BMC Genomics* 13, 458, doi:10.1186/1471-2164-13-458.
- Derynck, R., Zhang, Y., Feng, X. H., 1998. Smads: transcriptional activators of TGF-beta responses. *Cell* 95, 737-40, doi:10.1016/s0092-8674(00)81696-7.
- Dhingra, A., Täger, J., Bressan, E., Rodriguez-Nieto, S., Bedi, M. S., Bröer, S., Sadikoglou, E., Fernandes, N., Castillo-Lizardo, M., Rizzu, P., Heutink, P., 2020. Automated Production of Human Induced Pluripotent Stem Cell-Derived Cortical and Dopaminergic Neurons with Integrated Live-Cell Monitoring. *J Vis Exp*, doi:10.3791/61525.
- Di Battista, M. E., Pascale, E., Purcaro, C., Passarelli, F., Passarelli, E., Guglielmi, R., Vanacore, N., Meco, G., 2014. Clinical subtypes in Parkinson's disease: the impact of MAPT haplotypes. *J Neural Transm (Vienna)* 121, 353-6, doi:10.1007/s00702-013-1117-7.
- Dickson, D. W., 1998. Pick's disease: a modern approach. *Brain Pathol* 8, 339-54, doi:10.1111/j.1750-3639.1998.tb00158.x.
- Dickson, D. W., Ahmed, Z., Algom, A. A., Tsuboi, Y., Josephs, K. A., 2010. Neuropathology of variants of progressive supranuclear palsy. *Curr Opin Neurol* 23, 394-400, doi:10.1097/WCO.0b013e32833be924.
- Dickson, D. W., Bergeron, C., Chin, S. S., Duyckaerts, C., Horoupian, D., Ikeda, K., Jellinger, K., Lantos, P. L., Lippa, C. F., Mirra, S. S., Tabaton, M., Vonsattel, J. P., Wakabayashi, K., Litvan, I., 2002. Office

- of Rare Diseases neuropathologic criteria for corticobasal degeneration. *J Neuropathol Exp Neurol* 61, 935-46, doi:10.1093/jnen/61.11.935.
- Dorval, V., Fraser, P. E., 2006. Small ubiquitin-like modifier (SUMO) modification of natively unfolded proteins tau and alpha-synuclein. *J Biol Chem* 281, 9919-24, doi:10.1074/jbc.M510127200.
- Drewes, G., Trinczek, B., Illenberger, S., Biernat, J., Schmitt-Ulms, G., Meyer, H. E., Mandelkow, E. M., Mandelkow, E., 1995. Microtubule-associated protein/microtubule affinity-regulating kinase (p110mark). A novel protein kinase that regulates tau-microtubule interactions and dynamic instability by phosphorylation at the Alzheimer-specific site serine 262. *J Biol Chem* 270, 7679-88, doi:10.1074/jbc.270.13.7679.
- Dugger, B. N., Dickson, D. W., 2017. Pathology of Neurodegenerative Diseases. *Cold Spring Harb Perspect Biol* 9, doi:10.1101/cshperspect.a028035.
- Ehrlich, M., Hallmann, A. L., Reinhardt, P., Arauzo-Bravo, M. J., Korr, S., Ropke, A., Psathaki, O. E., Ehling, P., Meuth, S. G., Oblak, A. L., Murrell, J. R., Ghetti, B., Zaehres, H., Scholer, H. R., Sternecker, J., Kuhlmann, T., Hargus, G., 2015. Distinct Neurodegenerative Changes in an Induced Pluripotent Stem Cell Model of Frontotemporal Dementia Linked to Mutant TAU Protein. *Stem Cell Reports* 5, 83-96, doi:10.1016/j.stemcr.2015.06.001.
- Eiraku, M., Watanabe, K., Matsuo-Takasaki, M., Kawada, M., Yonemura, S., Matsumura, M., Wataya, T., Nishiyama, A., Muguruma, K., Sasai, Y., 2008. Self-organized formation of polarized cortical tissues from ESCs and its active manipulation by extrinsic signals. *Cell Stem Cell* 3, 519-32, doi:10.1016/j.stem.2008.09.002.
- Elbaz, A., Ross, O. A., Ioannidis, J. P., Soto-Ortolaza, A. I., Moisan, F., Aasly, J., Annesi, G., Bozi, M., Brighina, L., Chartier-Harlin, M. C., Destée, A., Ferrarese, C., Ferraris, A., Gibson, J. M., Gispert, S., Hadjigeorgiou, G. M., Jasinska-Myga, B., Klein, C., Krüger, R., Lambert, J. C., Lohmann, K., van de Loo, S., Lorient, M. A., Lynch, T., Mellick, G. D., Mutez, E., Nilsson, C., Opala, G., Puschmann, A., Quattrone, A., Sharma, M., Silburn, P. A., Stefanis, L., Uitti, R. J., Valente, E. M., Vilariño-Güell, C., Wirdefeldt, K., Wszolek, Z. K., Xiromerisiou, G., Maraganore, D. M., Farrer, M. J., 2011. Independent and joint effects of the MAPT and SNCA genes in Parkinson disease. *Ann Neurol* 69, 778-92, doi:10.1002/ana.22321.
- Eliezer, D., Kutluay, E., Bussell, R., Jr., Browne, G., 2001. Conformational properties of alpha-synuclein in its free and lipid-associated states. *J Mol Biol* 307, 1061-73, doi:10.1006/jmbi.2001.4538.
- Escobar-Khondiker, M., Hollerhage, M., Muriel, M. P., Champy, P., Bach, A., Depienne, C., Respondek, G., Yamada, E. S., Lannuzel, A., Yagi, T., Hirsch, E. C., Oertel, W. H., Jacob, R., Michel, P. P., Ruberg, M., Hoglinger, G. U., 2007. Annonacin, a natural mitochondrial complex I inhibitor, causes tau pathology in cultured neurons. *J Neurosci* 27, 7827-37, doi:10.1523/jneurosci.1644-07.2007.
- Esteras, N., Rohrer, J. D., Hardy, J., Wray, S., Abramov, A. Y., 2017. Mitochondrial hyperpolarization in iPSC-derived neurons from patients of FTDP-17 with 10+16 MAPT mutation leads to oxidative stress and neurodegeneration. *Redox Biol* 12, 410-422, doi:10.1016/j.redox.2017.03.008.
- Ezquerro, M., Pastor, P., Valldeoriola, F., Molinuevo, J. L., Blesa, R., Tolosa, E., Oliva, R., 1999. Identification of a novel polymorphism in the promoter region of the tau gene highly associated to progressive supranuclear palsy in humans. *Neurosci Lett* 275, 183-6, doi:10.1016/s0304-3940(99)00738-7.
- Ezquerro, M., Pastor, P., Gaig, C., Vidal-Taboada, J. M., Cruchaga, C., Munoz, E., Marti, M. J., Valldeoriola, F., Aguilar, M., Calopa, M., Hernandez-Vara, J., Tolosa, E., 2011. Different MAPT haplotypes are associated with Parkinson's disease and progressive supranuclear palsy. *Neurobiol Aging* 32, 547.e11-6, doi:10.1016/j.neurobiolaging.2009.09.011.

- Fanciulli, A., Wenning, G. K., 2015. Multiple-system atrophy. *N Engl J Med* 372, 249-63, doi:10.1056/NEJMra1311488.
- Flach, K., Hilbrich, I., Schiffmann, A., Gärtner, U., Krüger, M., Leonhardt, M., Waschipky, H., Wick, L., Arendt, T., Holzer, M., 2012. Tau oligomers impair artificial membrane integrity and cellular viability. *J Biol Chem* 287, 43223-33, doi:10.1074/jbc.M112.396176.
- Fong, H., Wang, C., Knoferle, J., Walker, D., Balestra, M. E., Tong, L. M., Leung, L., Ring, K. L., Seeley, W. W., Karydas, A., Kshirsagar, M. A., Boxer, A. L., Kosik, K. S., Miller, B. L., Huang, Y., 2013. Genetic correction of tauopathy phenotypes in neurons derived from human induced pluripotent stem cells. *Stem Cell Reports* 1, 226-34, doi:10.1016/j.stemcr.2013.08.001.
- Fortin, D. L., Troyer, M. D., Nakamura, K., Kubo, S., Anthony, M. D., Edwards, R. H., 2004. Lipid rafts mediate the synaptic localization of alpha-synuclein. *J Neurosci* 24, 6715-23, doi:10.1523/jneurosci.1594-04.2004.
- Fuchs, J., Tichopad, A., Golub, Y., Munz, M., Schweitzer, K. J., Wolf, B., Berg, D., Mueller, J. C., Gasser, T., 2008. Genetic variability in the SNCA gene influences alpha-synuclein levels in the blood and brain. *Faseb j* 22, 1327-34, doi:10.1096/fj.07-9348com.
- Funk, K. E., Thomas, S. N., Schafer, K. N., Cooper, G. L., Liao, Z., Clark, D. J., Yang, A. J., Kuret, J., 2014. Lysine methylation is an endogenous post-translational modification of tau protein in human brain and a modulator of aggregation propensity. *Biochem J* 462, 77-88, doi:10.1042/bj20140372.
- Garcia-Leon, J. A., Cabrera-Socorro, A., Eggermont, K., Swijsen, A., Terryn, J., Fazal, R., Nami, F., Ordovas, L., Quiles, A., Lluís, F., Serneels, L., Wierda, K., Sierksma, A., Kreir, M., Pestana, F., Van Damme, P., De Strooper, B., Thorrez, L., Ebnet, A., Verfaillie, C. M., 2018. Generation of a human induced pluripotent stem cell-based model for tauopathies combining three microtubule-associated protein TAU mutations which displays several phenotypes linked to neurodegeneration. *Alzheimers Dement* 14, 1261-1280, doi:10.1016/j.jalz.2018.05.007.
- Gerson, J. E., Sengupta, U., Lasagna-Reeves, C. A., Guerrero-Muñoz, M. J., Troncoso, J., Kaye, R., 2014. Characterization of tau oligomeric seeds in progressive supranuclear palsy. *Acta Neuropathol Commun* 2, 73, doi:10.1186/2051-5960-2-73.
- Ghetti, B., Oblak, A. L., Boeve, B. F., Johnson, K. A., Dickerson, B. C., Goedert, M., 2015. Invited review: Frontotemporal dementia caused by microtubule-associated protein tau gene (MAPT) mutations: a chameleon for neuropathology and neuroimaging. *Neuropathol Appl Neurobiol* 41, 24-46, doi:10.1111/nan.12213.
- Giasson, B. I., Murray, I. V., Trojanowski, J. Q., Lee, V. M., 2001. A hydrophobic stretch of 12 amino acid residues in the middle of alpha-synuclein is essential for filament assembly. *J Biol Chem* 276, 2380-6, doi:10.1074/jbc.M008919200.
- Giasson, B. I., Forman, M. S., Higuchi, M., Golbe, L. I., Graves, C. L., Kotzbauer, P. T., Trojanowski, J. Q., Lee, V. M., 2003. Initiation and synergistic fibrillization of tau and alpha-synuclein. *Science* 300, 636-40, doi:10.1126/science.1082324.
- Goedert, M., 2005. Tau gene mutations and their effects. *Mov Disord* 20 Suppl 12, S45-52, doi:10.1002/mds.20539.
- Goedert, M., Jakes, R., 1990. Expression of separate isoforms of human tau protein: correlation with the tau pattern in brain and effects on tubulin polymerization. *Embo j* 9, 4225-30.
- Goedert, M., Jakes, R., Crowther, R. A., 1999. Effects of frontotemporal dementia FTDP-17 mutations on heparin-induced assembly of tau filaments. *FEBS Lett* 450, 306-11, doi:10.1016/s0014-5793(99)00508-6.

- Goedert, M., Klug, A., Crowther, R. A., 2006. Tau protein, the paired helical filament and Alzheimer's disease. *J Alzheimers Dis* 9, 195-207, doi:10.3233/jad-2006-9s323.
- Goedert, M., Spillantini, M. G., Jakes, R., Rutherford, D., Crowther, R. A., 1989a. Multiple isoforms of human microtubule-associated protein tau: sequences and localization in neurofibrillary tangles of Alzheimer's disease. *Neuron* 3, 519-26, doi:10.1016/0896-6273(89)90210-9.
- Goedert, M., Spillantini, M. G., Potier, M. C., Ulrich, J., Crowther, R. A., 1989b. Cloning and sequencing of the cDNA encoding an isoform of microtubule-associated protein tau containing four tandem repeats: differential expression of tau protein mRNAs in human brain. *Embo j* 8, 393-9.
- Goedert, M., Jakes, R., Spillantini, M. G., Hasegawa, M., Smith, M. J., Crowther, R. A., 1996. Assembly of microtubule-associated protein tau into Alzheimer-like filaments induced by sulphated glycosaminoglycans. *Nature* 383, 550-3, doi:10.1038/383550a0.
- Grundke-Iqbal, I., Iqbal, K., Tung, Y. C., Quinlan, M., Wisniewski, H. M., Binder, L. I., 1986. Abnormal phosphorylation of the microtubule-associated protein tau (tau) in Alzheimer cytoskeletal pathology. *Proc Natl Acad Sci U S A* 83, 4913-7, doi:10.1073/pnas.83.13.4913.
- Gu, Y., Oyama, F., Ihara, Y., 1996. Tau is widely expressed in rat tissues. *J Neurochem* 67, 1235-44.
- Guo, T., Noble, W., Hanger, D. P., 2017. Roles of tau protein in health and disease. *Acta Neuropathol* 133, 665-704, doi:10.1007/s00401-017-1707-9.
- Hamilton, R. L., 2000. Lewy bodies in Alzheimer's disease: a neuropathological review of 145 cases using alpha-synuclein immunohistochemistry. *Brain Pathol* 10, 378-84, doi:10.1111/j.1750-3639.2000.tb00269.x.
- Hanger, D. P., Anderton, B. H., Noble, W., 2009. Tau phosphorylation: the therapeutic challenge for neurodegenerative disease. *Trends Mol Med* 15, 112-9, doi:10.1016/j.molmed.2009.01.003.
- Hasegawa, M., Smith, M. J., Goedert, M., 1998. Tau proteins with FTDP-17 mutations have a reduced ability to promote microtubule assembly. *FEBS Lett* 437, 207-10, doi:10.1016/s0014-5793(98)01217-4.
- Hofer, A., Berg, D., Asmus, F., Niwar, M., Ransmayr, G., Riemenschneider, M., Bonelli, S. B., Steffelbauer, M., Ceballos-Baumann, A., Haussermann, P., Behnke, S., Krüger, R., Prestel, J., Sharma, M., Zimprich, A., Riess, O., Gasser, T., 2005. The role of alpha-synuclein gene multiplications in early-onset Parkinson's disease and dementia with Lewy bodies. *J Neural Transm (Vienna)* 112, 1249-54, doi:10.1007/s00702-004-0263-3.
- Höglinger, G. U., Michel, P. P., Champy, P., Feger, J., Hirsch, E. C., Ruberg, M., Lannuzel, A., 2005. Experimental evidence for a toxic etiology of tropical parkinsonism. *Mov Disord* 20, 118-9, doi:10.1002/mds.20300.
- Höglinger, G. U., Melhem, N. M., Dickson, D. W., Sleiman, P. M., Wang, L. S., Klei, L., Rademakers, R., de Silva, R., Litvan, I., Riley, D. E., van Swieten, J. C., Heutink, P., Wszolek, Z. K., Uitti, R. J., Vandrovцова, J., Hurtig, H. I., Gross, R. G., Maetzler, W., Goldwurm, S., Tolosa, E., Borroni, B., Pastor, P., Cantwell, L. B., Han, M. R., Dillman, A., van der Brug, M. P., Gibbs, J. R., Cookson, M. R., Hernandez, D. G., Singleton, A. B., Farrer, M. J., Yu, C. E., Golbe, L. I., Revesz, T., Hardy, J., Lees, A. J., Devlin, B., Hakonarson, H., Muller, U., Schellenberg, G. D., 2011. Identification of common variants influencing risk of the tauopathy progressive supranuclear palsy. *Nat Genet* 43, 699-705, doi:10.1038/ng.859.
- Hong, M., Zhukareva, V., Vogelsberg-Ragaglia, V., Wszolek, Z., Reed, L., Miller, B. I., Geschwind, D. H., Bird, T. D., McKeel, D., Goate, A., Morris, J. C., Wilhelmsen, K. C., Schellenberg, G. D., Trojanowski, J. Q., Lee, V. M., 1998. Mutation-specific functional impairments in distinct tau isoforms of hereditary FTDP-17. *Science* 282, 1914-7, doi:10.1126/science.282.5395.1914.

- Hoover, B. R., Reed, M. N., Su, J., Penrod, R. D., Kotilinek, L. A., Grant, M. K., Pitstick, R., Carlson, G. A., Lanier, L. M., Yuan, L. L., Ashe, K. H., Liao, D., 2010. Tau mislocalization to dendritic spines mediates synaptic dysfunction independently of neurodegeneration. *Neuron* 68, 1067-81, doi:10.1016/j.neuron.2010.11.030.
- Hu, B. Y., Weick, J. P., Yu, J., Ma, L. X., Zhang, X. Q., Thomson, J. A., Zhang, S. C., 2010. Neural differentiation of human induced pluripotent stem cells follows developmental principles but with variable potency. *Proc Natl Acad Sci U S A* 107, 4335-40, doi:10.1073/pnas.0910012107.
- Hutton, M., Lendon, C. L., Rizzu, P., Baker, M., Froelich, S., Houlden, H., Pickering-Brown, S., Chakraverty, S., Isaacs, A., Grover, A., Hackett, J., Adamson, J., Lincoln, S., Dickson, D., Davies, P., Petersen, R. C., Stevens, M., de Graaff, E., Wauters, E., van Baren, J., Hillebrand, M., Joosse, M., Kwon, J. M., Nowotny, P., Che, L. K., Norton, J., Morris, J. C., Reed, L. A., Trojanowski, J., Basun, H., Lannfelt, L., Neystat, M., Fahn, S., Dark, F., Tannenberg, T., Dodd, P. R., Hayward, N., Kwok, J. B., Schofield, P. R., Andreadis, A., Snowden, J., Craufurd, D., Neary, D., Owen, F., Oostra, B. A., Hardy, J., Goate, A., van Swieten, J., Mann, D., Lynch, T., Heutink, P., 1998. Association of missense and 5'-splice-site mutations in tau with the inherited dementia FTDP-17. *Nature* 393, 702-5, doi:10.1038/31508.
- Imamura, K., Sahara, N., Kanaan, N. M., Tsukita, K., Kondo, T., Kutoku, Y., Ohsawa, Y., Sunada, Y., Kawakami, K., Hotta, A., Yawata, S., Watanabe, D., Hasegawa, M., Trojanowski, J. Q., Lee, V. M., Suhara, T., Higuchi, M., Inoue, H., 2016. Calcium dysregulation contributes to neurodegeneration in FTLD patient iPSC-derived neurons. *Sci Rep* 6, 34904, doi:10.1038/srep34904.
- Iovino, M., Agathou, S., Gonzalez-Rueda, A., Del Castillo Velasco-Herrera, M., Borroni, B., Alberici, A., Lynch, T., O'Dowd, S., Geti, I., Gaffney, D., Vallier, L., Paulsen, O., Karadottir, R. T., Spillantini, M. G., 2015. Early maturation and distinct tau pathology in induced pluripotent stem cell-derived neurons from patients with MAPT mutations. *Brain* 138, 3345-59, doi:10.1093/brain/awv222.
- Irwin, D. J., 2016. Tauopathies as clinicopathological entities. *Parkinsonism Relat Disord* 22 Suppl 1, S29-33, doi:10.1016/j.parkreldis.2015.09.020.
- Irwin, D. J., Cohen, T. J., Grossman, M., Arnold, S. E., Xie, S. X., Lee, V. M., Trojanowski, J. Q., 2012. Acetylated tau, a novel pathological signature in Alzheimer's disease and other tauopathies. *Brain* 135, 807-18, doi:10.1093/brain/aws013.
- Irwin, D. J., Cohen, T. J., Grossman, M., Arnold, S. E., McCarty-Wood, E., Van Deerlin, V. M., Lee, V. M., Trojanowski, J. Q., 2013. Acetylated tau neuropathology in sporadic and hereditary tauopathies. *Am J Pathol* 183, 344-51, doi:10.1016/j.ajpath.2013.04.025.
- Iseki, E., Togo, T., Suzuki, K., Katsuse, O., Marui, W., de Silva, R., Lees, A., Yamamoto, T., Kosaka, K., 2003. Dementia with Lewy bodies from the perspective of tauopathy. *Acta Neuropathol* 105, 265-70, doi:10.1007/s00401-002-0644-3.
- Ishizawa, T., Mattila, P., Davies, P., Wang, D., Dickson, D. W., 2003. Colocalization of tau and alpha-synuclein epitopes in Lewy bodies. *J Neuropathol Exp Neurol* 62, 389-97.
- Ittner, L. M., Ke, Y. D., Delerue, F., Bi, M., Gladbach, A., van Eersel, J., Wölfing, H., Chieng, B. C., Christie, M. J., Napier, I. A., Eckert, A., Staufienbiel, M., Hardeman, E., Götz, J., 2010. Dendritic function of tau mediates amyloid-beta toxicity in Alzheimer's disease mouse models. *Cell* 142, 387-97, doi:10.1016/j.cell.2010.06.036.
- Janning, D., Igaev, M., Sündermann, F., Brühmann, J., Beutel, O., Heinisch, J. J., Bakota, L., Piehler, J., Junge, W., Brandt, R., 2014. Single-molecule tracking of tau reveals fast kiss-and-hop interaction with microtubules in living neurons. *Mol Biol Cell* 25, 3541-51, doi:10.1091/mbc.E14-06-1099.

- Jeganathan, S., von Bergen, M., Mandelkow, E. M., Mandelkow, E., 2008. The natively unfolded character of tau and its aggregation to Alzheimer-like paired helical filaments. *Biochemistry* 47, 10526-39, doi:10.1021/bi800783d.
- Jeganathan, S., von Bergen, M., Bruchlach, H., Steinhoff, H. J., Mandelkow, E., 2006. Global hairpin folding of tau in solution. *Biochemistry* 45, 2283-93, doi:10.1021/bi0521543.
- Jellinger, K. A., 2010. Basic mechanisms of neurodegeneration: a critical update. *J Cell Mol Med* 14, 457-87, doi:10.1111/j.1582-4934.2010.01010.x.
- Jellinger, K. A., 2011. Interaction between alpha-synuclein and tau in Parkinson's disease comment on Wills et al.: elevated tauopathy and alpha-synuclein pathology in postmortem Parkinson's disease brains with and without dementia. *Exp Neurol* 2010; 225: 210-218. *Exp Neurol* 227, 13-8, doi:10.1016/j.expneurol.2010.10.006.
- Jellinger, K. A., 2014. Neuropathology of multiple system atrophy: new thoughts about pathogenesis. *Mov Disord* 29, 1720-41, doi:10.1002/mds.26052.
- Jicha, G. A., Bowser, R., Kazam, I. G., Davies, P., 1997. Alz-50 and MC-1, a new monoclonal antibody raised to paired helical filaments, recognize conformational epitopes on recombinant tau. *J Neurosci Res* 48, 128-32, doi:10.1002/(sici)1097-4547(19970415)48:2<128::aid-jnr5>3.0.co;2-e.
- Kim, T. G., Yao, R., Monnell, T., Cho, J. H., Vasudevan, A., Koh, A., Peeyush, K. T., Moon, M., Datta, D., Bolshakov, V. Y., Kim, K. S., Chung, S., 2014. Efficient specification of interneurons from human pluripotent stem cells by dorsoventral and rostrocaudal modulation. *Stem Cells* 32, 1789-804, doi:10.1002/stem.1704.
- Kirkeby, A., Grealish, S., Wolf, D. A., Nelander, J., Wood, J., Lundblad, M., Lindvall, O., Parmar, M., 2012. Generation of regionally specified neural progenitors and functional neurons from human embryonic stem cells under defined conditions. *Cell Rep* 1, 703-14, doi:10.1016/j.celrep.2012.04.009.
- Klein, C., Kramer, E. M., Cardine, A. M., Schraven, B., Brandt, R., Trotter, J., 2002. Process outgrowth of oligodendrocytes is promoted by interaction of fyn kinase with the cytoskeletal protein tau. *J Neurosci* 22, 698-707.
- Koechling, T., Lim, F., Hernandez, F., Avila, J., 2010. Neuronal models for studying tau pathology. *Int J Alzheimers Dis* 2010, doi:10.4061/2010/528474.
- Köpke, E., Tung, Y. C., Shaikh, S., Alonso, A. C., Iqbal, K., Grundke-Iqbal, I., 1993. Microtubule-associated protein tau. Abnormal phosphorylation of a non-paired helical filament pool in Alzheimer disease. *J Biol Chem* 268, 24374-84.
- Kouri, N., Ross, O. A., Dombroski, B., Younkin, C. S., Serie, D. J., Soto-Ortolaza, A., Baker, M., Finch, N. C. A., Yoon, H., Kim, J., Fujioka, S., McLean, C. A., Ghetti, B., Spina, S., Cantwell, L. B., Farlow, M. R., Grafman, J., Huey, E. D., Ryung Han, M., Beecher, S., Geller, E. T., Kretschmar, H. A., Roeber, S., Gearing, M., Juncos, J. L., Vonsattel, J. P. G., Van Deerlin, V. M., Grossman, M., Hurtig, H. I., Gross, R. G., Arnold, S. E., Trojanowski, J. Q., Lee, V. M., Wenning, G. K., White, C. L., Hoglinger, G. U., Muller, U., Devlin, B., Golbe, L. I., Crook, J., Parisi, J. E., Boeve, B. F., Josephs, K. A., Wszolek, Z. K., Uitti, R. J., Graff-Radford, N. R., Litvan, I., Younkin, S. G., Wang, L. S., Ertekin-Taner, N., Rademakers, R., Hakonarson, H., Schellenberg, G. D., Dickson, D. W., 2015. Genome-wide association study of corticobasal degeneration identifies risk variants shared with progressive supranuclear palsy. *Nat Commun* 6, 7247, doi:10.1038/ncomms8247.
- Kovacs, G. G., Budka, H., 2010. Current concepts of neuropathological diagnostics in practice: neurodegenerative diseases. *Clin Neuropathol* 29, 271-88, doi:10.5414/npp29271.

- Kovacs, G. G., Botond, G., Budka, H., 2010. Protein coding of neurodegenerative dementias: the neuropathological basis of biomarker diagnostics. *Acta Neuropathol* 119, 389-408, doi:10.1007/s00401-010-0658-1.
- Kovacs, G. G., Rozemuller, A. J., van Swieten, J. C., Gelpi, E., Majtenyi, K., Al-Sarraj, S., Troakes, C., Bódi, I., King, A., Hortobágyi, T., Esiri, M. M., Ansorge, O., Giaccone, G., Ferrer, I., Arzberger, T., Bogdanovic, N., Nilsson, T., Leisser, I., Alafuzoff, I., Ironside, J. W., Kretschmar, H., Budka, H., 2013. Neuropathology of the hippocampus in FTLD-Tau with Pick bodies: a study of the BrainNet Europe Consortium. *Neuropathol Appl Neurobiol* 39, 166-78, doi:10.1111/j.1365-2990.2012.01272.x.
- Krüger, R., Kuhn, W., Müller, T., Woitalla, D., Graeber, M., Kösel, S., Przuntek, H., Eppelen, J. T., Schöls, L., Riess, O., 1998. Ala30Pro mutation in the gene encoding alpha-synuclein in Parkinson's disease. *Nat Genet* 18, 106-8, doi:10.1038/ng0298-106.
- Kuret, J., Chirita, C. N., Congdon, E. E., Kannanayakal, T., Li, G., Necula, M., Yin, H., Zhong, Q., 2005. Pathways of tau fibrillization. *Biochim Biophys Acta* 1739, 167-78, doi:10.1016/j.bbadis.2004.06.016.
- Kwok, J. B., Teber, E. T., Loy, C., Hallupp, M., Nicholson, G., Mellick, G. D., Buchanan, D. D., Silburn, P. A., Schofield, P. R., 2004. Tau haplotypes regulate transcription and are associated with Parkinson's disease. *Ann Neurol* 55, 329-34, doi:10.1002/ana.10826.
- Landino, L. M., Skreslet, T. E., Alston, J. A., 2004. Cysteine oxidation of tau and microtubule-associated protein-2 by peroxynitrite: modulation of microtubule assembly kinetics by the thioredoxin reductase system. *J Biol Chem* 279, 35101-5, doi:10.1074/jbc.M405471200.
- Lantos, P. L., 1998. The definition of multiple system atrophy: a review of recent developments. *J Neuropathol Exp Neurol* 57, 1099-111, doi:10.1097/00005072-199812000-00001.
- Lasagna-Reeves, C. A., Castillo-Carranza, D. L., Sengupta, U., Clos, A. L., Jackson, G. R., Kaye, R., 2011. Tau oligomers impair memory and induce synaptic and mitochondrial dysfunction in wild-type mice. *Mol Neurodegener* 6, 39, doi:10.1186/1750-1326-6-39.
- Ledesma, M. D., Bonay, P., Colaço, C., Avila, J., 1994. Analysis of microtubule-associated protein tau glycation in paired helical filaments. *J Biol Chem* 269, 21614-9.
- Lee, C. C., Nayak, A., Sethuraman, A., Belfort, G., McRae, G. J., 2007. A three-stage kinetic model of amyloid fibrillation. *Biophys J* 92, 3448-58, doi:10.1529/biophysj.106.098608.
- Lee, G., Newman, S. T., Gard, D. L., Band, H., Panchamoorthy, G., 1998. Tau interacts with src-family non-receptor tyrosine kinases. *J Cell Sci* 111 (Pt 21), 3167-77.
- Lee, V. M., Giasson, B. I., Trojanowski, J. Q., 2004. More than just two peas in a pod: common amyloidogenic properties of tau and alpha-synuclein in neurodegenerative diseases. *Trends Neurosci* 27, 129-34, doi:10.1016/j.tins.2004.01.007.
- Lei, P., Ayton, S., Moon, S., Zhang, Q., Volitakis, I., Finkelstein, D. I., Bush, A. I., 2014. Motor and cognitive deficits in aged tau knockout mice in two background strains. *Mol Neurodegener* 9, 29, doi:10.1186/1750-1326-9-29.
- Lill, C. M., Roehr, J. T., McQueen, M. B., Kavvoura, F. K., Bagade, S., Schjeide, B. M., Schjeide, L. M., Meissner, E., Zauft, U., Allen, N. C., Liu, T., Schilling, M., Anderson, K. J., Beecham, G., Berg, D., Biernacka, J. M., Brice, A., DeStefano, A. L., Do, C. B., Eriksson, N., Factor, S. A., Farrer, M. J., Foroud, T., Gasser, T., Hamza, T., Hardy, J. A., Heutink, P., Hill-Burns, E. M., Klein, C., Latourelle, J. C., Maraganore, D. M., Martin, E. R., Martinez, M., Myers, R. H., Nalls, M. A., Pankratz, N., Payami, H., Satake, W., Scott, W. K., Sharma, M., Singleton, A. B., Stefansson, K., Toda, T., Tung, J. Y., Vance, J., Wood, N. W., Zabetian, C. P., Young, P., Tanzi, R. E., Khoury, M. J., Zipp, F., Lehrach, H., Ioannidis, J. P., Bertram, L., 2012. Comprehensive research synopsis and

- systematic meta-analyses in Parkinson's disease genetics: The PDGene database. *PLoS Genet* 8, e1002548, doi:10.1371/journal.pgen.1002548.
- Linnertz, C., Saucier, L., Ge, D., Cronin, K. D., Burke, J. R., Browndyke, J. N., Hulette, C. M., Welsh-Bohmer, K. A., Chiba-Falek, O., 2009. Genetic regulation of alpha-synuclein mRNA expression in various human brain tissues. *PLoS One* 4, e7480, doi:10.1371/journal.pone.0007480.
- Liu, F., Gong, C. X., 2008. Tau exon 10 alternative splicing and tauopathies. *Mol Neurodegener* 3, 8, doi:10.1186/1750-1326-3-8.
- Löhle, M., Hermann, A., Glass, H., Kempe, A., Schwarz, S. C., Kim, J. B., Poulet, C., Ravens, U., Schwarz, J., Schöler, H. R., Storch, A., 2012. Differentiation efficiency of induced pluripotent stem cells depends on the number of reprogramming factors. *Stem Cells* 30, 570-9, doi:10.1002/stem.1016.
- Magnani, E., Fan, J., Gasparini, L., Golding, M., Williams, M., Schiavo, G., Goedert, M., Amos, L. A., Spillantini, M. G., 2007. Interaction of tau protein with the dynactin complex. *Embo j* 26, 4546-54, doi:10.1038/sj.emboj.7601878.
- Majounie, E., Cross, W., Newsway, V., Dillman, A., Vandrovcova, J., Morris, C. M., Nalls, M. A., Ferrucci, L., Owen, M. J., O'Donovan, M. C., Cookson, M. R., Singleton, A. B., de Silva, R., Morris, H. R., 2013. Variation in tau isoform expression in different brain regions and disease states. *Neurobiol Aging* 34, 1922.e7-1922.e12, doi:10.1016/j.neurobiolaging.2013.01.017.
- Mandelkow, E. M., Schweers, O., Drewes, G., Biernat, J., Gustke, N., Trinczek, B., Mandelkow, E., 1996. Structure, microtubule interactions, and phosphorylation of tau protein. *Ann N Y Acad Sci* 777, 96-106, doi:10.1111/j.1749-6632.1996.tb34407.x.
- Maroteaux, L., Campanelli, J. T., Scheller, R. H., 1988. Synuclein: a neuron-specific protein localized to the nucleus and presynaptic nerve terminal. *J Neurosci* 8, 2804-15, doi:10.1523/jneurosci.08-08-02804.1988.
- Mata, I. F., Shi, M., Agarwal, P., Chung, K. A., Edwards, K. L., Factor, S. A., Galasko, D. R., Ghingina, C., Griffith, A., Higgins, D. S., Kay, D. M., Kim, H., Leverenz, J. B., Quinn, J. F., Roberts, J. W., Samii, A., Snapinn, K. W., Tsuang, D. W., Yearout, D., Zhang, J., Payami, H., Zabetian, C. P., 2010. SNCA variant associated with Parkinson disease and plasma alpha-synuclein level. *Arch Neurol* 67, 1350-6, doi:10.1001/archneurol.2010.279.
- McCarthy, J. J., Linnertz, C., Saucier, L., Burke, J. R., Hulette, C. M., Welsh-Bohmer, K. A., Chiba-Falek, O., 2011. The effect of SNCA 3' region on the levels of SNCA-112 splicing variant. *Neurogenetics* 12, 59-64, doi:10.1007/s10048-010-0263-4.
- McKee, A. C., Cantu, R. C., Nowinski, C. J., Hedley-Whyte, E. T., Gavett, B. E., Budson, A. E., Santini, V. E., Lee, H. S., Kibilus, C. A., Stern, R. A., 2009. Chronic traumatic encephalopathy in athletes: progressive tauopathy after repetitive head injury. *J Neuropathol Exp Neurol* 68, 709-35, doi:10.1097/NEN.0b013e3181a9d503.
- McKee, A. C., Stern, R. A., Nowinski, C. J., Stein, T. D., Alvarez, V. E., Daneshvar, D. H., Lee, H. S., Wojtowicz, S. M., Hall, G., Baugh, C. M., Riley, D. O., Kibilus, C. A., Cormier, K. A., Jacobs, M. A., Martin, B. R., Abraham, C. R., Ikezu, T., Reichard, R. R., Wolozin, B. L., Budson, A. E., Goldstein, L. E., Kowall, N. W., Cantu, R. C., 2013. The spectrum of disease in chronic traumatic encephalopathy. *Brain* 136, 43-64, doi:10.1093/brain/aws307.
- Menden, K., Francescato, M., Nyima, T., Blauwendraat, C., Dhingra, A., Castillo-Lizardo, M., Fernandes, N., Kaurani, L., Kronenberg-Versteeg, D., Atarsu, B., Sadikoglou, E., Borroni, B., Rodriguez-Nieto, S., Simon-Sanchez, J., Fischer, A., Craig, D. W., Neumann, M., Bonn, S., Rizzu, P., Heutink, P., 2021. Integrated multi-omics analysis reveals common and distinct dysregulated pathways for genetic subtypes of Frontotemporal Dementia. *bioRxiv*, 2020.12.01.405894, doi:10.1101/2020.12.01.405894.

- Miguel, L., Rovelet-Lecrux, A., Feyeux, M., Frebourg, T., Nassoy, P., Campion, D., Lecourtois, M., 2019. Detection of all adult Tau isoforms in a 3D culture model of iPSC-derived neurons. *Stem Cell Res* 40, 101541, doi:10.1016/j.scr.2019.101541.
- Min, S. W., Chen, X., Tracy, T. E., Li, Y., Zhou, Y., Wang, C., Shirakawa, K., Minami, S. S., Defensor, E., Mok, S. A., Sohn, P. D., Schilling, B., Cong, X., Ellerby, L., Gibson, B. W., Johnson, J., Krogan, N., Shamloo, M., Gestwicki, J., Masliah, E., Verdin, E., Gan, L., 2015. Critical role of acetylation in tau-mediated neurodegeneration and cognitive deficits. *Nat Med* 21, 1154-62, doi:10.1038/nm.3951.
- Miyasaka, T., Watanabe, A., Saito, Y., Murayama, S., Mann, D. M., Yamazaki, M., Ravid, R., Morishima-Kawashima, M., Nagashima, K., Ihara, Y., 2005. Visualization of newly deposited tau in neurofibrillary tangles and neuropil threads. *J Neuropathol Exp Neurol* 64, 665-74, doi:10.1097/01.jnen.0000173890.79058.1d.
- Mondragón-Rodríguez, S., Trillaud-Doppia, E., Dudilot, A., Bourgeois, C., Lauzon, M., Leclerc, N., Boehm, J., 2012. Interaction of endogenous tau protein with synaptic proteins is regulated by N-methyl-D-aspartate receptor-dependent tau phosphorylation. *J Biol Chem* 287, 32040-53, doi:10.1074/jbc.M112.401240.
- Moon, J., Schwarz, S. C., Lee, H. S., Kang, J. M., Lee, Y. E., Kim, B., Sung, M. Y., Hoglinger, G., Wegner, F., Kim, J. S., Chung, H. M., Chang, S. W., Cha, K. Y., Kim, K. S., Schwarz, J., 2016. Preclinical Analysis of Fetal Human Mesencephalic Neural Progenitor Cell Lines: Characterization and Safety In Vitro and In Vivo. *Stem Cells Transl Med*, doi:10.5966/sctm.2015-0228.
- Moreira, P. I., Smith, M. A., Zhu, X., Nunomura, A., Castellani, R. J., Perry, G., 2005. Oxidative stress and neurodegeneration. *Ann N Y Acad Sci* 1043, 545-52, doi:10.1196/annals.1333.062.
- Morfini, G. A., Burns, M., Binder, L. I., Kanaan, N. M., LaPointe, N., Bosco, D. A., Brown, R. H., Jr., Brown, H., Tiwari, A., Hayward, L., Edgar, J., Nave, K. A., Garberrn, J., Atagi, Y., Song, Y., Pigino, G., Brady, S. T., 2009. Axonal transport defects in neurodegenerative diseases. *J Neurosci* 29, 12776-86, doi:10.1523/jneurosci.3463-09.2009.
- Mori, H., Oda, M., Komori, T., Arai, N., Takanashi, M., Mizutani, T., Hirai, S., Mizuno, Y., 2002. Lewy bodies in progressive supranuclear palsy. *Acta Neuropathol* 104, 273-8, doi:10.1007/s00401-002-0555-3.
- Mukrasch, M. D., Bibow, S., Korukottu, J., Jeganathan, S., Biernat, J., Griesinger, C., Mandelkow, E., Zweckstetter, M., 2009. Structural polymorphism of 441-residue tau at single residue resolution. *PLoS Biol* 7, e34, doi:10.1371/journal.pbio.1000034.
- Myers, A. J., Kaleem, M., Marlowe, L., Pittman, A. M., Lees, A. J., Fung, H. C., Duckworth, J., Leung, D., Gibson, A., Morris, C. M., de Silva, R., Hardy, J., 2005. The H1c haplotype at the MAPT locus is associated with Alzheimer's disease. *Hum Mol Genet* 14, 2399-404, doi:10.1093/hmg/ddi241.
- Myers, A. J., Pittman, A. M., Zhao, A. S., Rohrer, K., Kaleem, M., Marlowe, L., Lees, A., Leung, D., McKeith, I. G., Perry, R. H., Morris, C. M., Trojanowski, J. Q., Clark, C., Karlawish, J., Arnold, S., Forman, M. S., Van Deerlin, V., de Silva, R., Hardy, J., 2007. The MAPT H1c risk haplotype is associated with increased expression of tau and especially of 4 repeat containing transcripts. *Neurobiol Dis* 25, 561-70, doi:10.1016/j.nbd.2006.10.018.
- Nacharaju, P., Lewis, J., Easson, C., Yen, S., Hackett, J., Hutton, M., Yen, S. H., 1999. Accelerated filament formation from tau protein with specific FTDP-17 missense mutations. *FEBS Lett* 447, 195-9, doi:10.1016/s0014-5793(99)00294-x.
- Nakamura, K., Nemani, V. M., Azarbal, F., Skibinski, G., Levy, J. M., Egami, K., Munishkina, L., Zhang, J., Gardner, B., Wakabayashi, J., Sesaki, H., Cheng, Y., Finkbeiner, S., Nussbaum, R. L., Masliah, E., Edwards, R. H., 2011. Direct membrane association drives mitochondrial fission by the

- Parkinson disease-associated protein alpha-synuclein. *J Biol Chem* 286, 20710-26, doi:10.1074/jbc.M110.213538.
- Nakamura, M., Shiozawa, S., Tsuboi, D., Amano, M., Watanabe, H., Maeda, S., Kimura, T., Yoshimatsu, S., Kisa, F., Karch, C. M., Miyasaka, T., Takashima, A., Sahara, N., Hisanaga, S. I., Ikeuchi, T., Kaibuchi, K., Okano, H., 2019. Pathological Progression Induced by the Frontotemporal Dementia-Associated R406W Tau Mutation in Patient-Derived iPSCs. *Stem Cell Reports* 13, 684-699, doi:10.1016/j.stemcr.2019.08.011.
- Neve, R. L., Harris, P., Kosik, K. S., Kurnit, D. M., Donlon, T. A., 1986. Identification of cDNA clones for the human microtubule-associated protein tau and chromosomal localization of the genes for tau and microtubule-associated protein 2. *Brain Res* 387, 271-80, doi:10.1016/0169-328x(86)90033-1.
- Nonaka, T., Watanabe, S. T., Iwatsubo, T., Hasegawa, M., 2010. Seeded aggregation and toxicity of {alpha}-synuclein and tau: cellular models of neurodegenerative diseases. *J Biol Chem* 285, 34885-98, doi:10.1074/jbc.M110.148460.
- Pan, F., Ding, H., Dong, H., Ye, M., Liu, W., Cui, G., Chen, J., Wu, Y., Wang, H., Dai, X., Shi, H., Ding, X., 2013. Association of polymorphism in rs2736990 of the α -synuclein gene with Parkinson's disease in a Chinese population. *Neurol India* 61, 360-4, doi:10.4103/0028-3886.117595.
- Pascale, E., Di Battista, M. E., Rubino, A., Purcaro, C., Valente, M., Fattapposta, F., Ferraguti, G., Meco, G., 2016. Genetic Architecture of MAPT Gene Region in Parkinson Disease Subtypes. *Front Cell Neurosci* 10, 96, doi:10.3389/fncel.2016.00096.
- Pastor, P., Ezquerra, M., Tolosa, E., Muñoz, E., Martí, M. J., Valldeoriola, F., Molinuevo, J. L., Calopa, M., Oliva, R., 2002. Further extension of the H1 haplotype associated with progressive supranuclear palsy. *Mov Disord* 17, 550-6, doi:10.1002/mds.10076.
- Peeraer, E., Bottelbergs, A., Van Kolen, K., Stancu, I. C., Vasconcelos, B., Mahieu, M., Duytschaever, H., Ver Donck, L., Torremans, A., Sluydts, E., Van Acker, N., Kemp, J. A., Mercken, M., Brunden, K. R., Trojanowski, J. Q., Dewachter, I., Lee, V. M., Moechars, D., 2015. Intracerebral injection of preformed synthetic tau fibrils initiates widespread tauopathy and neuronal loss in the brains of tau transgenic mice. *Neurobiol Dis* 73, 83-95, doi:10.1016/j.nbd.2014.08.032.
- Peng, C., Gathagan, R. J., Lee, V. M., 2018. Distinct α -Synuclein strains and implications for heterogeneity among α -Synucleinopathies. *Neurobiol Dis* 109, 209-218, doi:10.1016/j.nbd.2017.07.018.
- Perry, S. W., Norman, J. P., Litzburg, A., Gelbard, H. A., 2004. Antioxidants are required during the early critical period, but not later, for neuronal survival. *J Neurosci Res* 78, 485-92, doi:10.1002/jnr.20272.
- Pittman, A. M., Fung, H. C., de Silva, R., 2006. Untangling the tau gene association with neurodegenerative disorders. *Hum Mol Genet* 15 Spec No 2, R188-95, doi:10.1093/hmg/ddl190.
- Pittman, A. M., Myers, A. J., Duckworth, J., Bryden, L., Hanson, M., Abou-Sleiman, P., Wood, N. W., Hardy, J., Lees, A., de Silva, R., 2004. The structure of the tau haplotype in controls and in progressive supranuclear palsy. *Hum Mol Genet* 13, 1267-74, doi:10.1093/hmg/ddh138.
- Pittman, A. M., Myers, A. J., Abou-Sleiman, P., Fung, H. C., Kaleem, M., Marlowe, L., Duckworth, J., Leung, D., Williams, D., Kilford, L., Thomas, N., Morris, C. M., Dickson, D., Wood, N. W., Hardy, J., Lees, A. J., de Silva, R., 2005. Linkage disequilibrium fine mapping and haplotype association analysis of the tau gene in progressive supranuclear palsy and corticobasal degeneration. *J Med Genet* 42, 837-46, doi:10.1136/jmg.2005.031377.
- Polymeropoulos, M. H., Lavedan, C., Leroy, E., Ide, S. E., Dehejia, A., Dutra, A., Pike, B., Root, H., Rubenstein, J., Boyer, R., Stenroos, E. S., Chandrasekharappa, S., Athanassiadou, A.,

- Papapetropoulos, T., Johnson, W. G., Lazzarini, A. M., Duvoisin, R. C., Di Iorio, G., Golbe, L. I., Nussbaum, R. L., 1997. Mutation in the alpha-synuclein gene identified in families with Parkinson's disease. *Science* 276, 2045-7, doi:10.1126/science.276.5321.2045.
- Poorkaj, P., Bird, T. D., Wijsman, E., Nemens, E., Garruto, R. M., Anderson, L., Andreadis, A., Wiederholt, W. C., Raskind, M., Schellenberg, G. D., 1998. Tau is a candidate gene for chromosome 17 frontotemporal dementia. *Ann Neurol* 43, 815-25, doi:10.1002/ana.410430617.
- Reinhardt, P., Glatza, M., Hemmer, K., Tsytsyura, Y., Thiel, C. S., Hoing, S., Moritz, S., Parga, J. A., Wagner, L., Bruder, J. M., Wu, G., Schmid, B., Ropke, A., Klingauf, J., Schwamborn, J. C., Gasser, T., Scholer, H. R., Sternecker, J., 2013. Derivation and expansion using only small molecules of human neural progenitors for neurodegenerative disease modeling. *PLoS One* 8, e59252, doi:10.1371/journal.pone.0059252.
- Reyes, J. F., Reynolds, M. R., Horowitz, P. M., Fu, Y., Guillozet-Bongaarts, A. L., Berry, R., Binder, L. I., 2008. A possible link between astrocyte activation and tau nitration in Alzheimer's disease. *Neurobiol Dis* 31, 198-208, doi:10.1016/j.nbd.2008.04.005.
- Robakis, D., Cortes, E., Clark, L. N., Vonsattel, J. P., Virmani, T., Alcalay, R. N., Crary, J. F., Levy, O. A., 2016. The effect of MAPT haplotype on neocortical Lewy body pathology in Parkinson disease. *J Neural Transm (Vienna)* 123, 583-8, doi:10.1007/s00702-016-1552-3.
- Rösler, T. W., Costa, M., Höglinger, G. U., 2020. Disease-modifying strategies in primary tauopathies. *Neuropharmacology* 167, 107842, doi:10.1016/j.neuropharm.2019.107842.
- Rösler, T. W., Tayanian Marvian, A., Brendel, M., Nykänen, N. P., Höllerhage, M., Schwarz, S. C., Hopfner, F., Koeglsperger, T., Respondek, G., Schweyer, K., Levin, J., Villemagne, V. L., Barthel, H., Sabri, O., Müller, U., Meissner, W. G., Kovacs, G. G., Höglinger, G. U., 2019. Four-repeat tauopathies. *Prog Neurobiol* 180, 101644, doi:10.1016/j.pneurobio.2019.101644.
- Schwarz, S. C., Schwarz, J., 2010. Translation of stem cell therapy for neurological diseases. *Transl Res* 156, 155-60, doi:10.1016/j.trsl.2010.07.002.
- Selkoe, D. J., Hardy, J., 2016. The amyloid hypothesis of Alzheimer's disease at 25 years. *EMBO Mol Med* 8, 595-608, doi:10.15252/emmm.201606210.
- Sengupta, A., Kabat, J., Novak, M., Wu, Q., Grundke-Iqbal, I., Iqbal, K., 1998. Phosphorylation of tau at both Thr 231 and Ser 262 is required for maximal inhibition of its binding to microtubules. *Arch Biochem Biophys* 357, 299-309, doi:10.1006/abbi.1998.0813.
- Sergeant, N., Delacourte, A., Buée, L., 2005. Tau protein as a differential biomarker of tauopathies. *Biochim Biophys Acta* 1739, 179-97, doi:10.1016/j.bbadis.2004.06.020.
- Shi, Y., Kirwan, P., Livesey, F. J., 2012. Directed differentiation of human pluripotent stem cells to cerebral cortex neurons and neural networks. *Nat Protoc* 7, 1836-46, doi:10.1038/nprot.2012.116.
- Silva, M. C., Cheng, C., Mair, W., Almeida, S., Fong, H., Biswas, M. H., Zhang, Z., Huang, Y., Temple, S., Coppola, G., Geschwind, D. H., Karydas, A., Miller, B. L., Kosik, K. S., Gao, F. B., Steen, J. A., Haggarty, S. J., 2016. Human iPSC-Derived Neuronal Model of Tau-A152T Frontotemporal Dementia Reveals Tau-Mediated Mechanisms of Neuronal Vulnerability. *Stem Cell Reports* 7, 325-40, doi:10.1016/j.stemcr.2016.08.001.
- Spillantini, M. G., Goedert, M., 2013. Tau pathology and neurodegeneration. *Lancet Neurol* 12, 609-22, doi:10.1016/s1474-4422(13)70090-5.
- Spillantini, M. G., Schmidt, M. L., Lee, V. M., Trojanowski, J. Q., Jakes, R., Goedert, M., 1997. Alpha-synuclein in Lewy bodies. *Nature* 388, 839-40, doi:10.1038/42166.

- Spillantini, M. G., Murrell, J. R., Goedert, M., Farlow, M. R., Klug, A., Ghetti, B., 1998. Mutation in the tau gene in familial multiple system tauopathy with presenile dementia. *Proc Natl Acad Sci U S A* 95, 7737-41, doi:10.1073/pnas.95.13.7737.
- Sposito, T., Preza, E., Mahoney, C. J., Seto-Salvia, N., Ryan, N. S., Morris, H. R., Arber, C., Devine, M. J., Houlden, H., Warner, T. T., Bushell, T. J., Zagnoni, M., Kunath, T., Livesey, F. J., Fox, N. C., Rossor, M. N., Hardy, J., Wray, S., 2015. Developmental regulation of tau splicing is disrupted in stem cell-derived neurons from frontotemporal dementia patients with the 10 + 16 splice-site mutation in MAPT. *Hum Mol Genet* 24, 5260-9, doi:10.1093/hmg/ddv246.
- Stamer, K., Vogel, R., Thies, E., Mandelkow, E., Mandelkow, E. M., 2002. Tau blocks traffic of organelles, neurofilaments, and APP vesicles in neurons and enhances oxidative stress. *J Cell Biol* 156, 1051-63, doi:10.1083/jcb.200108057.
- Steele, J. C., McGeer, P. L., 2008. The ALS/PDC syndrome of Guam and the cycad hypothesis. *Neurology* 70, 1984-90, doi:10.1212/01.wnl.0000312571.81091.26.
- Steele, J. C., Richardson, J. C., Olszewski, J., 1964. PROGRESSIVE SUPRANUCLEAR PALSY. A HETEROGENEOUS DEGENERATION INVOLVING THE BRAIN STEM, BASAL GANGLIA AND CEREBELLUM WITH VERTICAL GAZE AND PSEUDOBULBAR PALSY, NUCHAL DYSTONIA AND DEMENTIA. *Arch Neurol* 10, 333-59, doi:10.1001/archneur.1964.00460160003001.
- Stefansson, H., Helgason, A., Thorleifsson, G., Steinthorsdottir, V., Masson, G., Barnard, J., Baker, A., Jonasdottir, A., Ingason, A., Gudnadottir, V. G., Desnica, N., Hicks, A., Gylfason, A., Gudbjartsson, D. F., Jonsdottir, G. M., Sainz, J., Agnarsson, K., Birgisdottir, B., Ghosh, S., Olafsdottir, A., Cazier, J. B., Kristjansson, K., Frigge, M. L., Thorgeirsson, T. E., Gulcher, J. R., Kong, A., Stefansson, K., 2005. A common inversion under selection in Europeans. *Nat Genet* 37, 129-37, doi:10.1038/ng1508.
- Strauß, T., Marvian-Tayaranian, A., Sadikoglou, E., Dhingra, A., Wegner, F., Trümbach, D., Wurst, W., Heutink, P., Schwarz, S. C., Höglinger, G. U., 2021. iPSC Cell-Based Model for MAPT Haplotype as a Risk Factor for Human Tauopathies Identifies No Major Differences in TAU Expression. *Frontiers in Cell and Developmental Biology* 9, doi:10.3389/fcell.2021.726866.
- Sultan, A., Nessler, F., Violet, M., Bégard, S., Loyens, A., Talahari, S., Mansuroglu, Z., Marzin, D., Sergeant, N., Humez, S., Colin, M., Bonnefoy, E., Buée, L., Galas, M. C., 2011. Nuclear tau, a key player in neuronal DNA protection. *J Biol Chem* 286, 4566-75, doi:10.1074/jbc.M110.199976.
- Takahashi, K., Tanabe, K., Ohnuki, M., Narita, M., Ichisaka, T., Tomoda, K., Yamanaka, S., 2007. Induction of pluripotent stem cells from adult human fibroblasts by defined factors. *Cell* 131, 861-72, doi:10.1016/j.cell.2007.11.019.
- Tao, Y., Zhang, S. C., 2016. Neural Subtype Specification from Human Pluripotent Stem Cells. *Cell Stem Cell* 19, 573-586, doi:10.1016/j.stem.2016.10.015.
- Tashiro, K., Hasegawa, M., Ihara, Y., Iwatsubo, T., 1997. Somatodendritic localization of phosphorylated tau in neonatal and adult rat cerebral cortex. *Neuroreport* 8, 2797-801.
- Tolnay, M., Clavaguera, F., 2004. Argyrophilic grain disease: a late-onset dementia with distinctive features among tauopathies. *Neuropathology* 24, 269-83, doi:10.1111/j.1440-1789.2004.00591.x.
- Trabzuni, D., Wray, S., Vandrovicova, J., Ramasamy, A., Walker, R., Smith, C., Luk, C., Gibbs, J. R., Dillman, A., Hernandez, D. G., Arepalli, S., Singleton, A. B., Cookson, M. R., Pittman, A. M., de Silva, R., Weale, M. E., Hardy, J., Ryten, M., 2012. MAPT expression and splicing is differentially regulated by brain region: relation to genotype and implication for tauopathies. *Hum Mol Genet* 21, 4094-103, doi:10.1093/hmg/dds238.
- Trojanowski, J. Q., Schuck, T., Schmidt, M. L., Lee, V. M., 1989. Distribution of tau proteins in the normal human central and peripheral nervous system. *J Histochem Cytochem* 37, 209-15.

- Uversky, V. N., 2003. A protein-chameleon: conformational plasticity of alpha-synuclein, a disordered protein involved in neurodegenerative disorders. *J Biomol Struct Dyn* 21, 211-34, doi:10.1080/07391102.2003.10506918.
- Valenca, G. T., Srivastava, G. P., Oliveira-Filho, J., White, C. C., Yu, L., Schneider, J. A., Buchman, A. S., Shulman, J. M., Bennett, D. A., De Jager, P. L., 2016. The Role of MAPT Haplotype H2 and Isoform 1N/4R in Parkinsonism of Older Adults. *PLoS One* 11, e0157452, doi:10.1371/journal.pone.0157452.
- Verheyen, A., Diels, A., Reumers, J., Van Hoorde, K., Van den Wyngaert, I., van Outryve d'Ydewalle, C., De Bondt, A., Kuijlaars, J., De Muynck, L., De Hoogt, R., Bretteville, A., Jaensch, S., Buist, A., Cabrera-Socorro, A., Wray, S., Ebneith, A., Roevens, P., Royaux, I., Peeters, P. J., 2018. Genetically Engineered iPSC-Derived FTDP-17 MAPT Neurons Display Mutation-Specific Neurodegenerative and Neurodevelopmental Phenotypes. *Stem Cell Reports* 11, 363-379, doi:10.1016/j.stemcr.2018.06.022.
- Violet, M., Delattre, L., Tardivel, M., Sultan, A., Chauderlier, A., Caillierez, R., Talahari, S., Nesslany, F., Lefebvre, B., Bonnefoy, E., Buée, L., Galas, M. C., 2014. A major role for Tau in neuronal DNA and RNA protection in vivo under physiological and hyperthermic conditions. *Front Cell Neurosci* 8, 84, doi:10.3389/fncel.2014.00084.
- Volpato, V., Smith, J., Sandor, C., Ried, J. S., Baud, A., Handel, A., Newey, S. E., Wessely, F., Attar, M., Whiteley, E., Chintawar, S., Verheyen, A., Barta, T., Lako, M., Armstrong, L., Muschet, C., Artati, A., Cusulin, C., Christensen, K., Patsch, C., Sharma, E., Nicod, J., Brownjohn, P., Stubbs, V., Heywood, W. E., Gissen, P., De Filippis, R., Janssen, K., Reinhardt, P., Adamski, J., Royaux, I., Peeters, P. J., Terstappen, G. C., Graf, M., Livesey, F. J., Akerman, C. J., Mills, K., Bowden, R., Nicholson, G., Webber, C., Cader, M. Z., Lakics, V., 2018. Reproducibility of Molecular Phenotypes after Long-Term Differentiation to Human iPSC-Derived Neurons: A Multi-Site Omics Study. *Stem Cell Reports* 11, 897-911, doi:10.1016/j.stemcr.2018.08.013.
- von Bergen, M., Friedhoff, P., Biernat, J., Heberle, J., Mandelkow, E. M., Mandelkow, E., 2000. Assembly of tau protein into Alzheimer paired helical filaments depends on a local sequence motif ((306)VQIVYK(311)) forming beta structure. *Proc Natl Acad Sci U S A* 97, 5129-34, doi:10.1073/pnas.97.10.5129.
- Vuono, R., Winder-Rhodes, S., de Silva, R., Cisbani, G., Drouin-Ouellet, J., Spillantini, M. G., Cicchetti, F., Barker, R. A., 2015. The role of tau in the pathological process and clinical expression of Huntington's disease. *Brain* 138, 1907-18, doi:10.1093/brain/awv107.
- Wang, J. Z., Grundke-Iqbal, I., Iqbal, K., 1996. Glycosylation of microtubule-associated protein tau: an abnormal posttranslational modification in Alzheimer's disease. *Nat Med* 2, 871-5, doi:10.1038/nm0896-871.
- Wang, X., Campbell, M. R., Lacher, S. E., Cho, H. Y., Wan, M., Crowl, C. L., Chorley, B. N., Bond, G. L., Kleeberger, S. R., Slattery, M., Bell, D. A., 2016. A Polymorphic Antioxidant Response Element Links NRF2/sMAF Binding to Enhanced MAPT Expression and Reduced Risk of Parkinsonian Disorders. *Cell Rep* 15, 830-842, doi:10.1016/j.celrep.2016.03.068.
- Wang, Y., Mandelkow, E., 2016. Tau in physiology and pathology. *Nature Reviews Neuroscience* 17, 22-35, doi:10.1038/nrn.2015.1.
- Weingarten, M. D., Lockwood, A. H., Hwo, S. Y., Kirschner, M. W., 1975. A protein factor essential for microtubule assembly. *Proc Natl Acad Sci U S A* 72, 1858-62, doi:10.1073/pnas.72.5.1858.
- Wider, C., Ross, O. A., Nishioka, K., Heckman, M. G., Vilarino-Guell, C., Jasinska-Myga, B., Erketin-Taner, N., Rademakers, R., Graff-Radford, N. R., Mash, D. C., Papapetropoulos, S., Duara, R., Uchikado, H., Wszolek, Z. K., Farrer, M. J., Dickson, D. W., 2012. An evaluation of the impact of MAPT, SNCA and APOE on the burden of Alzheimer's and Lewy body pathology. *J Neurol Neurosurg Psychiatry* 83, 424-9, doi:10.1136/jnnp-2011-301413.

- Williams, D. R., Lees, A. J., 2009. Progressive supranuclear palsy: clinicopathological concepts and diagnostic challenges. *Lancet Neurol* 8, 270-9, doi:10.1016/s1474-4422(09)70042-0.
- Winkler, S., Hagenah, J., Lincoln, S., Heckman, M., Haugarvoll, K., Lohmann-Hedrich, K., Kostic, V., Farrer, M., Klein, C., 2007. alpha-Synuclein and Parkinson disease susceptibility. *Neurology* 69, 1745-50, doi:10.1212/01.wnl.0000275524.15125.f4.
- Wray, S., 2017. Modeling tau pathology in human stem cell derived neurons. *Brain Pathol* 27, 525-529, doi:10.1111/bpa.12521.
- Wray, S., Hardy, J., 2010. All MAPT out?: Well-travelled pathways into neurodegeneration. *The Biochemist* 32, 14-17, doi:10.1042/bio03202014.
- Zabetian, C. P., Hutter, C. M., Factor, S. A., Nutt, J. G., Higgins, D. S., Griffith, A., Roberts, J. W., Leis, B. C., Kay, D. M., Yearout, D., Montimurro, J. S., Edwards, K. L., Samii, A., Payami, H., 2007. Association analysis of MAPT H1 haplotype and subhaplotypes in Parkinson's disease. *Ann Neurol* 62, 137-44, doi:10.1002/ana.21157.
- Zarranz, J. J., Alegre, J., Gómez-Esteban, J. C., Lezcano, E., Ros, R., Ampuero, I., Vidal, L., Hoenicka, J., Rodriguez, O., Atarés, B., Llorens, V., Gomez Tortosa, E., del Ser, T., Muñoz, D. G., de Yebenes, J. G., 2004. The new mutation, E46K, of alpha-synuclein causes Parkinson and Lewy body dementia. *Ann Neurol* 55, 164-73, doi:10.1002/ana.10795.
- Zhang, B., Maiti, A., Shively, S., Lakhani, F., McDonald-Jones, G., Bruce, J., Lee, E. B., Xie, S. X., Joyce, S., Li, C., Toleikis, P. M., Lee, V. M., Trojanowski, J. Q., 2005. Microtubule-binding drugs offset tau sequestration by stabilizing microtubules and reversing fast axonal transport deficits in a tauopathy model. *Proc Natl Acad Sci U S A* 102, 227-31, doi:10.1073/pnas.0406361102.
- Zhang, C. C., Zhu, J. X., Wan, Y., Tan, L., Wang, H. F., Yu, J. T., Tan, L., 2017. Meta-analysis of the association between variants in MAPT and neurodegenerative diseases. *Oncotarget* 8, 44994-45007, doi:10.18632/oncotarget.16690.
- Zhang, Y., Pak, C., Han, Y., Ahlenius, H., Zhang, Z., Chanda, S., Marro, S., Patzke, C., Acuna, C., Covy, J., Xu, W., Yang, N., Danko, T., Chen, L., Wernig, M., Sudhof, T. C., 2013. Rapid single-step induction of functional neurons from human pluripotent stem cells. *Neuron* 78, 785-98, doi:10.1016/j.neuron.2013.05.029.
- Zhong, Q., Congdon, E. E., Nagaraja, H. N., Kuret, J., 2012. Tau isoform composition influences rate and extent of filament formation. *J Biol Chem* 287, 20711-9, doi:10.1074/jbc.M112.364067.